Characterization of Mouse NOA1:
Subcellular Localization, G-Quadruplex Binding & Proteolysis

Dissertation
Zur Erlangung des Doktorgrades
der Naturwissenschaften

vorgelegt beim Fachbereich 14
der Johann Wolfgang Goethe - Universität
in Frankfurt am Main

von
Natalie Al-Furoukh
aus Freudenstadt im Schwarzwald

Bad Nauheim 2013
(D30)

vom Fachbereich 14 der
Johann Wolfgang Goethe – Universität als Dissertation angenommen.

Dekan: Prof. Dr. Thomas Prisner

Gutachter:

Prof. Dr. Dr. Thomas Braun
Max-Planck-Institut für Herz- und Lungenforschung
Abteilung I: Entwicklung und Umbau des Herzens
Ludwigstraße 43, 61231 Bad Nauheim

Prof. Dr. Robert Tampé
Institut für Biochemie, Biocenter
Johann Wolfgang Goethe-Universität Frankfurt
Max-von-Laue Str. 9, 60438 Frankfurt am Main

Datum der Disputation: 30. September 2013

PER ASPERA AD ASTRA

I. Zusammenfassung

Mitochondrien sind sich selbst replizierende Zellorganellen. Ihre zentrale Rolle ist die Produktion von ATP. Hierzu besitzen Mitochondrien Transmembran-Atmungskettenkomplexe, die in der inneren mitochondrialen Membran lokalisiert sind und durch Elektronenübertragung einen Protonengradienten erzeugen, der Voraussetzung für die ATP-Produktion an der mitochondrialen ATP-Synthase ist. Die Energiebereitstellung in Form von ATP ist essentiell für das Überleben der Zelle. Organe mit hohem Energiebedarf wie z.B. Muskel, Herz und Gehirn, zeichnen sich durch ihren hohen Mitochondriengehalt aus.

Mitochondrien enthalten eine zirkuläre doppelsträngige DNA (Figure 1, Figure 2). Diese mtDNA kodiert 13 Proteine, 22 tRNAs und zwei ribosomale RNAs (Figure 3). Die 13 Proteine sind Bestandteil der Komplexe I, III, IV und V der Atmungskette. Zur Translation der mitochondrial kodierten Gene haben Mitochondrien einen autonomen Proteinsyntheseapparat (Figure 4, Table 1). Mitoribosomen werden unabhängig vom zytoplasmatischen Proteinsyntheseapparat assembliert und sind aufgrund des bakteriellen Ursprungs der Mitochondrien den prokaryotischen sehr ähnlich. Neben einer Vielzahl von kernkodierten Proteinen enthalten Mitoribosomen auch die zwei mtDNA kodierten ribosomalen RNAs (12S rRNA und 16S rRNA). Die exakten Mechanismen der Ribosomen-Assemblierung in Mitochondrien sind weitgehend unbekannt. Dennoch gibt es einige evolutionär hochkonservierte GTPasen, denen eine Schlüsselrolle als Assemblierungsfaktoren zugeschrieben wird[1,2].

Über 95% der mitochondrialen Proteine sind im Zellkern kodiert und müssen aus dem Zytosol in die Mitochondrien importiert werden. Es sind fünf Wege beschrieben, die sich in der Platzierung ihrer Substrate unterscheiden (Figure 5, Figure 6). Klassisch benötigen Membranproteine Signalsequenzen und Topologie-Signale, die für die korrekte Platzierung notwendig sind. Die Signalsequenz von Proteinen, die für das endoplasmatische Retikulum, die bakteriellen Plasmamembran oder die Innenmembranen von Chloroplasten bestimmt sind, wird vom ‚Signal Recognition Particle' (SRP) erkannt, gebunden und an den Zielort gebracht (Figure 7). Ein Mitochondrien-spezifischer SRP wurde bisher noch nicht entdeckt.

Mitochondrien enthalten eigenständige Protein-Abbausysteme. Die Matrix enthält drei ATP-abhängige Proteasen, die alle aus mehreren Untereinheiten bestehen und ringförmige Strukturen bilden (Figure 8). Die in der Membran verankerte m-AAA-Protease kontrolliert den Abbau der Atmungskettenkomplexe und anderer Innenmembranproteine. Während einige Substrate der Lon-Protease bekannt sind (z.B. der mitochondriale Transkritptionsfaktor Tfam) fehlt jegliche Information über die Substratspezifität von ClpXP in höheren Eukaryoten. ClpXP besteht aus der katalytischen Peptidasedomäne ClpP, welche Substrate abbaut und der regulatorischen Erkennungsdomäne ClpX. Die ATPase Aktivität ist auf die ClpX Untereinheit beschränkt, die unabhängig von ClpP auch als Chaperon funktioniert.

NOA1 (Nitric Oxide Associated Protein-1) ist eine im Zellkern kodierte GTPase[3]. In Abhängigkeit seiner GTPase Aktivität beeinflusst NOA1 die mitochondriale Atmung und die damit verbundene ATP-Produktion[4]. Außerdem wurde NOA1 eine Rolle in der Assemblierung von Mitoribosomen zugeschrieben[5]. Es wurde gezeigt, dass NOA1 mit der kleinen 28S Untereinheit der Mitoribosmen interagiert[6,7]. Die Autoren leiteten unterschiedliche Funktionen für NOA1 aus ihren Daten ab. Eine Rolle als Assemblierungsfaktor, der den Aufbau von Mitoribosomen reguliert[5,7,8] wird generell akzeptiert. Alternativ wird angenommen, dass NOA1 ein RNA-Chaperon oder ein ribosomale RNA prozessierendes Enzym wäre[2,6,9]. Die Aufklärung des molekularen Mechanismus, der den beobachteten Effekten zu Grunde liegt, steht jedoch aus.

Proteinstruktur und -funktion stehen oft in einem engen Zusammenhang. Die Analyse der Funktion von Einzel-Domänen kann Aufschluss über die oft komplexe, zelluläre Funktion des Gesamtproteins geben, die sich aus dem Entgegen- oder Zusammenwirken mehrerer Domänen ergibt. Deshalb wurde im Rahmen dieser Dissertation eine zellbiologische und biochemische Analyse der Funktion einiger bisher wenig untersuchter Motive des NOA1 Proteins vorgenommen werden. Die Arbeiten wurden entweder in murinen Zellkulturen, oder mit im Rahmen dieser Arbeit rekombinant hergestelltem NOA1 Protein durchgeführt.

Die gewonnenen Daten tragen dazu bei, ein umfangreicheres Model für die molekulare Funktion von NOA1 in der Zelle zu entwickeln. Die Zielsetzung umfasste die folgenden Bereiche:

- Charakterisierung der Kernlokalisation von NOA1 und Untersuchung des Zusammenhangs von Kernlokalisation und mitochondrialer Funktion

- Beschreibung der RNA-bindenden Eigenschaften von NOA1 und Analyse des Einflusses von RNA-Bindung auf die GTPase Funktion.
- Aufklärung des Abbauweges von NOA1.

Zu Beginn der Arbeit wurden die Domänen und Motive von NOA1 schematisch dargestellt (Figure 9) und deren Funktion beschrieben (Table 2). Ein speziesübergreifender Sequenzvergleich spiegelt den hohe Konservierungsgrad des NOA1 Proteins und seine essentielle Funktion wider. Im Säugerreich haben die NOA1 Homologe >70% Identität. Wirbellose, Pflanzen und Bakterien zeigen rund 30% Identität zum murinen NOA1 Protein (Table 3). In Überexpressionsstudien überlagerte NOA1 mit Mitochondrien spezifischen Marker-Proteinen. Das Entfernen des N-terminalen Signalpeptids (NOA1ΔMTS) führt zu einer Verteilung im Zytoplasma und der Akkumulation im Zellkern (Figure 10). Um auszuschließen, dass es sich bei der dualen Lokalisation um Isoformen handelte, wurden PCR basierte Studien durchgeführt. Diese zeigten klar, dass NOA1 ein einzelnes Protein ist und von einem spezifischen Gen und Transkript kodiert wird (Figure 11).

Zur zellbiologischen Expression wurden DNA-Konstrukte unterschiedlicher NOA1-Mutanten hergestellt (Figure 45). Das Abschneiden des N-Terminus verschob die subzelluläre Lokalisation von den Mitochondrien zum Zellkern, wohingegen das Abtrennen der C-terminalen RNA-Bindedomäne den Import von NOA1 in die Mitochondrien minderte (Figure 12). Die Entfernung der mitochondrialen Zielsequenz verursacht zudem einen Caspase-abhängigen Zelltod (Figure 13), der durch das Kappen des C-Terminus verhindert werden konnte. Aufgrund der vorliegenden Beobachtungen wird angenommen, dass die Kern- und Mitochondrien Lokalisation von NOA1 in dynamischem Zusammenhang stehen. Deshalb wurde der Einfluss von pharmakologisch aktiven Substanzen auf diese Dynamik getestet (Figure 15, Table 4, Figure 16). Histologische Analysen bestätigen die Lokalisation von NOA1 in den Nucleoli des Zellkerns (Figure 17, Figure 20). In einem *in vitro* Experiment wurde in isolierten Zellkernen der aktive Import von rekombinantem NOA1 Protein (Figure 18, Figure 19) bewiesen. Die Verwendung von Kernexport-Inhibitoren zeigte, dass NOA1 ein Exportin1/Crm1 spezifisches Kernexportsignal enthält (Figure 21), dessen isolierte Export-Eigenschaften durch Fusion an GFP bestätigt werden konnten (Figure 22). Die Inhibierung der cytosolischen Proteinsynthese bestätigte die Abfolge der subzellulären Lokalisationen. *De novo*

synthetisiertes NOA1 befindet sich im Zellkern wohingegen N-terminal prozessiertes NOA1 ausschließlich in den Mitochondrien zu finden ist (Figure 23). Demnach nimmt NOA1 einen Umweg durch den Zellkern, bevor es seinen Funktionsort, die Mitochondrien erreicht (Figure 41).

Die durch Akkumulation im Zellkern erzeugte Toxizität von NOA1 konnte durch Entfernung des C-Terminus aufgehoben werden. Dieser C-Terminus enthält eine noch uncharakterisierte RNA-binde Domäne. Deshalb wurde mit der SELEX-Methode (Systemic Evolution of Ligands by EXponential Enrichment) das Nucleotid Konsensus-Bindemotiv bestimmt (Figure 47). NOA1 bindet vornehmlich Guanin reiche Sequenzen (Figure 24), die nachfolgend als G-Quadruplexe identifiziert wurden (Figure 42). Ausführliche Bindungsstudien mit rekombinantem NOA1-Protein und radioaktiv markierten G-Quadruplexen bestätigten, das NOA1 G-Quadruplexe spezifisch bindet (Figure 25, Figure 26, Figure 27) und diese außerdem die GTPase Aktivität von NOA1 stimulieren (Figure 28). Eine NOA1 spezifischer zellulärer RNA-Ligand konnte bisher nicht identifiziert werden.

Die Studien der RNA-Bindung sowie die Lokalisation im Nucleolus, wo die Assemblierung von RNA/Protein-Komplexen stattfindet, charakterisieren NOA1 als Ribonukleoprotein. Bislang wurde kein mitochondriales Importsystem für Ribonukleoproteine beschrieben, obwohl der Import verschiedener solcher RNA/Protein Komplexe experimentell gezeigt werden konnte. Ein potentieller Importweg, mit Beteiligung von TOM Komplex und Porin in der Außenmembran, sowie TIM23 Komplex, Prohibitin Komplex und m-AAA Protease in der Innenmembran, wird hier diskutiert (Figure 43).

Die kurze Halbwertszeit des NOA1 Proteins und sein relativ niedriges Expressionsniveau wiesen auf einen streng kontrollierten Abbauweg hin. Im C-Terminus von NOA1 wurden potentielle Erkennungssignale für die Matrix Protease Komplex ClpXP identifiziert und durch Mutationsstudien bestätigt (Figure 35). Die Expression von ClpX war ausreichend, um zeitgleich überexprimiertes NOA1 komplett abzubauen (Figure 36). *In vitro* Abbaustudien bekräftigten die Spezifität von ClpXP für NOA1 (Figure 37). Dies ist der erste experimentelle Beweis für ein spezifisches ClpXP Substrat in Eukaryoten. Damit kann der ClpXP Protease eine übergeordnete Bedeutsamkeit zugeordnet werden, denn sie beeinflusst, durch den gezielten Abbau von NOA1, den zentralen Stoffwechsel der Mitochondrien.

Außerdem definiert dieser Abbau durch ClpXP NOA1's Weg über den Zellkern in die Mitochondrien als Einbahnstraße.

Zielsetzung dieser Arbeit war es, NOA1 eine molekulare Funktion zuzuordnen. Unter Einbeziehung der vorliegenden Daten wird die Rolle von NOA1 als mitochondrialer Membran-Insertions-Faktor für mtDNA kodierte Proteine diskutiert (Figure 44). Untersuchungen zur Bindung von NOA1 an intakte Mitoribosomen unterstützten das Model. Es wurde bereits gezeigt, dass die GTPase Aktivität für die Bindung und Freisetzung von NOA1 vom Mitoribosom notwendig ist[7]. Neu ist die Notwenigkeit einer naszierenden Peptidkette für die Interaktion von NOA1 und dem translatierenden Mitoribosom, was mithilfe des Translationsterminators Puromycin gezeigt werden konnte (Figure 39). Auch konnten zahlreiche Parallelelen von NOA1 zum klassischen Membran-Insertions-Faktor SRP gezogen werden (Table 8). Um den Einfluss von NOA1 auf die Insertion von mtDNA kodierten Proteinen zu visualisieren wurden invertierte Membranvesikel der inneren Mitochondrien Membran hergestellt. Der Ansatz enthielt eine krude Translationsmixtur, bestehend aus invertierten mitochondrialen Vesikeln, mtRNA, einem Ribosomen-reichen mitochondrialen Matrix-Extrakt und NOA1 Protein. Mehrere Peptide wurden abhängig von NOA1 in die Membranen eingebaut. Die GTPase Funktion war hierbei nicht essentiell.

Zusammenfassend konnte im Rahmen dieser Arbeit die Hypothese von NOA1 als mitochondrialem Membran-Insertions-Faktor experimentell unterstützt werden. Die vorliegende Arbeit bildet die Grundlage für weiterführende, differenzierte Untersuchungen. Einige Fragestellungen leiten sich direkt aus dem Model ab. Welche G-Quadruplex-RNA bindet NOA1 im Zellkern? Bindet NOA1 auch G-Quadruplex-RNA in Mitochondrien? Welche Zusammensetzung hat der Ribonukleoprotein-Import-Komplex in Mitochondrien? Gibt es transiente Interaktionen von NOA1 und Protein-Komplexen der inneren Mitochondrienmembran wie dem OXA-Komplex oder Bestandteilen des TIM23-Komlex?

Unabhängig von den Antworten auf diese Fragen steigt mit dem hier vorgeschlagenen Model die Bedeutsamkeit von NOA1 und ClpXP für die Mitochondrien-Forschung.

II. Abstract

Mitochondria contain their own protein synthesis machinery with mitoribosomes that are similar to prokaryotic ribosomes. The thirteen proteins encoded in the mitochondrial genome are members of the respiratory chain complexes that generate a proton gradient, which is the electromotoric force for ATP synthesis.

NOA1 (Nitric Oxide Associated Protein-1) is a nuclear encoded GTPase that positively influences mitochondrial respiration and ATP production. Although a role in mitoribosome assembly was assigned to NOA1 the underlying molecular mechanism is poorly understood. This work shows that the multi-domain protein NOA1 serves multiple purposes for the function of mitochondria. NOA1 is a dual localized protein that makes a detour through the nucleus before mitochondrial import. The nuclear shuttling is mediated by a nuclear localization signal and the now identified nuclear export signal. SELEX (Systemic Evolution of Ligands by Exponential Enrichment) analysis revealed a G-quadruplex binding motif that characterizes NOA1 as ribonucleoprotein (RNP). G-quadruplex binding was coupled to the GTPase activity and increased the GTP hydrolysis rate. The sequence of localization events and the identification of NOA1 being a RNP lead to the discussion of an alternative import pathway for RNPs into mitochondria. The short-lived NOA1 contains ClpX recognition motifs and is specifically degraded by the mitochondrial matrix protease ClpXP. NOA1 is the first reported substrate of ClpXP in higher eukaryotes and augments the contribution of the ClpXP protease for mitochondrial metabolism. To assess the direct action of NOA1 on the mitoribosome co-sedimentation assays were performed. They showed that the interaction of NOA1 and the mitoribosome is dependent on the GTPase function and the nascent peptide chain. *In vitro*, NOA1 facilitated the membrane insertion of newly translated and isotope labeled mitochondrial translation products into inverted mitochondrial inner membrane vesicles. In conclusion, NOA1 is a G-quadruplex-RNP that acts as mitochondrial membrane insertion factor for mtDNA-encoded proteins.

This thesis provides a comprehensive model of the molecular function of NOA1 and is the basis for future research. The identification of NOA1 as ClpXP substrate is a major contribution to the field of mitochondrial research.

III. Publications

In preparation:
Unexpected detour through the nucleus is required for the essential mitochondrial function of NOA1, a novel ClpXP substrate. Al-Furoukh N, Kardon J, Krüger M, Szibor M, Baker TA, Braun T.

Binding to G-quadruplex RNA activates the mitochondrial GTPase NOA1. Al-Furoukh N, Goffart S, Szibor M, Wanrooij S, Braun T. Biochim Biophys Acta. 2013 Aug 8; 1833(12):2933-2942

NOA1 is necessary for oxygen-dependent regulation of mitochondrial respiratory complexes. Heidler J, Al-Furoukh N, Kukat C, Salwig I, Ingelmann ME, Seibel P, Krüger M, Holtz J, Wittig I, Braun T, Szibor M. J Biol Chem 2011 Sep 16;286(37):32086-93

Pulications not related to this thesis:
Postnatal cardiomyocyte growth and mitochondrial reorganization cause multiple changes in the proteome of human heart cardiomyocytes. Pohjoismaki JL, Krüger M, Al-Furoukh N, Lagerstedt A, Karhunen P, Braun T. Molecular BioSystems. 2013 Jun;9(6):1210-9

Hypoxic transcription gene profiles under the modulation of nitric oxide in nuclear-run-on microarray and proteomics. Igwe E, Essler S, Al-Furoukh N, Dehne N, Brüne B. BMC Genomics. 2009 Sep 2;10:408.

Noncovalent, site-specific biotinylation of histidine-tagged proteins. Reichel A, Schaible D, Al-Furoukh N, Cohen M, Schreiber G, Piehler J. Anal Chem. 2007 Nov 15;79(22):8590-600.

IV. Introduction

A. Mitochondria

„The immense literature ... concerning theses minute bodies found in the cytosplasm of various cells ... of vertebrate and invertebrate animals but also of plants, ... must neccessarily arouse even more general interest and increased observation and discussion. A multiplicity of names has already been given these bodies: mitochondria and chondromiten...; chondrioconten, chondriosomen, chondrion and plastosomen...; plasmafaden, plasmakörner...; paramiton or miton...; microsomen...; granule and filament...“, shortened quote from “Mitochondria in Tissue Culture” by Lewis published in Science, 1914[10].

Mitochondria were discovered in the 19th century when microscopes became available. These membranous organelles are distributed in the cytosol of eukaryotic cells (Figure 1) and they carry genetic information. Therefore, the eukaryotic cell has two genomes: the nucleus contains the genetic information packed into chromosomes and the mitochondria contain several hundred copies of the circular mitochondrial genome, the mtDNA.

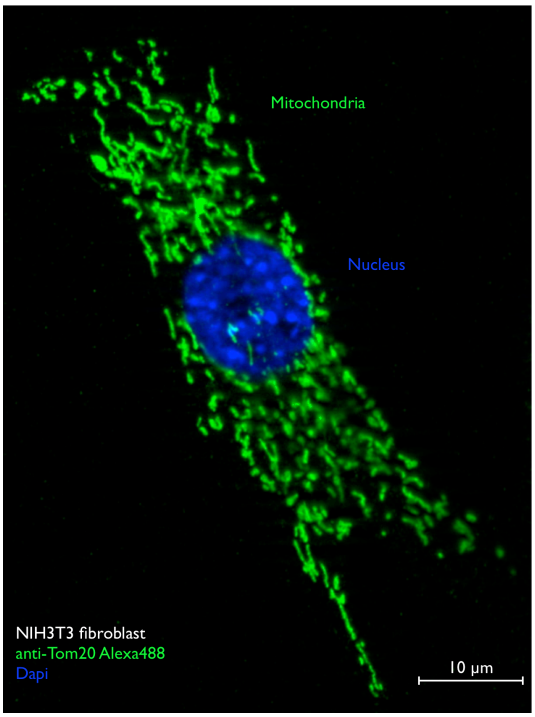

Figure 1 A eukaryotic cell with stained mitochondria and nucleus.

The definitions from the beginning of the last century, "mitochondrion" and "chondromites", origin from the Greek words "mitos and chondros" that mean "filament and granule". These terms are the best descriptions for the main characteristic of mitochondria, which is dynamics. They form a tubular network but in a situation of stress this network is disrupted and mitochondria appear fragmented (Figure 2).

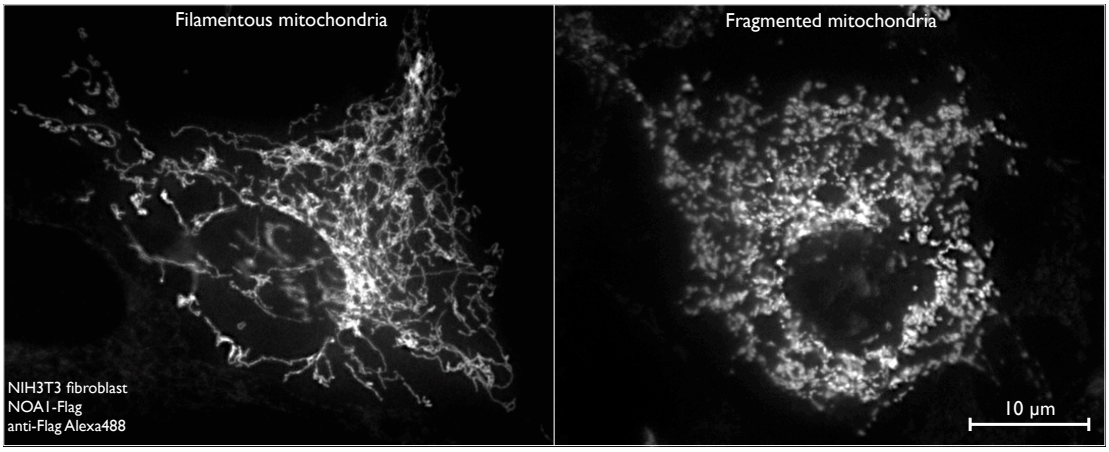

Figure 2 Mitochondria - dynamic organelles. Picture of filamentous and fragmented mitochondria of mouse fibroblast cells.

Today, it is known that the mitochondrial network is constantly undergoing fission and fusion. When these processes become disturbed, an imbalance is generated leading to hyper-fusion or complete fragmentation of the mitochondria. These extreme states can be beneficial but also pathological for the cell. The rather descriptive mitochondrial research of the past changed quickly and today we have gained vast knowledge of the biochemical processes inside these organelles. Mitochondria are named "powerhouse[11]" or "metabolic sensors" because they produce the main energy source of the cell, which is adenosine triphosphate (ATP), and they can quickly adapt to changes in the complex signaling networks that communicate cellular energy demands. Outer and inner membranes compartmentalize mitochondria and form inter-membrane space, cristae and matrix. The outer membrane is permeable for molecules and proteins <5 kDa and contains a variety of transmembrane protein complexes that mediate transport of proteins from the cytosol into the inter-membrane space or the matrix. The intermembrane space is a storage compartment for signaling molecules that are released during

apoptosis, e.g. cytochrome c (cyt c) and apoptosis-inducing factor (AIF). The inner membrane is forming invaginations, called "cristae". The cristae membrane contains the protein complexes of the respiratory chain (complexes I-IV) executing electron transport and thereby generating a proton gradient. This gradient is used by the mitochondrial ATP-synthase (complex V) to produce ATP by oxidative phosphorylation. Clusters of ATP-synthase are localized at the tip of the cristae[12] and release ATP into the matrix. The inner membrane is impermeable and contains transport protein complexes for different metabolites. The proteins responsible for fission and fusion are also localized in the inner membrane.

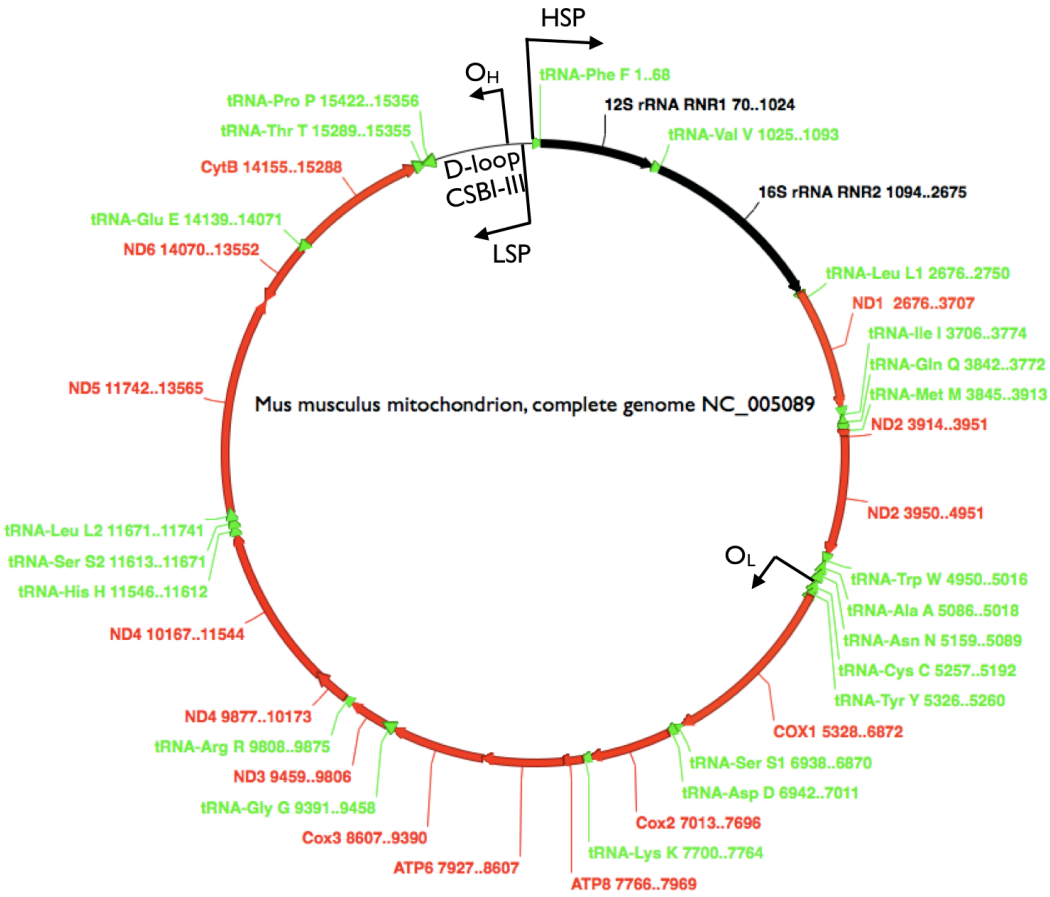

Figure 3 Scheme of the mouse mitochondrial genome. rRNAs black; tRNAs green; genes coding for proteins red; O_H origin of heavy strand replication; O_L origin of light strand replication; D-loop displacement loop; CSB conserved sequence block.

The matrix is the place of pyruvate oxidation, citric acid cycle and fatty acid biosynthesis. Additionally it contains the proteins that participate in mitochondrial transcription and translation. mtDNA has a size of ~16 kilo bases (Figure 3) and encodes 13 membrane proteins that are integral members of the respiratory chain

complexes I, III, IV and V. For protein synthesis the matrix contains the mitochondrial ribosomes that are different in structure and function from the cytosolic ribosomes[13]. Additionally to protein coding transcripts, two ribosomal RNAs (12s rRNA and 16S rRNA) and 22 tRNAs are transcribed from the mtDNA. They are involved in translation of the mitochondrially-encoded proteins. During transcription polycistronic transcripts are generated starting from heavy and light strand promoter. The polycistronic transcripts are then processed resulting in single RNAs. The promoters for both strands and evolutionary conserved regulatory domains are localized in the displacement loop (D-loop), a non-coding region lying between the proline tRNA and the phenylalanine tRNA codons.

Beside transcription, the mtDNA undergoes continuous replication also in post mitotic cells. Different models of replication are discussed in the literature[14-17].

Small defects like mutations in mtDNA, oxidative damage of proteins or mtDNA due to excess of reactive oxygen species, the by-product of respiration, or mutations in nuclear-encoded mitochondrial proteins can lead to severe pathologies. The interest in mitochondriopathies is growing proportional to the understanding of the system. Mitochondrial dysfunction plays a critical role in a variety of disorders like cardiac, neuromuscular and neurodegenerative diseases[18-20]. However, the understanding of the underlying fundamental molecular mechanisms is poor which is why the development of therapies to treat these severe pathologies remains very difficult.

B. Protein synthesis in mitochondria

The mitochondrial protein synthesis apparatus is more similar to the prokaryotic than to the cytosolic eukaryotic translation machinery. This is explained by the endosymbiont theory, which tells that mitochondria derived from the phagocytosis of prokaryotes. Protein synthesis of the 13 mtDNA-encoded polypeptides occurs at the mitochondrial 55S ribosome that consists of 28S small subunit and the 39S large subunit containing 16S rRNA and 12S rRNA, respectively.

The mammalian mitochondrial ribosome (mitoribosome) has ~20% minimized rRNA content but extended protein content in comparison to the bacterial counterpart[13]. This reduced amount of structurally stabilizing rRNA segments leads to a loss of compaction of the mitoribosome. Therefore mitochondrial ribosomes are more porous compared to the prokaryotic ribosomes (Figure 4). The lack in rRNAs is counterbalanced by new or enlarged homologs of mitochondrial ribosomal proteins

(MRPs). Although structurally different, the assignment of tasks is the same for all ribosomes, which is mRNA decoding on the small subunit and peptide bond formation on the large subunit[13]. Mitochondrial rRNAs are highly shielded by MRPs so that the majority of the surface of the mitoribosome is largely made up of MRPs. These proteins not only provide structural stability but also adopted functions during the protein synthesis process at the interface of small and large subunit. The phenotype of buried mitochondrial rRNAs is unique for mitoribosomes. The evolutionary related chloroplasts contain ribosomes, with a similar rRNA:rProtein ratio but the rRNA is not buried but patchy distributed over the surface. From the comparison of cryo-electron microscopy (cryo-EM) data it became obvious that the structure of ribosomes from different organelles has diverged significantly. These differences in structure hint to significant functional and regulatory differences.

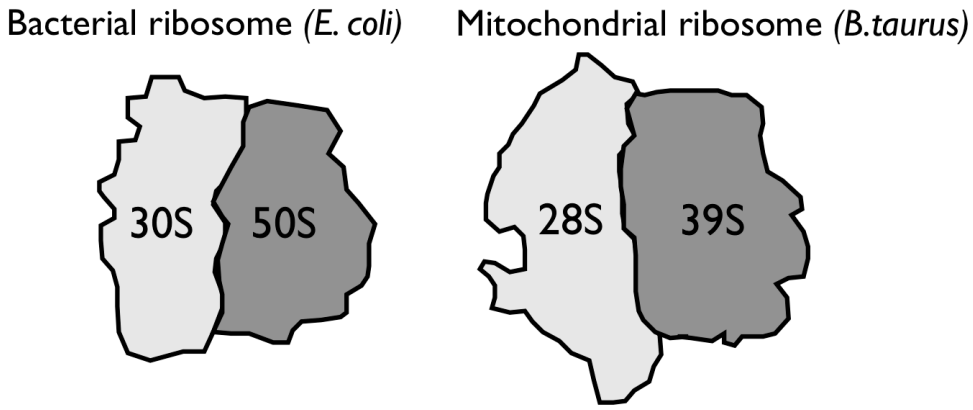

Figure 4 Contours of bacterial and mitochondrial ribosomes based on cryo-EM data. The *E.coli* ribosome has higher density and appears more compact in comparison to mammalian mitochondrial ribosomes, here *B.taurus*. Contours adapted from [21].

Table 1 compares the main features of bacterial and mammalian mitochondrial ribosomes. Structural data supporting the presence of alternative rRNAs, which are not 12S rRNA and 16S rRNA, is lacking. However, biochemical studies revealed that 5S rRNA is transported into mitochondria together with the ribosomal protein MRPL18[22,23]. Therefore it cannot be excluded that the composition of mitoribsomes as drawn from cryo-EM studies, could be complemented with to date unidentified rRNAs and MRPs.

Table 1 Comparison of the properties of bacterial ribosomes (*E.coli)* and mammalian mitochondrial ribosomes (*B.taurus)*.

	Bacterial ribosome (*E. coli*)	Mammalian mitochondrial ribosome (*B. taurus*)
Molecular mass	2.3 MDa	2.7 MDa
Sedimentation coefficient	70S	55S
RNA:protein ratio	~2:1	~1:2
Subunits	30S + 50 S	28S + 39S
Small subunit composition	16S rRNA (1542 nt) + 21 proteins	12S rRNA (950 nt) + 29 proteins
Large subunit composition	23S rRNA and 5S rRNA (total 3024 nt) + 34 proteins	16S rRNA (1560 nt) + 50 proteins
Diameter	~260 Å	~320 Å

adapted from Agrawal & Sharma et al. 2012

The dynamics of mitoribosome assembly and translation in the mitochondria is poorly characterized due to the lack of *in vitro* systems. The available data mainly derive from experiments with yeast or from cryo-EM analyses of isolated mitoribosomes. Unlike mammalian cells, some yeast species are facultative anaerobic organisms and can survive independently of mitochondrial function. Most experiments are based on the introduction of mutations in the nuclear and/or the mitochondrial genome of such facultative anaerob yeast species. The majority of such mutations would be lethal in a mammalian cell. Moreover, genetic modification of mtDNA is not feasible in mammalian cells to date. The following section gives an overview about the processes of ribosome assembly and translation.

Protein synthesis can be divided into five major phases: mitoribosome assembly, initiation, elongation, termination and mitoribosome recycling[24]. Mitoribosome assembly is rather uncharacterized. A few RNA chaperones and putative assembly factors have been identified but the spatiotemporal organization of assembly still remains unclear. It is assumed that the assembly process is separated into independent subassembly steps since single knockouts of MRPs rather result in the degradation of subcomplexes than in the degradation of the whole mitoribosome. The mitoribosomal binding sites for tRNAs are defined as A-, P- and E-site according to the activity of the binding tRNAs. The aminoacyl-tRNA (aa-tRNA) is loaded onto

the A-site, the peptidyl-tRNA is moved to the P-site and the E-site defines the exit for the free tRNA. Mitochondria contain two initiation factors: $IF3_{mt}$ and $IF2_{mt}$. In a first step $IF3_{mt}$ binds to the 55S ribosome and induces the loosening of the subunits resulting in a $IF3_{mt}$:28S complex. In the following GTP:$IF2_{mt}$ is recruited, then mRNA and fMet-tRNA bind to the complex. When this $IF3_{mt}$:GTP:$IF2_{mt}$:28S:mRNA:fMet-tRNA initiation complex is formed the large 39S mitoribosomal subunit is bound accompanied by GTP hydrolysis and the release of $IF3_{mt}$ and $IF2_{mt}$. This 55S:fMet-tRNA:mRNA complex undergoes the elongation process that is highly conserved and works similar to prokaryotic and cytosolic elongation. Three elongation factors are involved: EF-Tu_{mt}, EF-Ts_{mt} and EF-$G1_{mt}$. EF-Tu_{mt} form a complex with an aa-tRNA and GTP. This ternary complex consisting of EF-Tu_{mt}:GTP:aa-tRNA binds to the A-site of the 55S ribosome. The large subunit of the ribosome catalyzes peptide bond formation of aa-tRNA and the existing peptide chain. In parallel GTP hydrolysis occurs and EF-Tu_{mt}:GDP is released. EF-Ts_{mt} replaces the GDP with GTP to recycle EF-Tu_{mt}:GTP for the next cycle. The binding of EF-$G1_{mt}$:GTP translocates the deacylated peptidyl-tRNA from the A-site to the P-site where it is converted into a free tRNA upon transfer of the peptide chain on the new aa-tRNA in the next cycle. The free tRNA exits the ribosome from the E-site. The process of translation termination in mitochondria was comprehensively investigated[25-27]. Three release factors are involved in termination and ribosome recycling: mtRF1a, $RRF1_{mt}$ (=mtRRF) and $RRF2_{mt}$ (=EF-$G2_{mt}$). First, mtRF1a:GTP binds to the A site of the 55S ribosome and induces its own release and the release of the protein chain triggered by GTP hydrolysis. In a second step $RRF1_{mt}$ binds to the A-site, where it is joined by $RRF2_{mt}$:GTP. Thereafter, GTP hydrolysis promots the dissociation of 28S and 39S subunits and the release of the mRNA. The elongation factor EF-$G1_{mt}$ and the termination factor EF-$G2_{mt}$ are isoforms.

Although a lot of details were described, the exact mechanism of the mitochondrial translation process remains unclear. It is due to this lack of information that a pure functional *in vitro* system for cytosolic as well as mitochondrial translation still could not be established. Additionally, the initiation of mitochondrial translation is very different from cytosolic and prokaryotic translation initiation since mtDNA transcripts are leaderless. That means that they neither carry prokaryotic Shine-Delgarno nor eukaryotic Kozak initiation sequences. It is assumed that the differences in protein and rRNA composition of the mitoribosome in combination

with secondary structure motifs of the mitochondrial mRNAs could compensate for the lack of classical leader sequences.

C. Protein targeting to mitochondrial membranes

All mitochondrial encoded proteins are membrane proteins and essential members of the respiratory chain complexes I, III, IV and V. Besides the 13 mtDNA-encoded proteins, all other mitochondrial proteins are nuclear encoded, synthesized by the cytosolic translation apparatus and need to be imported co- or post-translationally. Therefore, mitochondria contain different import pathways that target proteins to their final localization. A recent review[28] summarizes the five protein import pathways of mitochondria in very detail. The review also addresses the contribution of the import pathways to other mitochondrial functions like mitochondrial membrane organization, quality control and endoplasmic reticulum-mitochondria junctions. In the following section, the five main mitochondrial protein import routes are roughly described (Figure 5).

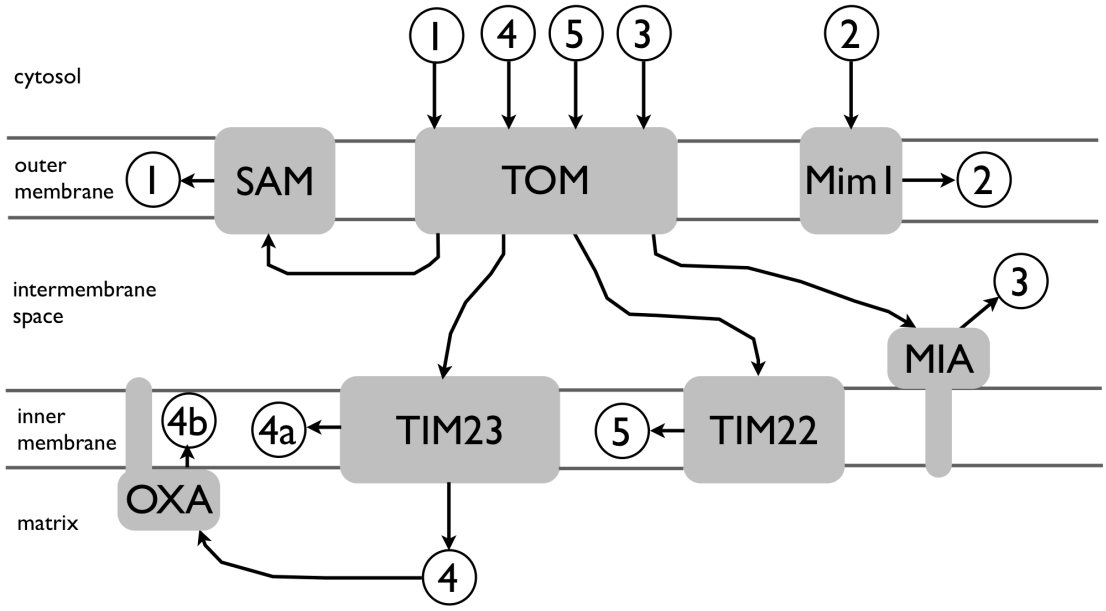

Figure 5 Five major mitochondrial import and sorting pathways for nuclear encoded mitochondrial proteins (based on [28]). SAM: sorting and assembly machinery, import of β-barrel proteins in the outer membrane; TOM: translocase of the outer mitochondrial membrane, main protein entry channel; Mim1: mitochondrial import protein 1, insertion of α-helical proteins in the outer membrane; TIM23: presequence translocase of the inner membrane, transport of precursor containing proteins into the matrix and the innermembrane; TIM22: carrier translocase of the inner membrane, insertion of non-cleavable inner membrane proteins; MIA: mitochondrial intermembrane space import and assembly machinery, oxidative folding of intermembrane space proteins; OXA: oligomeric

complex of Oxa1, export of mitochondrial precursor proteins from the matrix to the inner membrane.

The majority of proteins enter the mitochondria by the TOM complex (translocase of the outer mitochondrial membrane) with its channel-forming core protein Tom40. Other Tom proteins act as receptor proteins or support the assembly of the TOM complex. For outer membrane insertion there are two main pathways described that are specific for evolutionary origin and secondary structure of the inserted proteins. Outer mitochondrial membrane proteins of bacterial origin form β-barrels and use the TOM complex to enter the intermembrane space where chaperones assist the precursor to insert into the outer mitochondrial membrane by the SAM (sorting and assembly machinery) complex (Figure 5-1). The Mim1 (mitochondrial import protein 1) protein inserts α-helical proteins into the outer mitochondrial membrane. These proteins have eukaryotic origin. Mim1 interacts with the TOM receptor Tom70 but the membrane insertion is independent of the pore of the TOM complex (Figure 5-2). SAM and Mim1 pathways function independently, but it was shown that they cooperate during the assembly of some outer membrane multi-domain proteins, e.g. the TOM complex. Intermembrane space proteins mainly use the TOM complex and the recently identified MIA (mitochondrial intermembrane space import and assembly) complex. Most intermembrane space proteins are cysteine rich and the MIA complex binds to these cysteine-motifs. MIA facilitates oxidative folding of the precursor proteins by the transient formation of cysteine bonds (Figure 5-3). Oxidative protein folding is a common principle that is present in the periplasm of bacteria and in the endoplasmic reticulum. Mitochondrial matrix proteins classically contain a cleavable precursor sequence at their N-terminus. The presequence containing protein is imported to the intermembrane space by the TOM complex and directly targeted to the matrix by the TIM23 (presequence translocase of inner mitochondrial membrane) complex (Figure 5-4). In the matrix the presequence is cleaved by a matrix metalloprotease. Presequence cleavage and further amino terminal truncations by other matrix proteases increase the stability of the protein according to the N-end rule of stability[29,30]. Some presequence containing proteins are hydrophobic and therefore either laterally released from Tom23 to insert into the inner mitochondrial membrane (Figure 5-4a) or translocated to the matrix, processed and subsequently

inserted into the inner membrane by the OXA complex (Figure 5-4b). Alternatively, proteins are targeted to the inner mitochondrial membrane by less defined internal signal sequences. These so-called carrier-precursors are recognized by cytosolic chaperones that initiate import by the TOM complex to the intermembrane space. The carrier-precursor is then transferred by small TIM chaperones to the TIM22 (carrier translocase of inner mitochondrial membrane) complex that mediates inner membrane insertion (Figure 5-5). Recently, it was shown that the OXA complex[31] plays a role in the biogenesis of carrier preproteins[32] of the inner membrane by supporting folding and assembly into preassembled subcomplexes[33]. However, the character of cooperation of TIM22 and Oxal remain unclear[32].

In contrast to the different targeting possibilities for proteins translated by cytosolic ribosomes, the mtDNA-encoded proteins synthesized by the mitoribosomes seem to have limited possibilities. It is assumed that these hydrophobic polypeptides are co-translationally inserted into the inner mitochondrial membrane.

For membrane insertion in general a targeting sequence, a recognition molecule and an insertion receptor is required. The most famous mammalian membrane insertion system is the co-translational insertion of transmembrane proteins to the endoplasmic reticulum by the signal recognition particle (SRP), the SRP-receptor and the Sec-translocon (analog to Figure 7). The mammalian SRP is a protein complex consisting of the core protein SRP54 and five addional polypeptides that were named according to their molecular weight (SRP9, SRP14, SRP19, SRP68, SRP72). The scaffold of the particle is the ribosomal RNA 7SL-RNA, which has a length of 300 nucleotides. Yeast and primitive eukaryotes have SRPs that are built of different protein homologs and are smaller in size. Prokaryotes have very simple SRPs that consist of the core protein SRP54 and the 114 nucleotide 4.5S rRNA.

Higher plants contain a SRP in their chloroplasts that mediates the insertion of the light-harvesting complex subunits into the thylakoid membranes. While lower plants still contain SRP-rRNA together with the cpSRP54, higher plants lost their RNA component due to mutations of the RNA binding site but added a protein component resulting in the cpSRP54/cpSRP43 complex[34]. The lack of rRNA makes the chloroplast SRP unique among SRPs.

The SRP-RNA contains two structural folding motifs that fulfill specific function. The S-domain mediates the interaction of SRP with the ER-signal presequence of the nascent polypeptide chain and with the SRP-receptor, a transmembrane protein that

is localized to the endoplasmic reticulum. The ALU domain is responsible for the deceleration of translation after SRP binding to the nascent chain:ribosome complex. The interaction of SRP and SRP-receptor at the ER-membrane induces targeting of the nascent chain towards the translocon channel. Binding of SRP and SRP-receptor trigger GTP hydrolysis of both binding partners leading to the release of SRP from the ribosome and restart of the translation activity. The membrane insertion mechanism and the protein complexes involved in ER-membrane insertion evolved from the bacterial Type II secretory pathway system that transports proteins across the bacterial plasma membrane. To date no mitochondrial homolog of SRP is identified. It is assumed that the close proximity of the mitoribosome to the inner membrane and the OXA complex mediate the co-translational insertion process of mtDNA-encoded translation products. Structural studies showed that the mitoribosome lacks a portion of rRNA in the large subunit at the site of interaction with the mitochondrial inner membrane. The polypeptide-exit tunnel and a site named polypeptide-accessible site are located at this interface where the large mitochondrial ribosomal subunit and inner mitochondrial membrane get together. These sites are exposed to solvent and therefore are surrounded by mitochondria-specific MRPs. Recent models showed that these proteins must be involved in the interaction of mitoribosome and inner mitochondrial membrane. It is assumed that the large subunit of the mitoribosome is virtually embedded into the inner membrane. In this model the polypeptide-exit tunnel lies directly inside of the inner mitochondrial membrane. However, the nascent chain would still be accessible for regulatory proteins because the polypeptide-accessible site faces the matrix right above the membrane insertion site. Together with the inner membrane protein Mba1, Oxa1 aligns to the polypeptide-exit tunnel at the interface of ribosome and inner membrane. However, the exact composition of the OXA complex is unclear. The Oxa1 protein is a five-transmembrane containing protein that has a C-terminal extention in the matrix. This C-terminal helix interacts with the large subunit of the mitoribosome. Oligomerization of Oxa1 leads to the formation of a pore. Dimers are sufficient to insert polypeptides into the inner mitochondrial membrane. Based on the studies of the Oxa1 protein and its interaction partners a model for mitochondrial inner membrane insertion of mtDNA-encoded was developed[31,32,35-37] (Figure 5). Additionally to Oxa1 its homolog Cox18 plays a role in the OXA complex. Although the proteins are highly similar, they cannot compensate each

other, indicating that they cooperate with different essential functions. Oxa1 is the primary insertase for the co-translational insertion of the N-terminus of transmembrane proteins. The analysis of Cox18 point mutants revealed that Cox18 is responsible for the post-translational insertion of C-terminus into the membrane[35]. This cooperative and specific action of Oxa1 and Cox18 ensures correct topology of the transmembrane proteins. These findings were preceded by some general considerations about membrane protein topology.

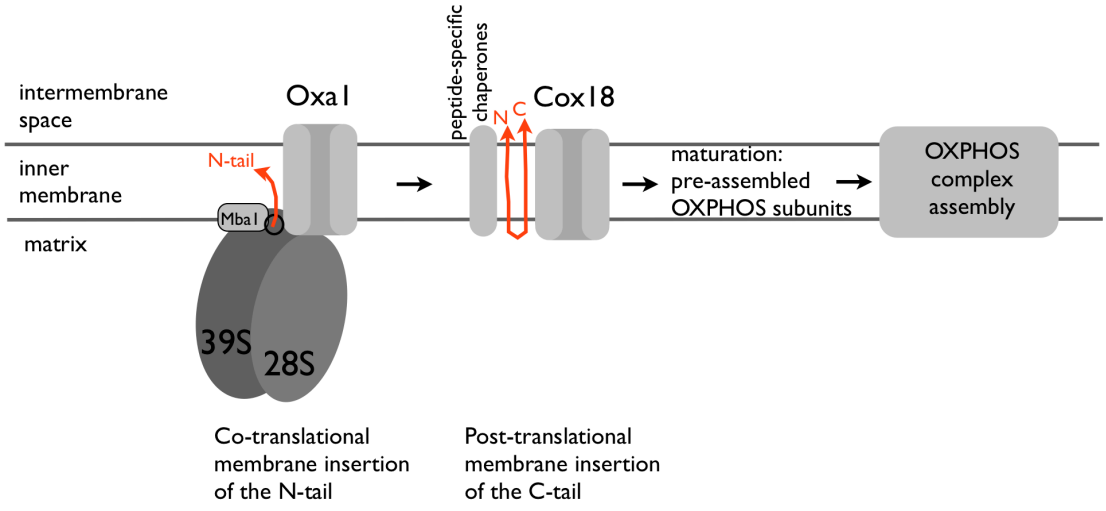

Figure 6 Model of protein insertion into the mitochondrial inner membrane by Oxa1 and Cox18 (from yeast). Peptide chain orientation is exemplary of COX2. [35,36,38]

Besides N-terminal or internal mitochondrial targeting signals (MTS), membrane proteins contain further signals that determine the orientation of the protein in the membrane. These topogenic signals are characterized by hydrophobicity of the transmembrane segment itself and by the charges of the flanking sites of the transmembrane segment. These charges define if a membrane segment is N-terminally or C-terminally inserted and follow the positive-inside rule[39] where negative charges at either terminus favor insertion while positive charged termini stay inside the matrix. Subunit 9 of the mitochondrial ATPase (ATP9) is nuclear encoded and contains a classical amino-terminal MTS and is imported into the mitochondrial matrix by TOM/TIM23. As described earlier, TIM23 can laterally release inner membrane proteins while they are imported. However, it was shown that the MTS of ATP9 is cleaved and there are other species like the yeast *S. cerevisiae* where ATP9 is encoded in the mitochondrial genome. Therefore, *S.*

cerevisiae ATP9 mutants were screened for a protein that is essential for the "export" of ATP9 from the matrix and its insertion into the inner membrane. The original ideas concerning membrane protein topology were proposed by nobel laureate Günter Blobel who reasoned that transmembrane proteins need so-called "stop-transfer" signals additionally to subcellular targeting signal and sorting sequences[37,40-43]. The actual concepts of membrane protein topology and their prediction are summarized in a comprehensive review[44].

Twenty years ago, the Oxa1 insertase was identified to be essential for correct insertion of ATP9 in yeast. The mechanism was conserved for mtDNA- and nuclear-encoded proteins. This new export system was named "conservative sorting model" since it implements the endosymbiont theory. The conservative sorting model mediated by OXA has intriguing similarities to the YidC sorting pathway in bacteria. YidC is the bacterial homolog of Oxa1 (Oxa1/Alb3/YidC family of proteins) and mediates SRP-dependent and independent insertion of transmembrane proteins into the plasma membrane of bacteria (Figure 7).

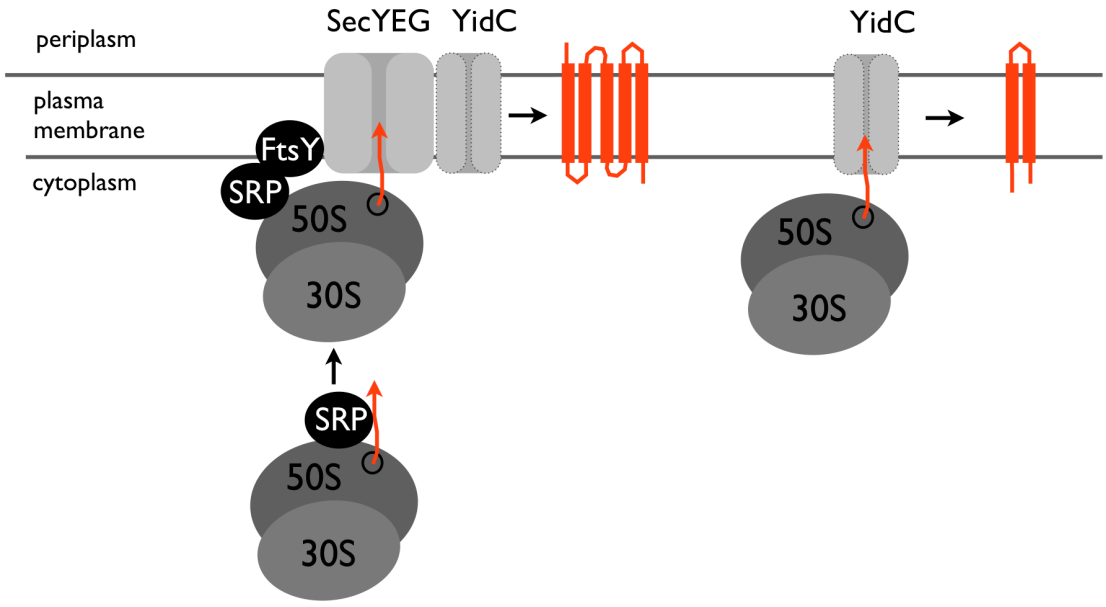

Figure 7 YidC mediated membrane protein insertion in bacteria. Sec-dependent protein insertion is not limited to the size of the substrate. Sec-independent membrane insertion by YidC is limited to small proteins with 1-2 transmembrane domains.

All substrates of YidC are integral membrane proteins of the bacterial plasma membrane and depend on YidC for insertion and folding. YidC can act independently and in association with the classical Sec-pathway components SecYEG, SRP and SRP-

receptor FtsY. The mechanism of SRP/SRP-receptor mediated co-translational protein insertion was detailed described earlier in this section. The essential protein YidC is available in higher amounts than the SEC translocon indicating that especially the autonomous function of YidC is highly relevant to the prokaryotic cell. Interestingly, the YidC insertion and folding capacity is limited to a maximum of two transmembrane helices per substrate. For larger substrates, YidC cooperates with the Sec machinery[45,46]. Although YidC depletion in *E.coli* is lethal, the insertion of Sec-dependent proteins is not affected in a ΔYidC background. Yeast Oxa1 and Cox18 can both carry out the Sec-independent functions of YidC in prokaryotes[47].

To date it is not known how mitochondrial Oxa1 and Cox18 manage the specific insertion of more than two transmembrane helix-containing proteins and how they recognize their substrates. Crosslinking studies identified heterodimers consisting of YidC and Oxa1 subunits that are stabilized by the large subunit of the mitoribosome and have similar physiochemical properties compared to the Sec-translocon[48]. This implies that YidC/Oxa1 dimers might complement for an inner membrane Sec-translocon in mitochondria although YidC/Oxa1 and Sec share no evolutionary relationship at all. It is tempting to hypothesize that transiently associated factors like Mba1 modulate the substrate specificity of the OXA complex. Besides, it is imaginable that components of the TIM complex are involved.

D. Mitochondrial protein degradation

The coexistence of protein synthesis and protein degradation guarantees cellular homeostasis. Mitochondrial protein turnover is in parts regulated by cytosolic events like mitophagy where parts of the mitochondrion are constricted and engulfed by autophago-lysosomal vesicles leading to the degradation of the content (mtDNA and proteins). Beside this coarse method to remove damaged material, mitochondria contain their own proteases for targeted protein degradation.

The mitochondrial matrix contains three major ATP-dependent proteases: ClpXP, Lon and m-AAA (Figure 8). All three proteases are ring-shaped complexes consisting of several subunits. Another similarity is the ATPase activity used to generate energy for peptide degradation.

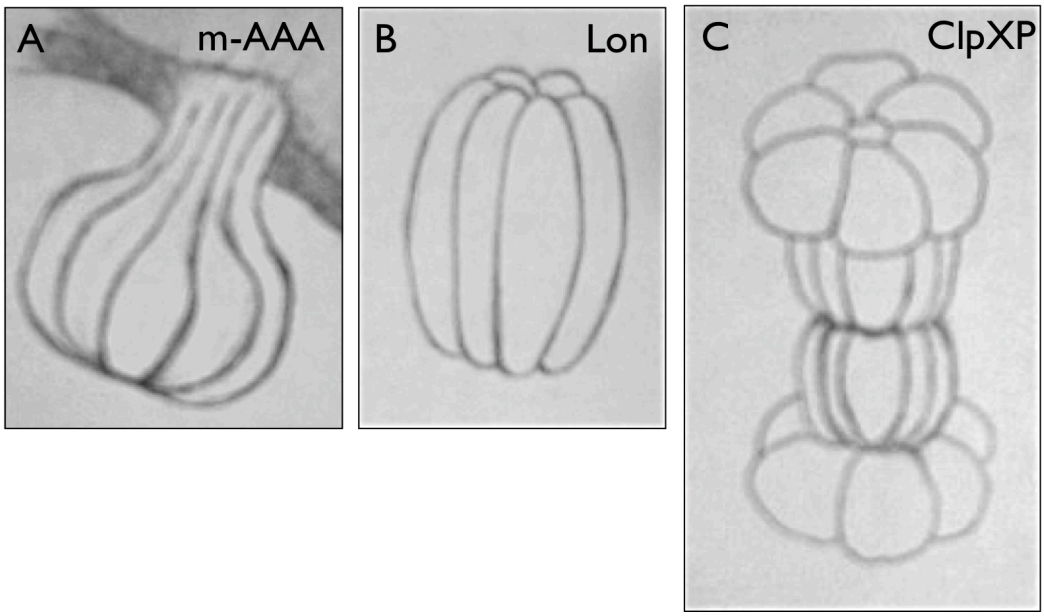

Figure 8 Schematic representation of the three major mitochondrial matrix proteases: ClpXP, Lon and m-AAA.

The m-AAA protease is an integral membrane protein that is anchored in the inner mitochondrial membrane facing the matrix (Figure 8A). m-AAA can either be built as homo-hexamer of AFG3L2 subunits or as hetero-hexamer consisting of AFG3L2 and paraplegin subunits. The two members of the inner membrane prohibitin complex PHB1 and PHB2 are substrates of m-AAA. In general m-AAA degrades inner membrane proteins that are part of the OXPHOS complex[49] and was shown to contribute to maturation of ribosomal proteins, e.g. MRPL23[50].

Lon protease (also named LonPl) and ClpXP are soluble matrix proteases. Lon is a homo-hexamer (Figure 8B). Each subunit has as well ATPase and proteolysis activity. The enzyme aconitase, the steroidogenic acute regulatory protein and the mitochondrial transcription factor Tfam are substrates of Lon protease. Since Lon protease degrades Tfam, a role in the maintenance and transcription of mtDNA was assigned to Lon. Furthermore, it was proposed that Lon could play a role in the turnover of other proteins that are involved in replication, transcription and translation of mtDNA[51].

Other than Lon and m-AAA, where every subunit has proteolysis and ATPase activity, the ClpXP protease consists of two multimeric subunits each of which carrying only one activity. The ATPase subunit is the hexamer ClpX that binds

substrates and adaptor proteins. The hydrolysis of ATP is needed for unfolding and translocation of the substrate. The protease subunit is the double-heptamer ClpP. Together, ClpX and ClpP form the ClpXP protease (Figure 8C). For binding of ClpX to ClpP ATP binding but not hydrolysis is required[52]. Notably, ClpX can also act autonomously as a disassembly chaperone when ClpP is absent. From studies with *E.coli* ClpXP it is known that substrate recognition can happen directly and indirectly via adapter molecule binding[52]. Proteomic studies revealed five classes of *E.coli* ClpXP recognition motifs[53]. In most cases tested, the tagging of proteins with one of the identified motifs lead to rapid degradation by ClpXP *in vitro*. The list of substrates includes transcription factors, metabolic enzymes and proteins that are involved in the response to starvation and oxidative stress[54,55]. However, to date there are no known endogenous mammalian substrates identified for ClpXP.

E. NOA1 - a ribosome assembly factor?

There are many mitochondrial proteins of unknown function. Some of these proteins are assigned to specific mitochondrial processes, like mitochondrial protein synthesis, since loss of function studies in yeast or plants revealed that they are essential for this specific event.

Based on such deletion studies in *Arabidopsis thaliana* the NOA1 protein was identified ten years ago. The knockout of NOA1 caused severe growth defects[56]. Primary studies linked NOAI with nitric oxide signaling and named the protein thereafter AtNOS1 (*Arabidopsis thaliana* Nitric Oxide Synthase I). Some years later, the protein was renamed NOA1 (Nitric Oxide Associated 1) because it was shown to be a GTPase rather than a nitric oxide synthase[3,57]. Today, the molecular function of NOA1 is investigated in bacteria, plants and mammalian cells. This work focuses on mammalian NOA1 hence the biology of plant NOA1 is not addressed any further. Due to the high degree of evolutionary conservation, studies of the bacterial homolog YqeH are described herein since they enlightened main features of the mammalian NOA1 protein. YqeH is a member of the Era/Obg family of GTPases[2]. Structural studies revealed that YeqH is a G-protein, which couples enzymatic GTPase activity with nucleic acid and/or protein recognition[57]. The GTPase domain is necessary for the function of YqeH. However, GTPase activity alone is not sufficient to complement for the loss of YqeH in knockout studies. It was shown that the C-terminal domain of YqeH contains a TRAP-like RNA binding domain, which is

essential for the function of YqeH[3]. In bacteria a variety of small GTPases were characterized based on their GTPase domain and the additional functional domains. YqeH belongs to the family of circularly permuted GTPases (cpGTPases) and it was early recognized that knockout or mutation of this family of GTPases results in defects in ribosomal function[38]. Further studies revealed that YqeH is involved in bacterial ribosome assembly and the stability of the small ribosomal subunit[2,9]. Since YqeH contains a RNA binding domain it was tested if YqeH was a RNA chaperone. Indeed, it was demonstrated that YqeH has rather unspecific affinity for RNA and that ribosomal particles/proteins stimulate the GTPase activity and the RNA binding activity of YqeH[5,6,8]. Like for other GTPases involved in the biogenesis of ribosomes, the YqeH cpGTPase activity is stimulated by potassium ions, which is a unique feature among Ras-like GTPases[1,8].

Mammalian NOA1 was investigated *in vivo* and *in vitro*. Unlike plants, mammalian cells cannot survive without their mitochondrial NOA1. As it was shown for YqeH bacterial ribosomal constituents stimulate the GTP hydrolysis rate of NOA1[5]. NOA1 co-sediments with the mitoribosomal small subunit 28S in sucrose gradients[7] and GTPase hydrolysis leads to release of NOA1 from ribosomes[7]. Loss of NOA1 is accompanied by severe OXPHOS defects. The detailed analysis of OXPHOS complexes revealed that the loss of NOA1 in knockdown cells is directly linked to a loss of supercomplexes/respirasomes[4]. Overexpression of NOA1 leads to an increase in respiration including ATP production, an effect that is dependent on the GTPase function of NOA1[4]. This was confirmed by work of others showing increased oxygen consumption in cells overexpressing NOA1[58]. Furthermore, the affinity of NOA1 for RNA/DNA was confirmed in the mammalian system[7]. Very recently, the NOA1 *S. cerevisiae* homolog MTG3 was investigated for its function during ribosome assembly in yeast mitochondria. As a result, MTG3 participates in the assembly of the small mitoribosomal subunit and affects the processing of an essential mitoribosomal RNA. This indicates that yeast NOA1 plays a role in the assembly of the small mitoribosomal subunit presumably as RNA chaperone[59]. However, the exact function and underlying mechanism of the NOA1 protein during mitochondrial protein synthesis is not yet clarified.

The NOA1 protein is a strong candidate for an essential regulator of mitochondrial function. Altered NOA1 protein levels have severe effects on mitoribosomal stability, protein synthesis and OXPHOS function. The presence of NOA1 is critical

for the cell. The analyses of NOA1's function were mainly performed by loss or gain of function experiments. The contribution of the GTPase domain was examined and found to be prerequisite for the proper function of NOAI. Although there are several hypotheses about the nature of NOA1, e.g. ribosome assembly factor or rRNA chaperone, the role of NOA1 in mitochondrial translation was not yet identified.

Here a cell biological and biochemical approach was chosen to analyze single domains and motifs of NOA1 and their functional relations. Previous studies suggested that NOA1 could be targeted to the nucleus, because it carries a nuclear localization signal[5]. Nevertheless, there are no data about this alternative subcellular localization. One aim of this study was the characterization of the nuclear localization and putative nucleo-mitochondrial dynamics of the NOA1. Furthermore, it was central to identify whether the two localizations are functionally linked. Moreover, the biochemical approach with recombinant produced NOAI is expected to shed light on the RNA-binding characteristics of NOA1 including the investigation if RNA-binding and GTPase functions are connected to each other. Since NOA1 was shown to be a relatively short-lived protein, the identification of the degradation pathway was a further aim of this work. Altogether, the project was supposed to provide a more comprehensive model for the mechanism of NOA1's mitochondrial activities that are closely associated to the area of mitochondrial translation.

V. Aim of the Study

The NOA1 protein is a regulator of mitochondrial function. Here, a cell biological and biochemical approach was chosen to acquire a comprehensive model for the underlying mechanism and the regulation of NOA1's cellular activities.

The main goals are outlined in brief:

- Characterization of the nuclear localization of NOA1 and identification whether mitochondrial and nuclear localization are functionally linked.
- Description of the RNA-binding features of NOA1 and study if the RNA-binding activity and the GTPase function are connected.
- Identification of the degradation pathway of NOA1.

VI. Results

A. *NOA1 is a conserved multi-domain protein.*

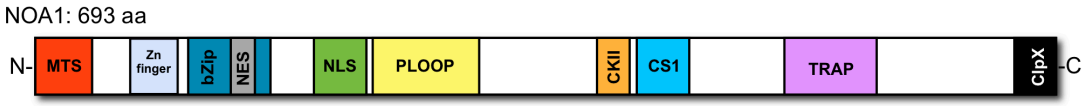

Figure 9 Schematic representations of domains and motifs of the mammalian NOA1 protein.

Mouse NOA1 is a ~77 kDa protein consisting of 693 amino acids. The predicted domains and motifs of NOA1 are depicted in Figure 9 and their putative functions are summarized in Table 2.

Table 2 Overview of the domains and motifs of NOA1 and their putative function

	Name	Function	Motif
MTS	Mitochondrial Targeting Signal	Import to the mitochondrial matrix; the MTS is cleaved by MMP after import	Residues 1-17
bZip	basic Leucine zipper domain	Dimerization domain	$(Lxxxxxx L)_6$
Zn finger	treble clef zinc finger	DNA binding fold with a metal-binding site to coordinates zinc ions	$CxxCn_{34}CxxC$
NES	(putative) Nuclear Export Signal	Nuclear export via Crm1	$Lx_{2-3}Lx_{2-3}LxL$
NLS	Nuclear Localization Signal	Nuclear import via the Importin α/β complex	LKRLRKRL
PLOOP	circularly permutted GTPase domain	GTP binding and hydrolysis	GTTNAGKS
CKII	Casein kinase II phosphorylation site	Phosphorylation by CKII at Serine 421 (could be related to nuclear export)	S_{421}
CS1	Caspase-1 cleavage site	Conserved recognition site for Caspase-1 mediated cleavage	F*DADS
TRAP	RNA-binding domain	RNA-binding site with conserved Arg/Asn/Trp triad	
ClpX	(putative) ClpX recognition motif	Putative recognition site for ClpX recognition and degradation by ClpXP	

The N-terminal mitochondrial targeting presequence (MTS) of NOA1 is typical for mitochondrial matrix proteins[60]. The zinc finger domain (Zn finger) is a Zn^{2+} ion coordinated nucleotide binding domain, which is likely to be involved in RNA/DNA interactions[57]. The leucine zipper predicted by ProSite[61] is a dimerization domain allowing NOA1 to form dimers[4]. Within the leucine zipper domain a potential nuclear export signal was identified. The bipartite nuclear localization signal (NLS)[62] targets proteins to the nucleus[63]. NOA1 contains a circularly permuted GTPase

domain (ProSite[61]), which means that the subdomains are alternatively arranged[3]. These cGTPases are abundant in RNA-binding proteins[2]. Such a conserved RNA-binding domain is found in the C-terminus (TRAP)[57]. Since NOA1 was correlated with cell death events[58], the online tool PeptideCutter at the ExPASy webserver was used to analyze the NOA1 protein sequence for enzymatic recognition sites. Beside a number of random enzymatic cleavage sites, there is exactly one potential caspase recognition site at amino acid 461 that is specific for caspase-1. In close proximity to this caspase-1 cleavage site a serine-specific phosphorylation site for Casein Kinase II (CKII) was predicted[61]. CKII is regulating nucleo-cytoplasmic shuttling events and modulates caspase-pathways of apoptosis[64]. The C-terminus contains putative recognition elements for the mitochondrial ClpXP protease. These motifs were identified by comparison of the NOA1 amino acid sequence to the five known classes of ClpXP sites. The C-terminus of NOA1 contains three double lysine-containing motifs that align to the described C-motif2[53].

The NOA1 protein is highly conserved throughout evolution, which is due to the fact that the RNA-binding domain and the cGTPase domain are conserved in all species. Table 3 summarizes the percentage of identities of NOA1 proteins from fifteen species in comparison to murine NOA1. The percentage of identity describes the degree of correspondence and indicates the similarity of two protein orthologues. As a rule of thumb it is accepted that an identity of > 25% indicates a similarity of structure and function whereas a minor identity of 18% - 25% implies a similarity of either structure or function[65]. The identity often underestimates the functional similarity because amino acid changes occur during evolution, which lowers the degree of identity while the function of the conserved domain can still be the same.

Overall, NOA1 is a highly conserved protein and its function is relevant to bacteria, yeast, plants and all eukaryotes.

Species	Symbol	% Identity	Peptide length	Protein ID
Eukaryotes				
Vertebrates				
Placental Mammals[1]				
Mus musculus (Mouse) - reference species	NOA1/mNOA1	100 %	693 aa	NP_062810.1
Rattus norvegicus (Rat)	NOA1/RGD1359460	92 % (~95% similarity)	694 aa	NP_001006960.1
Homo sapiens (Human)	NOA1/C4orf14/hNOA1	75 % (~84% similarity)	698 aa	NP_115689.1
Pan troglodytes (Chimpanzee)	LOC735814	75 %	698 aa	XP_001136575.2
Macaca mulatta (Rhesus macaque)	C4orf14/NOA1	75 %	698 aa	XP_001082521.1
Canis lupus (Dog)	NOA1	70 %	700 aa	XP_854207.1
Bos taurus (Cattle)	NOA1/BOS_6681	72 %	694 aa	NP_001033277.1
Sus scrofa (Pig)	LOC100621115	71 %	702 aa	XP_003356996.1
Sauropsida[2]				
Gallus gallus (Chicken)	NOA1	49 %	596 aa	XP_420579.3
Fish[3]				
Danio rerio (Zebrafish)	noa1	44 % (~64% similarity)	702 aa	NP_001107900.1
Invertebrates				
Drosophila melanogaster (Fruitfly)	CG10914	33 %	624 aa	NP_611297.3
Caenorhabditis elegans (Roundworm)	Y48E1B.2	23 %	890 aa	NP_496845.1
Prokaryotes				
Bacillus subtilis	YqeH	34 %	366 aa	NP_390445.1
Yeast				
Saccharomyces cerevisiae (Bakers yeast)	GEP3/Gep3p	9 %	556 aa	NP_014848.1
Plants				
Monocotyledones				
Oryza sative (Rice)	OsNOA1/RIF1	33 %	547 aa	NP_001045614.1
Dicotyledones				
Arabidopsis thaliana (Thale cress)	NOA1/AtNOA1	32 %	8561 aa	NP_850666.1

[1] Humans and other primates; Rodents, rabbits and related species; Carnivores, hoofed animals and insectivores
[2] Birds and reptiles
[3] Ray-finned fish

B. NOA1 is localized in mitochondria and in the nucleus.

It was shown before that NOA1 is a mitochondrial matrix protein[4]. To address the targeting capacity of the nuclear localization signal, cells were transfected with Flag-tagged full length NOA1 and a truncation mutant lacking the amino acids 1-17, which contain the MTS. Anti-Flag staining showed that NOA1 colocalizes with the mitochondrial marker protein Tom20. Truncation of the MTS resulted in cytosolic and nuclear localization with the tendency of nuclear accumulation (Figure 10A). A staining of the same cells with a polyclonal NOA1 antibody showed the endogenous and the overexpressed protein simultaneously. The endogenous protein was localized in both compartments, the nucleus and the mitochondria (Figure 10A), showing that NOA1-Flag and NOA1ΔMTS-Flag intensify either of the endogenous localizations. Western blot analysis of lysates of these transfected cells showed the expected mitochondrial presequence processing with the full length NOA1-Flag. The endogenous MTS was slightly larger than the predicted number of amino acids, that

was removed in the NOAIΔMTS-Flag mutant. However, a single band for truncated NOAIΔMTS-Flag was detected indicating that the removal of the first seventeen N-terminal amino acids was sufficient to destroy the MTS (Figure 10B). Expression of NOA1ΔMTS is lethal and induced cell death in the transfected cells.

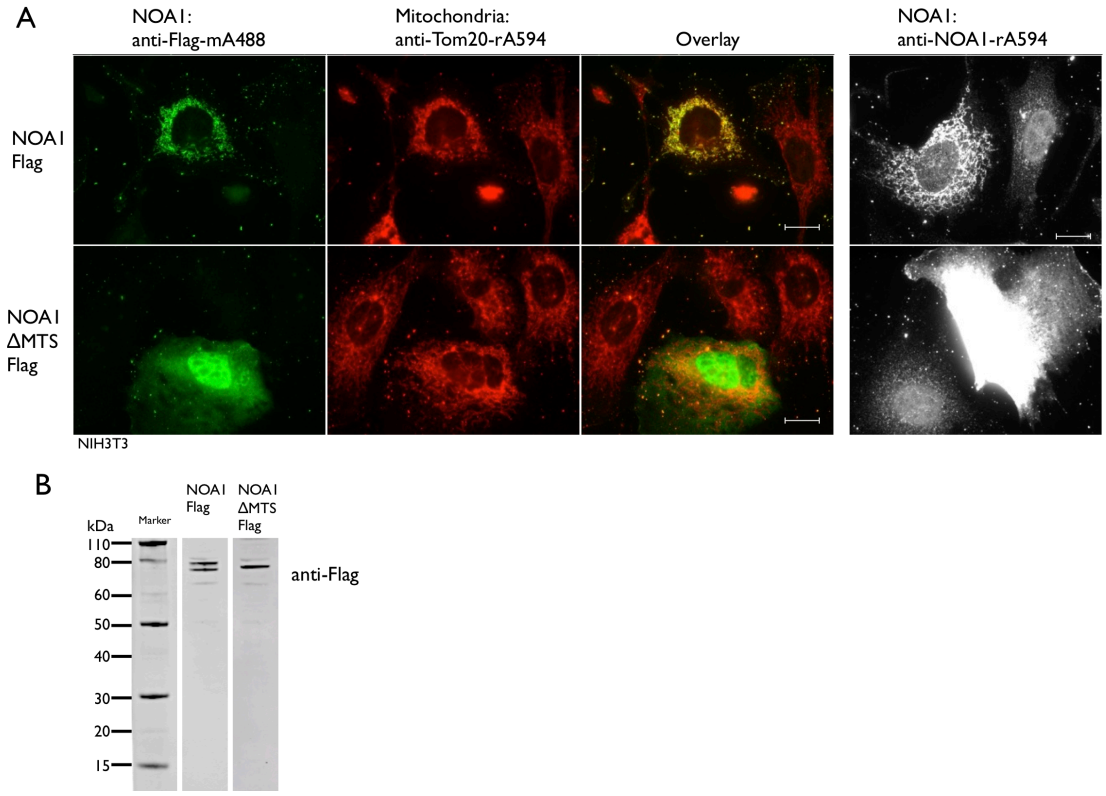

Figure 10 Localization of NOA1 and mitochondrial presequence processing. A) NOA1-Flag is colocalizing with Tom20 in mitochondria. Truncation of the mitochondrial targeting sequence leads to cellular distribution and nuclear accumulation of NOA1ΔMTS-Flag. Stainings with anti-NOA1 antibody shows overexpressed and endogenous protein (celltype: NIH3T3 fibroblasts; scale bar 10 µm). B) Presequence cleavage of mitochondrial NOA1-Flag is illustrated by Western Blot. The truncated NOA1ΔMTS-Flag protein is not processed.

C. The NOA1mRNA is ubiquitously expressed as a single transcript

Is a protein found in more than one subcellular localizion, the question arises if there are alternative transcripts or splice variants. One isoform could be mitochondrial while the other one could be targeted to the nucleus. To exclude the existence of such isoforms the NOA1 transcript was analyzed in detail.

NOA1 was ubiquitous and expressed in all mouse tissue as shown by a qualitative PCR using primers that amplified exon 1 of the NOA1 mRNA (Figure 11A). The

annotated transcript of NOA1 (NM_019836) has seven exons. Exon 1 is the largest exon coding for approximately 50% of the protein. At the time of the analysis, two annotations were available that predicted a second start codon that would lead to transcription of a shorter protein lacking the mitochondrial targeting sequence. The second unsteadiness was an annotation indicating the existence of a frame shift intron within exon 1. The intron was annotated with two bases and the consequence would have been a premature stop of translation leading to a shorter protein.

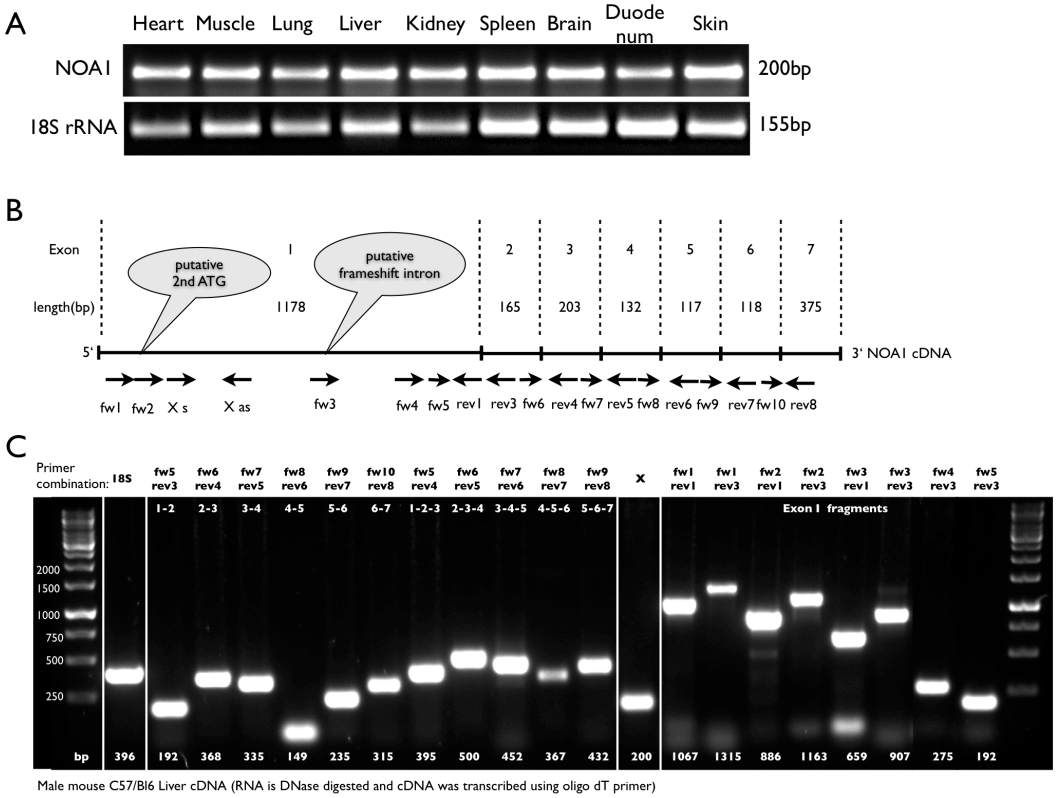

Figure 11 Analysis of the NOA1 transcript. A) Ubiquitous expression of NOA1 mRNA in different mouse tissues. B) Exon structure of the NOA1 cDNA and position of the primers for PCR analysis. C) PCR analysis of the NOA1 transcript investigating the integrity of Exon-Exon junctions and possible exon skipping.

Figure 11B depicts the exon structure and the position of primers. Figure 11C shows the result of the PCR with combinations of primer pairs. RNA was isolated from mouse liver and reverse transcribed with oligo-dT primers to amplify whole cell messenger RNA. The amplification of the six exon-exon-junctions resulted in single PCR products with the expected size. The amplification of larger fragments comprising exon-intron-exon, demonstrates that there is no evidence for exon

skipping. The analysis of exon 1 resulted in single, distinct bands clearly showing that there is a single specific NOA1 transcript.

In conclusion, there was no evidence for an alternative NOA1 transcript or a splice variant. The following experiments were performed on the basis that NOA1 is a unique protein with different functional domains and signaling peptides (Figure 9).

D. Nuclear accumulation of NOA1 leads to apoptosis that is rescued by truncation of the C-terminus

The expression of the NOA1 truncation constructs was tested in C2C12 myoblasts. Protein lysates were analyzed 24 hours after transfection by Western blot and the subcellular localization was visualized by antibody staining for the Flag-tag (Figure 12). NOA1 full length showed the typical double band of the precursor and mature mitochondrial protein. NOA1ΔMTS was detected in a faint band because as soon as expression started the transfected cells were undergoing cell death. N-terminal and/or C-terminal truncations resulted in strong expression. The NOA1ΔMTSΔC-terminus was not imported into mitochondria and showed a single band. NOA1ΔC-terminus was processed but to a smaller degree than the full-length (Figure 12A). The expression of the C-terminus of NOA1 alone does not result in a stable expression. To stabilize the protein it was linked to YFP-T2A using the intrinsic T2A self-cleaving activity[66] to create from a single chain precursor a free YFP and NOA1 C-terminus. With this construct a free C-terminus was detected (Figure 12B). To visualize the subcellular localization, cells were transfected with the constructs (Figure 12C). As expected, full-length NOA1 showed a mitochondrial pattern and NOA1ΔMTS showed a cytosolic distribution with nuclear accumulation. The lack of the C-terminus in the NOA1ΔCterminus variant interfered with mitochondrial import. This is comparable to the reduced processing of NOA1ΔC-terminus in the Western blot (Figure 12A). NOA1 lacking the MTS and the C-terminus showed cytosolic distribution and nuclear accumulation. In contrast to NOA1ΔMTS where the majority of cells were round shaped and apoptotic the expression of NOA1ΔMTSΔC-terminus had no lethal effects.

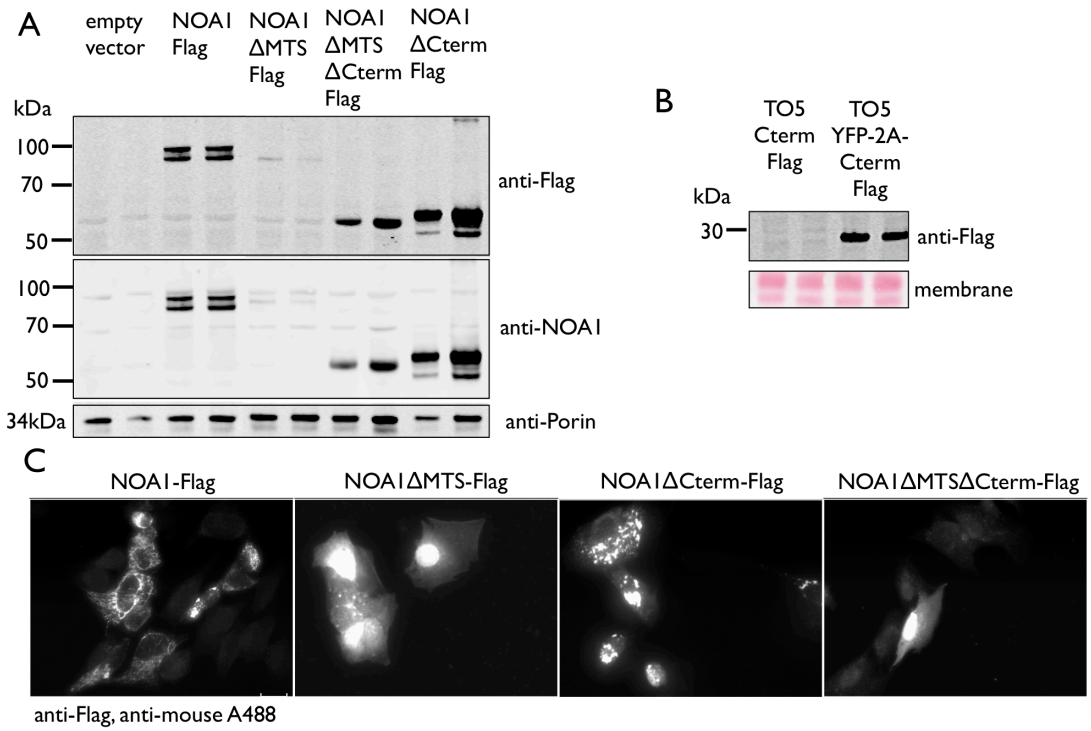

Figure 12 A) Expression test of truncation variants of NOA1 in C2C12 cells. 24 h after transfection protein lysates were analyzed by western blot. B) Expression of the C-terminus alone failed and a stabilization construct was generated by fusion of NOA1-C-terminus to YFP spaced by the self-cleaving T2A peptide. C) Localization of truncation variants. Full-length NOA1 shows mitochondrial distribution. Without MTS both proteins - NOA1ΔMTS and NOA1ΔMTSΔC-terminus - localize in the cytosol with nuclear accumulation. The NOA1ΔC-terminus is not properly localized to the mitochondria

To analyze the cell death induced by overexpression of NOA1ΔMTS cells were analyzed by FACS. The measurements were done 12 hours after transfection since protein expression started already ~6 hours after transfection and the transfected cells already started to die at this early time-point. Cells were stained with a combination of Annexin V-FITC and propidiumiodide. Figure 13A shows the increase in apoptosis upon NOA1ΔMTS transfection. The apoptosis was rescued by addition of 1 µM pan-Caspase-inhibitor Z-vad-fmk, showing that NOA1ΔMTS induced classical cell death. In general, rather low transfection efficiency was obtained in these experiments therefore the 15% dead cells reflect roughly the percentage of transfected cells.

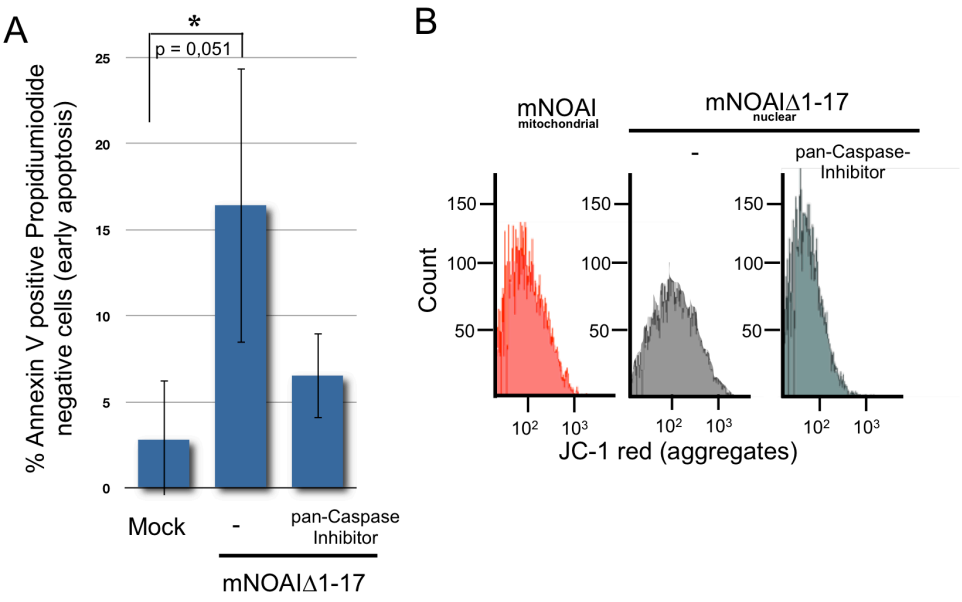

Figure 13 FACS analysis of NOA1ΔMTS induced cell death. A) FACS analysis of apoptosis in C2C12 cells. Cells transfected with NOA1ΔMTS were Annexin V-FITC positive and propidiumiodide negative. This was rescued by pan-caspase-inhibitor. B) Assessment of mitochondrial membrane potential by JC-1 labeling. The x-axis shows the intensity of red JC1-aggregates and the y-axis shows the number of cells. The number of JC-1 red aggregates is lower in NOA1ΔMTS transfected cells indicating the collapse of the mitochondrial membrane potential.

During apoptosis the mitochondrial membrane potential collapses in response to intrinsic queues. This can be measured by JC-1, a dye that is widely used for studying apoptosis. The dye is membrane permeable and exists in two forms. The monomer has a fluorescence emission in the green (~529 nm) whereas the red J-aggregates have red emission (~590 nm). The red J-aggregates form as a consequence of accumulation, e.g. in mitochondria. JC-1 cannot enter depolarized mitochondria. Thus, the more mitochondria become depolarized, the less J-aggregates can form. Figure 13B shows less J-aggregates in NOA1ΔMTS transfected cells showing the mitochondrial depolarization. The addition of pan-caspase-inhibitor rescued the membrane potential. Full length NOA1 did not alter the membrane potential in comparison to untransfected control cells.

In contrast to NOA1ΔMTS, NOA1ΔMTSΔC-terminus lacking the RNA-binding domain did not induce apoptosis in cell culture. During apoptosis mitochondria undergo morphological changes that are characterized by fission and peri-nuclear accumulation followed by the rounding of the whole cell. Figure 14 shows the effects

of overexpression of NOA1ΔMTS and NOA1ΔMTSΔC-terminus on mitochondrial morphology and the effect of NOA1C-terminus alone on cellular shape. NOA1ΔMTS was co-transfected with OMP25-EGFP, the membrane fragment of the outer mitochondrial protein OMP25 fused to EGFP. OMP25EGFP is an accepted marker of mitochondria[67,68]. In contrast to the apoptotic phenotype of aggregated mitochondria after transfection with NOA1ΔMTS (Figure 14A), a transfection with NOA1ΔMTSΔC-terminus did not change the mitochondrial morphology (Figure 14B). To visualize effect of the C-terminus alone the YFP-T2A-C-terminus fusion construct was used. Figure 14C shows the expression of NOA1-C-terminus by Flag-tag staining. The YFP signal demonstrates the transfection efficiency. The T2A peptide ensured a stoichiometric degree of YFP and NOA1-C-terminus. However cells with high fluorescence signal for Flag-tagged NOA1-C-terminus were round-shaped and underwent cell death whereas other cells that did not have high amounts of NOA1-C-terminus were flat and healthy.

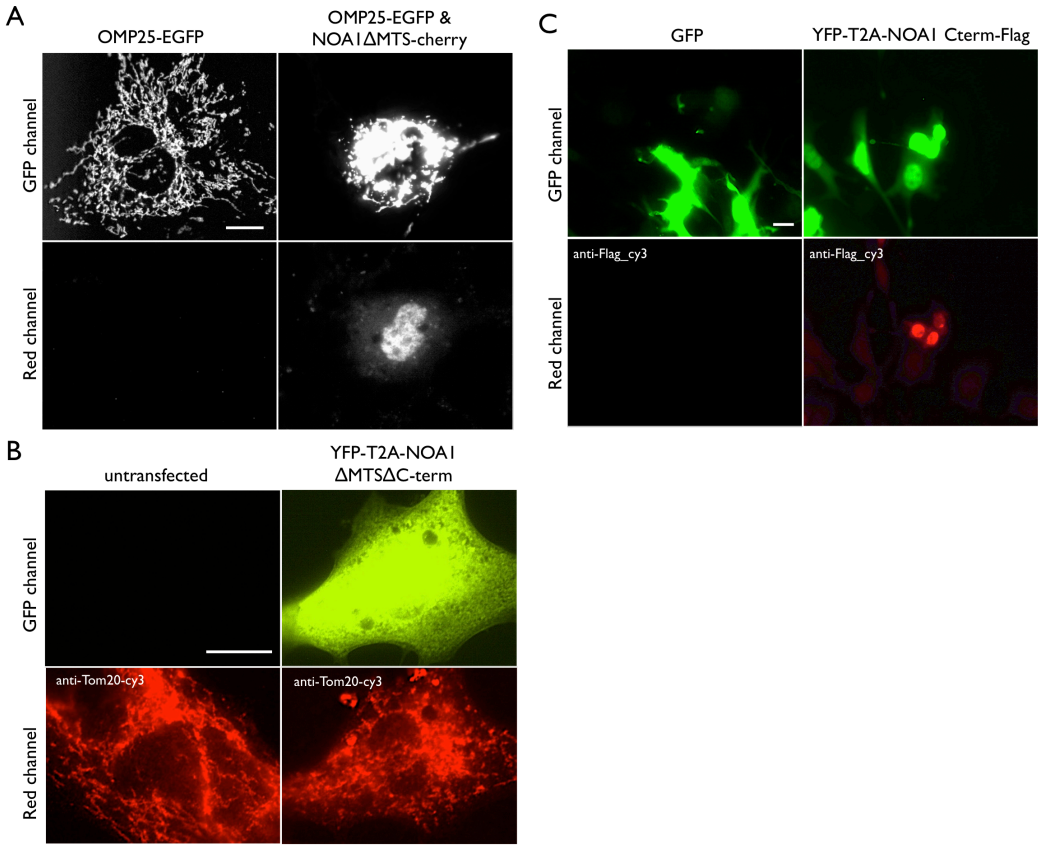

Figure 14 A) Lethality of nuclear NOA1 depends on the C-terminal domain. Expression of NOA1ΔMTS leads to mitochondrial morphology changes (visualized by OMP25-EGFP in

NIH3T3 cells) and subsequent cell death of the transfected cell. B) Expression of NOA1ΔMTSΔC-terminus rescued the cell death phenotype and confirms the functional importance of C-terminal RNA-binding TRAP-like domain. C) Expression of YFPT2A stabilized C-terminal fragment of NOA1 induced cell death.

In summary, NOA1 was imported into mitochondria and N-terminally processed. Truncation of the mitochondrial targeting presequence generated a cell death-inducing variant. This cell death was caspase-dependent and characterized by the loss of the mitochondrial membrane potential. The additional truncation of the C-terminus of NOA1 (NOA1ΔMTSΔC-terminus) rescued the apoptosis phenotype induced by truncation of the MTS alone. The expression of the NOA1C-terminus alone induced cell death dependent on the amount of protein expressed. This leads to the assumption that the C-terminus of NOA1 is responsible for the lethality of the NOA1 when a certain degree of accumulation is reached in a nuclear environment

E. Treatment of cells with pharamcological nuclear export inhibitors retain NOA1 in the nucleus

The endogenous NOA1 is predominantly localized to mitochondria. However the protein has a nuclear localization signal in the amino acid sequence. Furthermore, antibody stainings repetitively detected a small portion of the NOA1 protein in the nucleus. Therefore we analysed potential subcellular dynamics by appliying a variety of pharmacological substances.

The LOPAC^{1280} panel (Sigma Aldrich) was used to screen for factors that trigger nuclear localization of NOA1. LOPAC^{1280} is a library of pharmacological active chemical compounds. A transgenic C2C12 cell line was established that stably expressed a NOA1-EGFP fusion protein. Anti-GFP antibody staining showed the specificity of the NOA1-EGFP fluorescence (Figure 15A). Staining for endogenous NOA1 and counterstaining with mitotracker dye showed predominant mitochondrial localization of NOA1 in untreated cells (Figure 15B).

NOA1-EGFP expressing cells were seeded into 16-well LabTek chamber slides and treated either with a compound from the LOPAC^{1280} panel of compounds or diluent (DMSO). The result of the screen is summarized in Table 4. The primary screen for compounds was evaluated by nuclear fluorescence of NOA1-EGFP six hours after treatment with 100 µM concentrated substance.

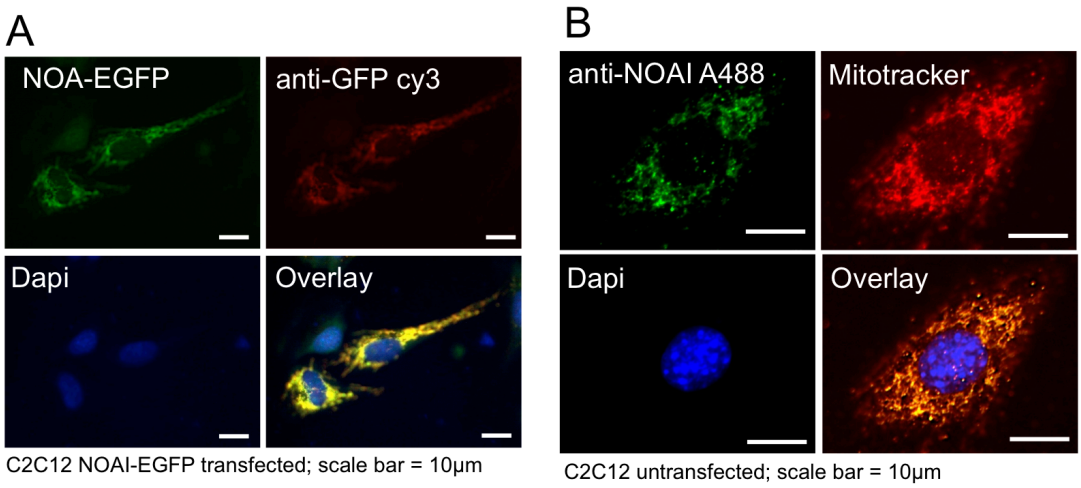

Figure 15 Establishment of a polyclonal cell line stably expressing NOA1-EGFP A) Cells are positive for NOA1-EGFP shown by counterstaining with anti-GFP antibody. B) Endogenous NOA1 is detected with anti-NOA1 antibody and colocalizes with the mitochochondrial costaining by Mitotracker Red 580.

Overall, nuclear accumulation was a heterogeneous process. In the primary screen, 3.2% (41/1280) of the compounds induced nuclear accumulation to a substantial degree. Substances that showed severe toxic effects on the cells were excluded. About 30.08% (385/1280) of the compounds were lethal at 100 µM concentration. One control for 1% DMSO and water were performed for every 15 substances. Nuclear accumulation of NOA1-EGFP was not affected by 1% DMSO. All 41 positive substances were retested and 17 (1.33% of total) substances full-filled the criteria of NOA1-EGFP accumulation in the nucleus in more than 10% of the cells. The highest accumulation rate showed four substances: trequinsine, quazinone, flunarizine and amiloride. These substances were used for further experiments. In summary, 0.31% (4/1280) of all compounds tested induced nuclear accumulation of NOA1-EGFP in C2C12 cells.

We further explored the effects of trequinsine, quazinone and flunarizine in additional experiments. The effect on nuclear accumulation of NOA1-EGFP was unequivocal at a concentration of 5 µM. The substances appeared to be non-toxic at the used concentrations and timeline.

Table 4 LOPAC pharmacological compounds that triggered nuclear accumulation of NOA1-EGFP (primary and secondary screen results)

Compound Names (1.33% hits of 1280 substances)	Class	Action	Selectivity	Description	Screen 1#	Screen 2##
5-(N,N-Dimethyl)amiloride hydrochloride	Ion Pump	Blocker	Na+/H+ Antiporter	Selective blocker of Na+/H+ Antiporter	+	+
Flunarizine dihydrochloride	Ion Pump	Blocker	Na+/Ca2+ channel	Na+/Ca2+ channel blocker, vasodilator	+	+
Quazinone	Cyclic Nucleotides	Inhibitor	PDEIII	Phosphodiesterase III (PDEIII) inhibitor	+	+
Trequinsin hydrochloride	Cyclic Nucleotides	Inhibitor	PDEIII	Phosphodiesterase III (PDEIII) inhibitor	+	+
9-Amino-1,2,3,4-tetrahydroacridine hydrochloride	Cholinergic	Inhibitor	Cholinesterase	Cholinesterase inhibitor	+	-
(±)-2-Amino-4-phosphonobutyric acid	Glutamate	Antagonist	NMDA	NMDA glutamate receptor antagonist	+	-
PK 11195	GABA	Antagonist	Benzodiazepine	Peripheral Benzodiazepine receptor antagonis	+	-
Chelerythrine chloride	Phophorylation	Inhibitor	PKC	PKC inhibitor; affects translocation of PKC from cytosol to plasma membrane	+	-
Cyclosporin A	Phophorylation	Inhibitor	Calcineurin phosphatase	Calcineurin phosphatase inhibitor; immunosuppressant	+	-
Farnesylthiosalicylic acid	G-protein	Antagonist	Ras	Non-toxic Ras inhibitor	+	-
Ethosuximide	Anticonvulsant			inhibits voltage-gated sodium channels	+	-
4-Amino-1,8-naphthalimide	Apoptosis	Inhibitor	PARP	Poly(ADP-ribose) polymerase (PARP) inhibitor	+	-
Calmidazolium chloride	Intracellular Calcium	Inhibitor	Ca2+ ATPase	Potent inhibitor of calmodulin activation of phosphodiesterase; strongly	+	-
GW2974	Phophorylation	Inhibitor	EGFR/ErbB-2	Dual EGFR and ErB-2 receptor tyrosine kinase inhibitor	+	-
GW5074	Phophorylation	Inhibitor	Raf1 kinase	cRaf1 kinase inhibitor	+	-
SQ 22536	Cyclic Nucleotides	Inhibitor	Adenylyl cyclase	Adenyly cyclase inhibitor	+	-
U0126	Phophorylation	Inhibitor	MEK1/MEK2	Specific inhibitor of MEK1 and MEK2 (MAPKK)	+	-

Treatment of NOA1-EGFP overexpressing C2C12 cells
Treatment of C2C12 cells and staining for endogenous NOA1

Figure 16A shows the nuclear accumulation of NOA1-EGFP after treatment with trequinsin, quazinone and flunarizine. By crude subcellular fractionation a slight increase in nuclear localized NOA1-EGFP was detected after treatment with trequinsin (Figure 16B). The pharmacological target of trequinsin and quazione is phosphodiesterase 3. Amiloride is a selective ion pump inhibitor and flunarizine is a sodium/calcium channel blocker. The common ground of these inhibitors is that they affect cellular calcium levels. It is known that the elevation of intracellular calcium prevents nuclear shuttling whereas calcium chelators enhance nuclear translocation[69].

As validation for the first LOPAC^{1280} screen the 41 primary positive substances were also applied on wild type cells that were stained for NOA1. Figure 16C shows either nuclear accumulation of overexpressed protein or a speckled, nucleolar-like localization of endogenous NOA1.

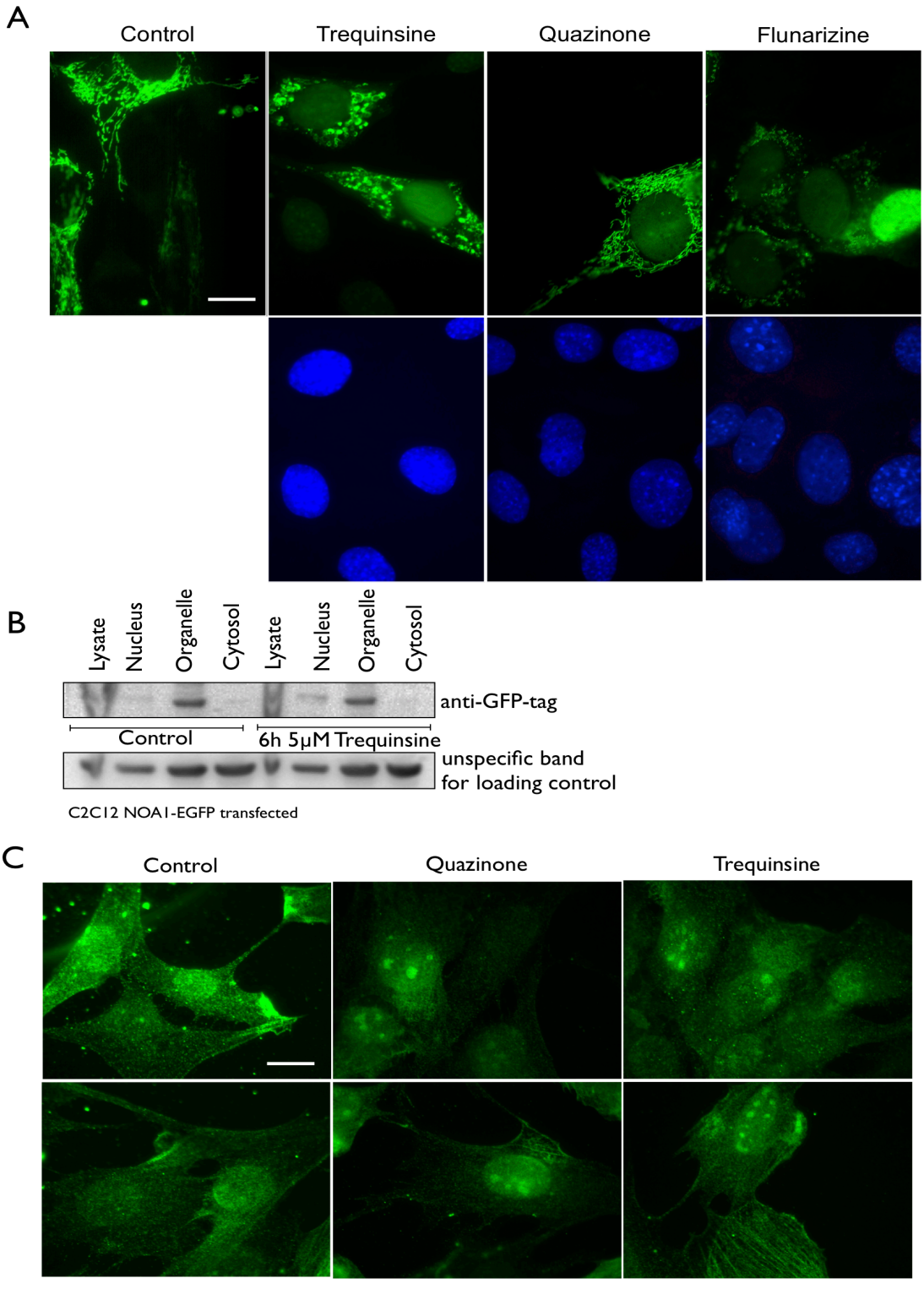

Figure 16 Analysis of the dynamics in the subcellular localization of NOA1 by treatment with LOPAC substances. A) NOA1-EGFP overexpression and treatment with LOPAC compounds showed nuclear accumulation of NOA1-EGFP. B) A crude cellular fractionation assay validated the increase in NOA1-EGFP in the nuclear fraction after treament with trequinsine. C) A nucleolar localization of endogenous NOA1 was observed after treatment with quazinone and trequinsin and antibody staining for NOA1; scale bar is 10 µm.

In summary, these experiments with NOA1-EGFP highlighted the dynamic nature of NOA1's subcellular localization. Treatment of cells with substances that influence nuclear import/export pathways induced nuclear accumulation of NOA1-EGFP. Furthermore, the speckled picture of nuclear, endogenous protein arose the question if there is a specific sub-nuclear localization.

F. Endogenous NOA1 can be found in the nucleus with association to the nucleolus

To validate the nuclear localization of NOA1 and to have a closer look on its sub-nuclear localization, freshly isolated, primary mouse myofibers were stained with NOA1 antibody and phalloidin-FITC (marker of actin) or Mitotracker dye (mitochondrial marker). Figure 17A showed localization of NOA1 in the nuclei that are spared by the phalloidin-FITC counterstain. Counterstaining of myofibers with the nucleolar marker protein UBF1 (Figure 17B) showed that NOA1 is distributed in speckles throughout the nucleus with association and partial co-localization with the nucleolus and UBF1. Intensity plots of the fluorescence signals and the distance were obtained from confocal pictures. The peaks of NOA1 and UBF1 fluorescence were centered supporting the fact that NOA1 speckles and UBF1 positive nucleoli are partially colocalized (Figure 17C).

Thus, while the majority of NOA1 protein is mitochondrially localized, a percentage of the endogenous NOA1 protein is forming speckles inside the nucleus. These NOA1 speckles associate with the nucleolus and co-localize partially with the nucleolar marker protein UBF1.

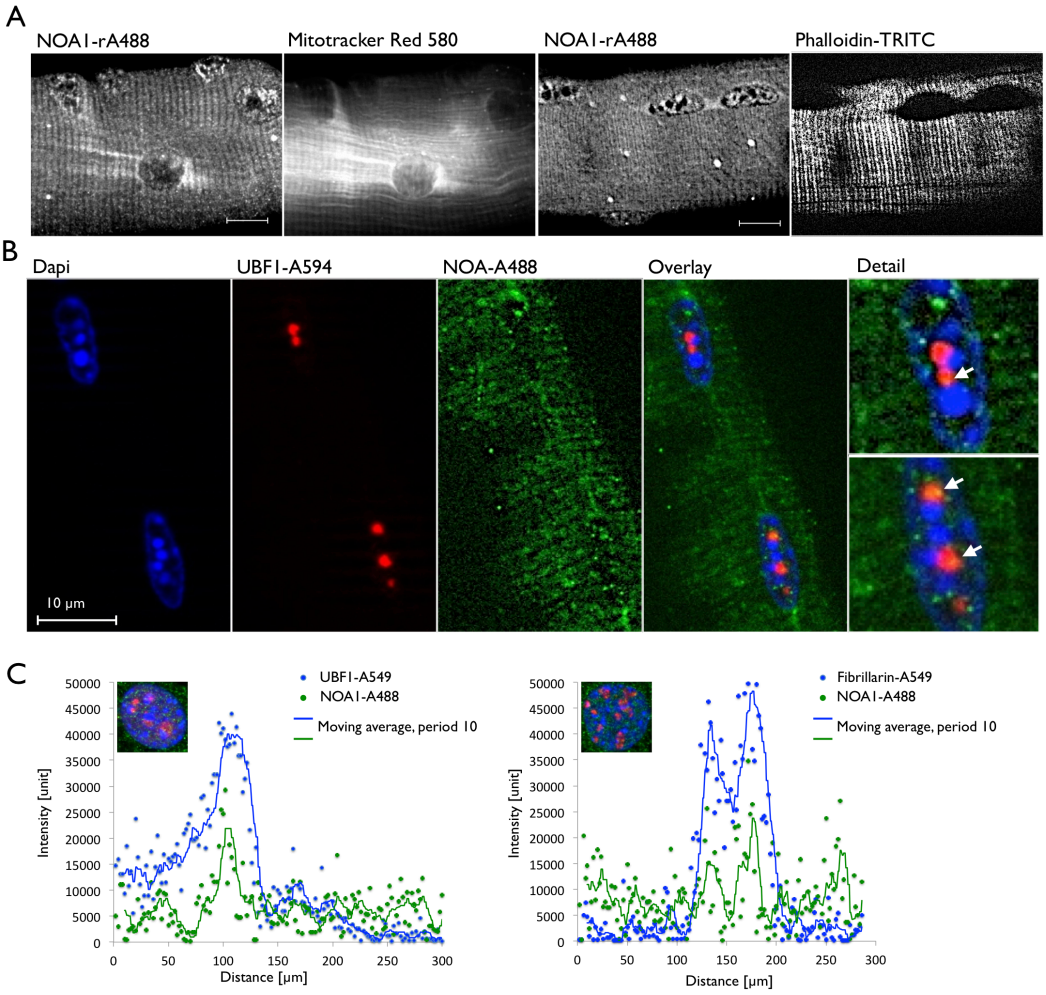

Colocalization of NOA1 with UBF1 and Fibrillarin in NIH3T3: Histogram (data obtained from confocal images)

Figure 17 Endogenous NOA1 is localized in the nucleus and associated to the nucleolus. A) Primary mouse myofibers show NOA1 staining in the nucleus that is spared by phalloidin. B) Co-staining with Dapi and UBF1 demonstrates the speckle-like association of NOA1 with the nucleolus. C) Confocal analysis validates the co-localization of NOA1 and UBF1.

G. Purification of recombinant NOA1-His$_6$ protein and GTPase activity test

In this thesis recombinant wild type, GTPase mutant and Caspase-mutant NOA1-His$_6$ protein was produced. As trials in *E.coli* failed, the immortalized Sf-9 insect cell line of *Spodoptera frugiperda* was used in combination with the baculovirus system to express recombinant NOA1. The protein production was performed in collaboration with the laboratory of Maria Falkenberg at the Sahlsgrenska academia in Gothenburg, Sweden. The infection with baculovirus, the selection and the induction of the expression were done in the Falkenberg laboratory. The expression

was robust and the protein purification was performed during a visit in the Falkenberg lab as described in the methods section.

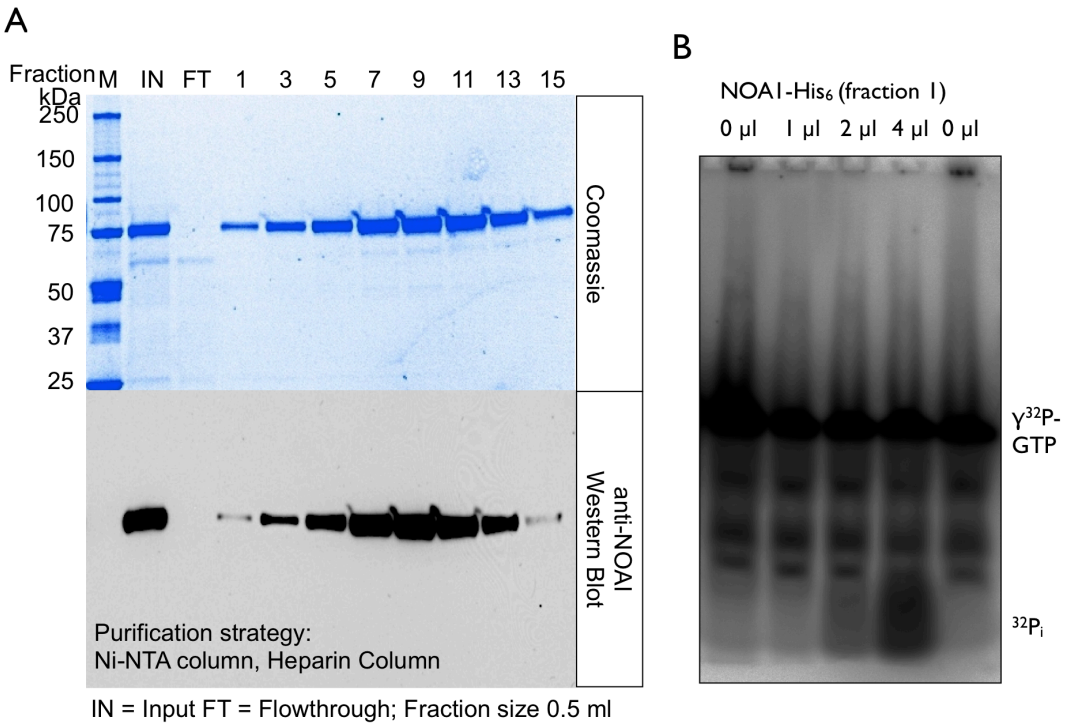

Figure 18 Recombinant NOA1-His_6 protein production in *S. frugiperda* cells A) Coomassie staining and Western blot after Ni-NTA and Heparin column purification. B) ^{32}P-labeled GTP was used for the GTPase assay and confirmed the activity of the recombinant NOA1-His_6 protein.

During purification, the peak fractions of the eluate were collected and analyzed by SDS-PAGE and coomassie staining. Figure 18A shows the purity of the elution peaks of wild type NOA1-His_6 after elution from the heparin column. The western blot showed no degradation during purification. For functional testing a GTPase activity assay was done. The presence of ^{32}P-γGTP enabled specific detection of hydrolyzed ^{32}P-labelled inorganic phosphate. The free $^{32}P_i$ is increasing with rising amounts of NOA1-wildtype protein. This *in vitro* GTP-hydrolysis activity attests the GTPase activity of the recombinant NOA1-His_6.

H. Nuclear import of recombinant NOA1-His$_6$ is GTP dependent.

To show that NOA1 is actively imported into the nucleus an *in vitro* nuclear import assay was set up. The available protocols for nuclear import assays rely on permeabilized whole cells and/or the addition of a cytosolic concentrate to the import reaction. Here, an *in vitro* assay without cytosol was established.

Isolated nuclei from mouse RAW264.7 macrophages and recombinant NOA1-His$_6$ protein was used. Additionally, an ATP regeneration system consisting of creatine phosphate kinase, ATP and creatine phosphate was added to recycle ATP from ADP and prevent system inhibition by nucleotidediphosphates. To block nuclear export Leptomycin B was included to the assay. Because nuclear import mediated by importinα/β is dependent on GTP, the non-hydrolysable GTP analogue GTPγS was used to block specific nuclear import in a control experiment. Proteins that are attached to the nuclear membrane like the importin-complex were involved in the assay and soluble cofactors were excluded since they were removed with the cytosol fraction. The availability of GTP exchange factors was limited in this assay but did not impair its function. After import the nuclei were washed and fixed. A staining with anti-Histidin-tag antibody visualized the localization of NOA1-His$_6$ protein.

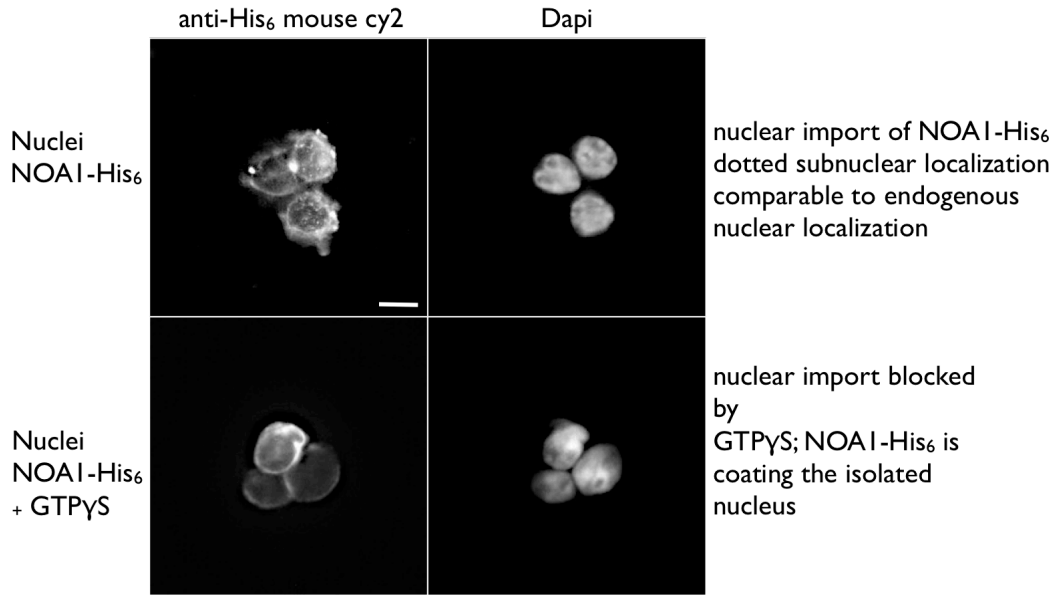

Figure 19 *In vitro* nuclear import assay with recombinant His-tagged NOA1 and isolated mouse macrophage nuclei (RAW26.7) shows active transport of NOA1 in a GTP dependent manner. The fixed nuclei were stained with anti-His$_6$ antibody to visualize the localization of NOA1-His$_6$ (Scale bar 10µm).

The confocal image of the *in vitro* nuclear import assay with recombinant NOA1-His_6 and isolated macrophage nuclei showed that NOA1 is actively imported into the nucleus (Figure 19). The antibody staining with His-tag antibody showed coating of the nuclei and dotted subnuclear localization equivalent to the nucleolus associated stainings in mouse myofibers. Addition of GTPγS to the import assay clearly prevented the import of NOA1. The nuclei were still coated with recombinant protein. This can be explained by the general interaction of the NLS of NOA1-His_6 with the protein import machinery in the nuclear membrane.

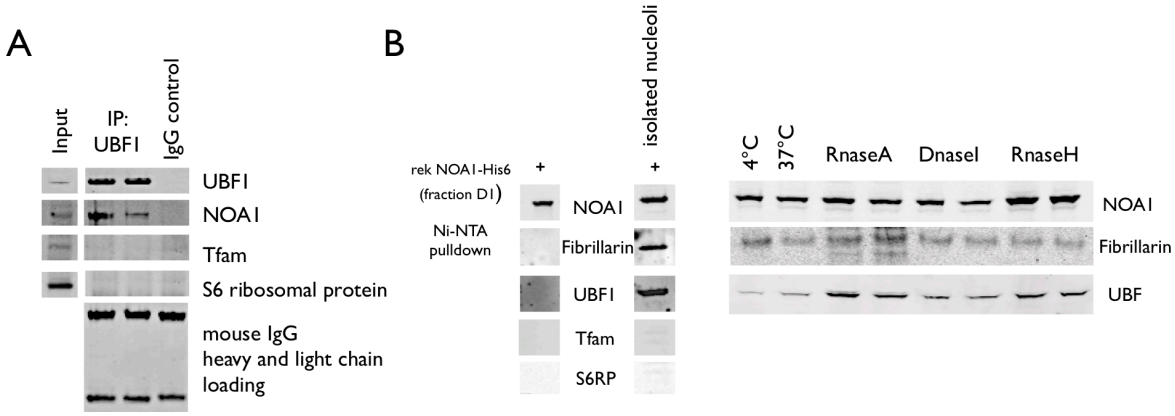

Figure 20 NOA interacts with the nucleolar marker protein UBF1. A) IP and B) Pulldown shows physical interaction of NOA1 and UBF1. The protein-protein interaction is independent of RNA and/or DNA bridges

After validation of nuclear localization and nuclear import the protein-protein-interaction of NOA1 and UBF1 was further analyzed by immunoprecipitation (IP) experiments (Figure 20A). IP of UBF1 pulls down endogenous NOA1 protein from RIPA buffer lysates. There was no interaction with Tfam or S6 ribosomal protein supporting the specificity of the interaction of NOA1 and UBF1 in the nucleus. The random association of mitochondrial NOA1 with the mitochondrial nucleoid was published recently[7]. S6 ribosomal protein is a control since NOA1 was reported to interact with a battery of ribosomal proteins (Figure 20A). UBF1 is a transcription factor that is localized at the site of transcription of ribosomal proteins in the nucleolus. Another member of this transcription initiation complex is Fibrillarin.

A pulldown experiment with recombinant NOA1-His_6 and RIPA lysate of nucleoli preparations showed that NOA1 interacts with this complex. NOA1-His_6 pulled down UBF1 and Fibrillarin (Figure 20B). The pulldown was repeated with whole cell

RIPA lysates and the addition of DNAse and RNases. The interaction of NOA1 with the UBF1/ Fibrillarin complex was independent of DNA bridges, DNA/RNA hybrids and RNA.

In conclusion, NOA1 was actively imported into nuclei in a GTP dependent manner. *In vitro* imported recombinant NOA1 showed the same speckled subnuclear localization pattern as endogenous NOA1 protein. NOA1 physically interacted with the nucleolar UBF1/Fibrillarin complex. This interaction is independent of DNA and/or RNA.

I. NOA1 is exported from the nucleus by Crm1 and carries a nuclear export signal (NES).

After investigating the nature of NOA1's sub-nuclear localization, nuclear protein-protein interactions and the nuclear import, the nuclear export was adressed. Fibroblasts were treated with the nuclear export blocker Leptomycin B (2 ng/ml) and the transcription inhibitor Actinomycin D (10µM). Leptomycin B is a bacterial macromolecule that targets Crm1 (exportin 1)[70]. Crm1 exports proteins from the nucleus that contain a leucine-rich nuclear export signal (NES). Crm1 exports the majority of shuttling proteins from the nucleus. Therefore, it was assumed that Crm1 exports NOA1, too. Inhibition of transcription by Actinomycin D leads to the nuclear accumulation of protein complexes localized at transcriptional initiation sites due to stalling of transcription. Actinomycin D is used as a control substance in nuclear export inhibition experiments and has often the same effect as Leptomycin B. Figure 21 shows that the nuclear localization of NOA1 was sensitive to Leptomycin B treatment. Similarily, stalling of transcription by Actinomycin D also led to a nuclear accumulation of NOA1.

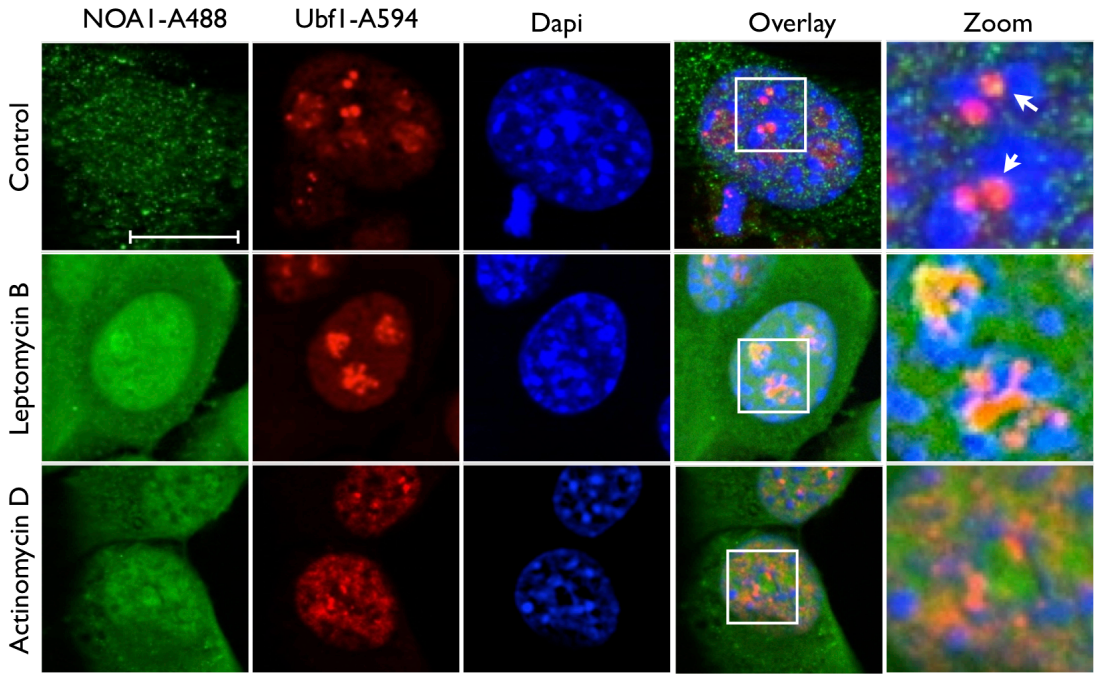

Figure 21 Crm1 exports NOA1 from the nucleus. The nuclear localization of NOA1 is sensitive to Leptomycin B and Actinomycin D. Nuclear export blockade lead to nuclear accumulation of NOA1 with nucleolar accentuation and increased co-localization with UBF1 (cell type: NIH3T3 fibroblasts, scale bar 10 µm).

After *in silico* tools failed to predict any nuclear export signal (NES) in the amino acid sequence of NOA1 the manual analysis resulted in the identification of the putative Crm1 dependent nuclear export signal (NES). This export signal lies within the predicted leucine zipper domain of NOA1 and is arranged in reverse order (Figure 22C). This is quite unusual and might be the reason why online tools did not detect the NES.

Fusion of NOA1's three localization signal sequences upstream of GFP provided a tool to test their effectiveness in targeting. MTS-GFP and NLS-GFP were strongly expressed. Combinations of targeting signals like MTS/NLS-GFP and NLS/NES-GFP resulted in weak expression (Figure 22A). The targeting performance was tested by transfection of the GFP fusion proteins into C2C12 cells and counterstaining for mitochondria with Tom20 antibody (Figure 22C). In control cells, the GFP is distributed throughout the whole cell. The GFP (~27 kDa) enters the nucleus by passive diffusion through the nuclear pores. Theses pores allow proteins up to a mass of 40 kDa to diffuse freely between nucleus and cytoplasm. The MTS of NOA1 clearly targets the GFP to mitochondria. The NLS of NOA1 targets the GFP to

active import into the nucleus. However, the distribution of GFP and NLS-GFP in the cell is similar because NLS-GFP can diffuse between nucleus and cytoplasm due to its small size, which masks the nuclear localization. The functionality of the NOA1-NES was shown before by the truncation of the MTS, which lead to a sustained nuclear accumulation of the NOA1ΔMTS mutant.

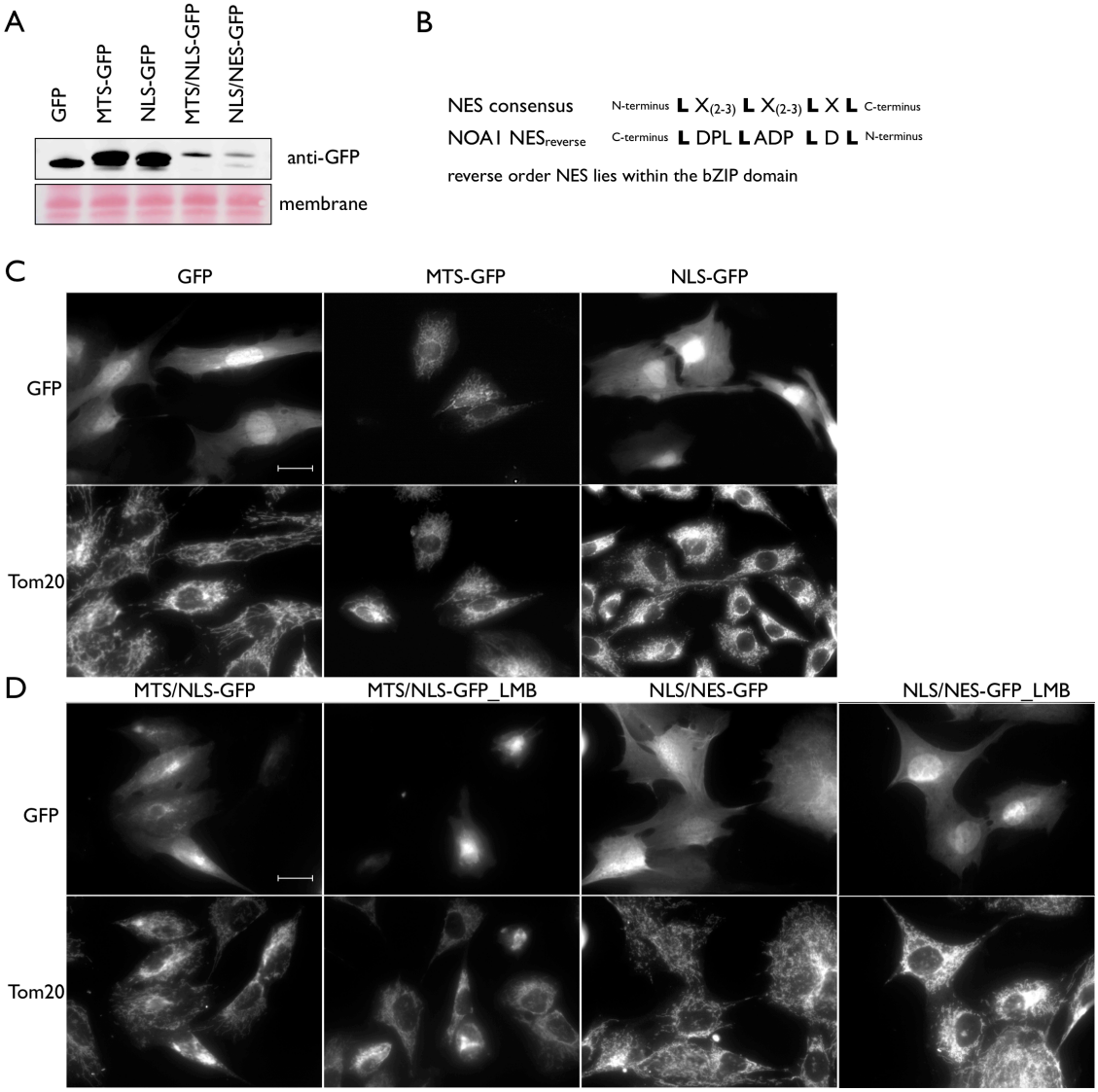

Figure 22 Analysis of the localization signals of the NOA1 protein and identification of the nuclear export signal (NES). A) Protein expression of localization signals fused to GFP. Dual tagged GFP constructs show weak expression. B) Alignment of the NES in NOA1 to the consensus sequence shows that the NOA-NES lies within the dimerization bZIP domain in reverse order. C) Targeting performance of NOA's localization signals fused to GFP. Tom20 antibody staining shows mitochondria. MTS-GFP is targeted to mitochondria. NLS-GFP is targeted to the nucleus. D) Subcellular distribution of MTS/NLS-GFP and NLS/NES-GFP is rather unspecific but nuclear export inhibition by Leptomycin B lead to partial retention of MTS/NLS and clear accumulation of NLS/NES-GFP in the nucleus (cell type: C2C12; scale bar = 10 µm).

The GFP tagged with MTS followed directly by the NLS of NOA1 was weakly expressed and showed no proper targeting to a specific compartment but a random distribution. The direct link of two subcellular localization signals might interfere with the sorting process. However, the treatment with Leptomycin B increased the amount of nuclear localized MTS/NLS-GFP in a population of cells (Figure 22C). The GFP fusion construct containing NLS linked to NES showed an even distribution of the GFP fluorescence throughout the cell. Treatment with Leptomycin B significantly increased the nuclear/cytosolic ratio of NLS/NES-GFP and lead to nuclear accumulation of NLS/NES-GFP (Figure 22B). The sensitivity of NLS/NES-GFP towards Leptomycin B validates the herein identified NES. The nuclear export signal of NOA1 that is localized within the leucine zipper dimerization domain is responsible for active nuclear export of NOA1 by Crm1 (Figure 22B).

Together, the export of NOA1 from the nucleus is dependent on Crm1 and therefore the export is sensitive to Leptomycin B. NOA1 contains a classical nuclear export signal (NES) that is arranged in reverse order in the amino acid sequence and is part of the leucine zipper domain which indicates that protein dimerization is likely to regulate nuclear export[71].

J. Nuclear localization of NOA1 occurs before mitochondrial import.

NOA1 has a classical N-terminal presequence for mitochondrial targeting. The previous experiments showed that NOA1 is also targeted to the nucleus where it is actively imported and exported, mediated by NLS and NES, respectively. Hence, NOA1 is a dual targeted protein. To clear the spatiotemporal sequence of the localization events NOA1-EGFP expressing cells were treated with trequinsin and flunarizine, compounds of the LOPAC[1280] library that showed the potential to accumulate NOA1 in the nucleus. NOA1 was accumulating in the nucleus upon treatment but in the presence of the translation inhibitor cycloheximide the nuclear accumulation was abolished (Figure 23A) showing that the nuclear accumulation process is dependent on translation. This lead to the conclusion that the newly translated NOA1 is targeted to the nucleus where it accumulates upon nuclear export blockade.

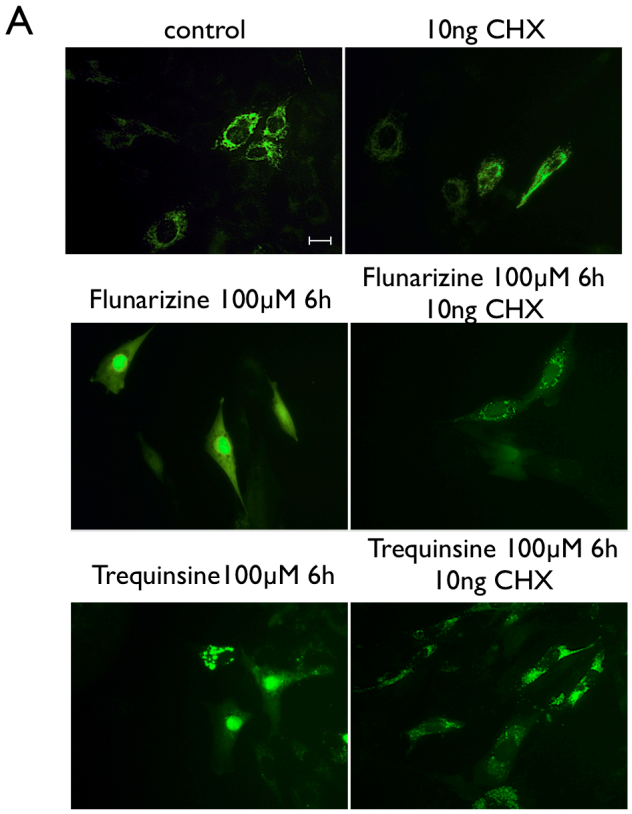

C2C12 NOA1-EGFP; scale bar 10 µm

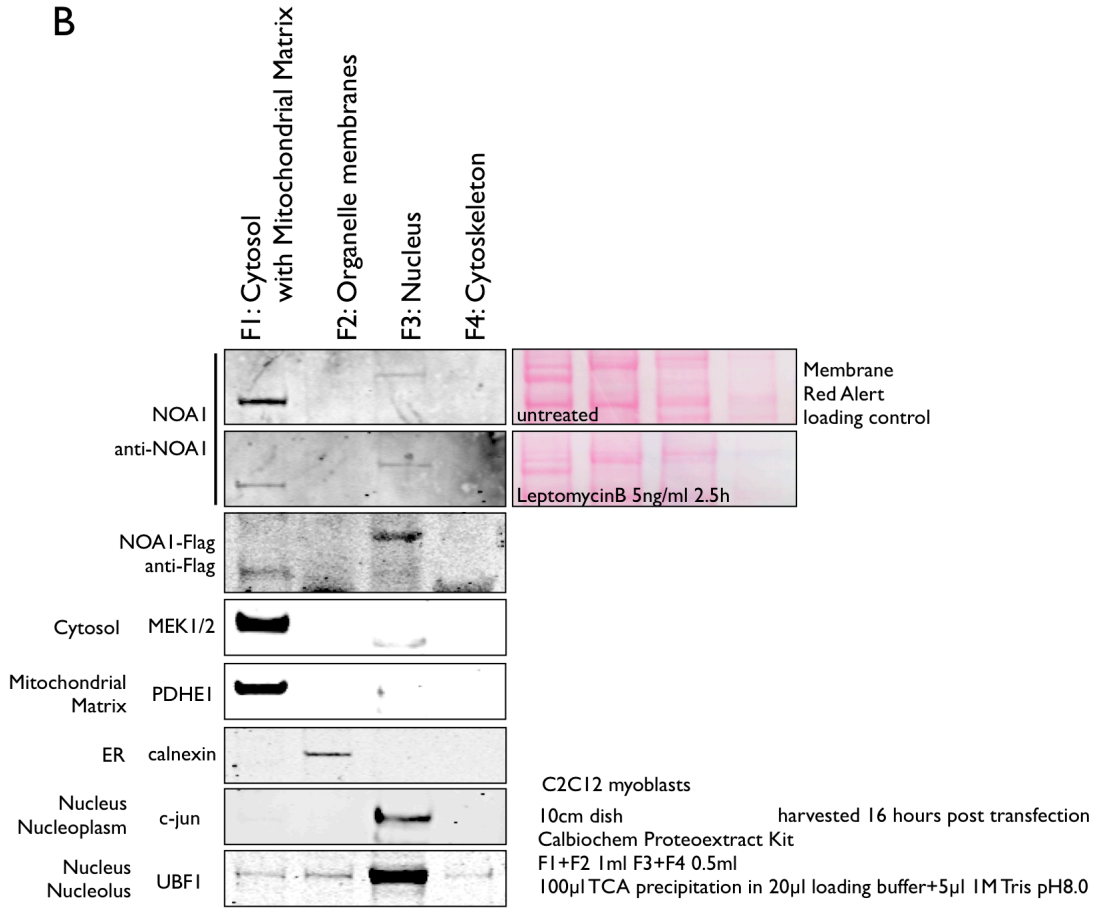

Figure 23 NOA1 is first nuclearly localized then mitochondrial. A) Newly synthesized NOA1-EGFP is accumulating in the nucleus upon treatment with flunarizine and trequinsin. B) Resolution in a 6% Bis-Tris SDS-PAGE gel reveals the nuclear form of NOA1 to be longer and having the size of the MTS containing precursor. NOA1-Flag overexpression showed the same result. Hence, nuclear localization occurs prior to the mitochondrial localization.

To clarify this, wild type and NOA1-Flag overexpressing cells were fractioned with a commercial fractionation kit. The fractions were separated on a 6% Bis-tris SDS-PAGE gel to ensure a clear separation of precursor and processed NOA1 protein. The shorter, mature NOA1 protein was detected in the F1 fraction containing the mitochondrial matrix proteins. The longer, unprocessed NOA1 precursor band was detected in the nuclear fraction F3 indicating that NOA1 is translated in the cytosol and as precursor form targeted to the nucleus before entering the mitochondria where the MTS is cleaved. Fraction purity was verified using pyruvate dehydrogenase (PDHE1) as mitochondrial (Figure 23B) c-jun and UBF1 as nuclear/nucleolar marker. Leptomycin B treatment decreased the amount of mitochondrial NOA1 in comparison to nuclear NOA1. A fractionation of NOA1-Flag overexpressing cells showed the same result.

It was demonstrated that nuclear localized NOA1 contains its MTS while mitochondrial NOA1 is fully processed lacking the MTS. Active protein synthesis is a requirement for nuclear accumulation of NOA1-EGFP.

K. NOA1-His$_6$ specifically binds G-quadruplexes

NOA1 contains a RNA-binding domain in the C-terminus. To get an idea of the RNA-binding selectivity of NOA1, a SELEX analysis was performed in order to identify a consensus binding sequence. SELEX is the "Selected Evolution of Ligands by EXponential Enrichment" and is based on multiple consecutive immunoprecipitations of the protein of interest (here: recombinant wild type NOA1-His$_6$) following PCR amplification of the bound consensus. A library of random DNA nucleotides with a length of 46 bases was used containing a core of 14 scrambled nucleotides.

Figure 24 summarizes the results of the SELEX experiment. After each round of immunoprecipitation with anti-His$_6$-tag antibody the DNA was precipitated and extracted from TBE-gels. The control experiment contained NOA1-His$_6$ protein but no antibody. In the second round a faster migrating band appeared in both samples. This faster migrating band was enriched in the third round and was dominant in the

experiment in the fourth round. The faster migrating bands and the standard 46 nt band were separately processed. The 46 nt bands emerged to be background. After six rounds of immunoprecipitation the faster migrating band was significantly enriched in the sample containing His_6-tag antibody (Figure 24A).

A

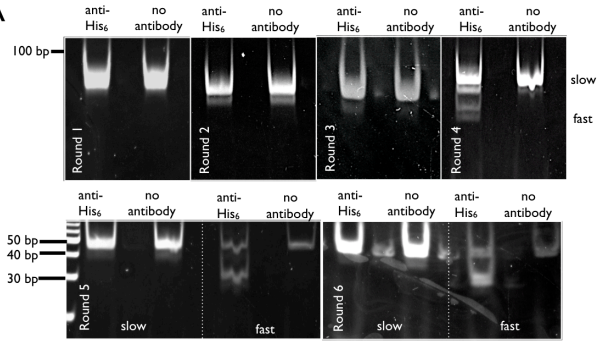

B

Table 4. Selex cloned consensus sequences

#	Sequence	Quadruplex Mapper (QGRS)	
1	GGGGGAACGGGGGG	GGGGGAACGGGGGG	2-1-3-1
2	GGCGGTATGGAGGG	GGCGGTATGGAGGG	2-1-3-1
3	GGCGTCCTCTTAGA	-	
4	CACCAGCAGCCCAA	-	
5	GGTAGTGCGGGGGG	-	
6	GGGTGAGGGGGGCG	-	
7	GGGGAGGGGGGGTG	GGGGAGGGGGGGTG	2-0-1-1
8	GGAAGGGAGTGGGG	GGAAGGGAGTGGGG	2-3-3-0
9	GGGGGAGGGGGGGTG	GGGGGAGGGGGGGTG	2-1-1-1
10	GACACGCAGGTGGGA	-	
11	GGGGGGGGGGTTGGG	GGGGGGGGGGTTGGG	3-1-0-2
consensus	GGGGGAGAGGAGGG	GGGGGAGAGGAGGG	2-1-3-1

C

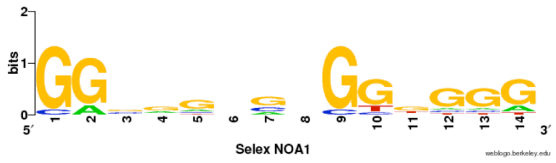

Figure 24 Selex results. A) Gels round 1 to round 6; a faster migrating band is enriched with each anti-His_6-tag IP round. B) Original sequences from the clones obtained from cloning the faster migrating band library and the consensus sequence. C) Weblogo pictrure of the SELEX consensus sequence for NOA1-His_6.

The clones from the 46 nt sized band of control and experiment contained random sequences with no consensus. The clones of the faster migrating band were analyzed the same way. All inserts had a size of exactly 46 nt. The characteristic of these clones was core sequences that were rich in guanines. A web-based application was used to identify the consensus sequence. WebLogo generates consensus sequences and creates graphical logos[72,73]. The WebLogo of the consensus binding sequence of NOA1 emphasizes the main feature, which is the richness in guanines (Figure 24C). Such G-rich sequences are prone to forming G-quadruplexes. The online tool "QGRS-Quadruplex mapper"[74] predicted each sequence of the faster migrating band to form a G-quadruplex (Figure 24B).

A Sequences of the oligonucleotides for quadruplex folding.

Oligo name	Sequence (5'-3')
G2 sense	AAAGGAAAGGAAAGGAAAGGAAA
G2 antisense	TTTCCTTTCCTTTCCTTTCCTTT
G3 sense	AAAGGGAAAGGGAAAGGGAAAGGGAAA
G3 antisense	TTTCCCTTTCCCTTTCCCTTTCCCTTT
G4 sense	AAAGGGGAAAGGGGAAAGGGGAAAGGGG
G4 antisense	TTTCCCCTTTCCCCTTTCCCCTTTCCCCTTT
G4 non	GAGAGAGAAGAGGAGAGAGGGAGAGAGG
G5 / Selex consensus	GGGGGAAAGGGGG

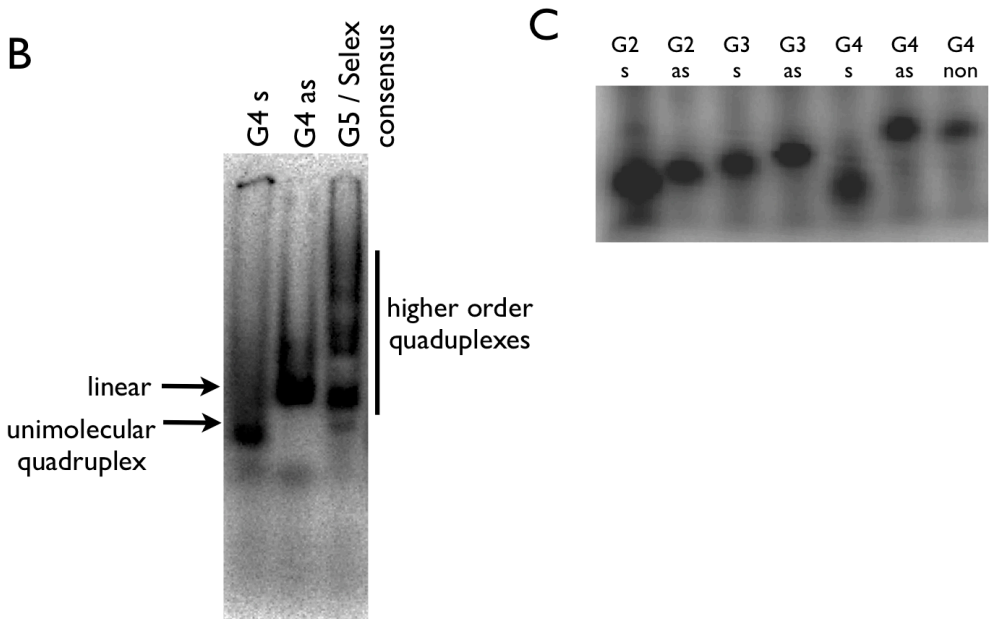

Figure 25 G-quadruplex folding. A) Sequences of the sense and antisense quadruplex oligonucleotides. B) Oligonucleotides were end-labeled with ^{32}P-γATP and folded with potassium to quadruplexes. The quadruplex runs faster in a 8% TBE gel than the corresponding antisense oligo that is not forming a quadruplex. Beside uni-molecular quadruplexes also higher order stacks can be formed resulting in retention in the gel.

Synthetic oligonucleotides (Figure 25A) were folded into G-quadruplexes by slowly cooling and the addition of potassium. The G4222 sense oligonucleotide consisted of four quartets of guanines flanked and spaced by triplets of arginine. The G4222 antisense oligonucleotide was the complementary sequence. The G-quadruplex G4222 sense ran faster than the antisense G4222 oligonucleotide having the same size (Figure 25B). The more guanines a sequence contains, the more complex the G-quadruplexes can become. Additionally, intermolecular stacks can be formed. Figure

25C compares the migration of G-quadruplex sense and antisense oligonucleotides with a G-rich oligo that is not predicted to form any G-quadruplexes although it contains the same number of guanines and adenines, but scrambled. This "G4 non" oligo ran at the same height as the antisense oligo. Thus, G-quadruplexes are formed *in vitro* with the chosen synthetic oligonucleotides. The oligos used in the SELEX analysis as well as in the gel shift assays were DNA although the assays were designed to investigate the RNA-binding domain of NOA1. RNA G-quadruplexes form comparable structures to their corresponding DNA G-quadruplexes and are even more stable than DNA G-quadruplexes[75]. Therefore, it was justifiable to perform the *in vitro* experiments with DNA oligonucleotides.

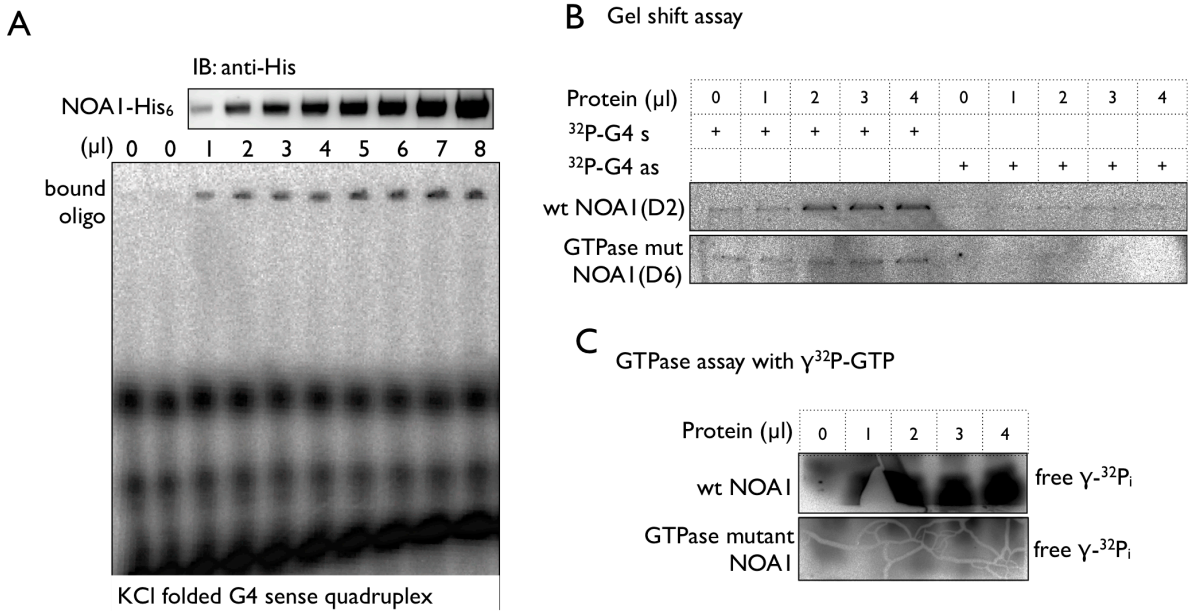

Figure 26 Recombinant NOA1 binds G-quadruplexes *in vitro*. A) NOA1-His_6 binds to ^{32}P-labelled G4 sense quadruplexes visualized by a gel shift assay. B) The GTPase mutant NOA1 binds to the quadruplex similar as the wild type protein. Both do not bind the antisense oligo, which is neither G-rich nor a quadruplex. C) GTPase assay of the wild type NOA1 and GTPase mutant NOA1 show that GTPase mutant NOA1 is unable to hydrolyze GTP.

In a gel shift assay with ^{32}P-γATP labeled prefolded oligos a binding of NOA1 to the G-quadruplexes could be seen (Figure 26A) therefore confirming the SELEX results. The GTPase mutant NOA1 lacks the ability to hydrolyze GTP (Figure 26C) but binds the G-quadruplex. Therefore, G-quadruplex binding is independent of the GTPase functionality of NOA1 (Figure 26B).

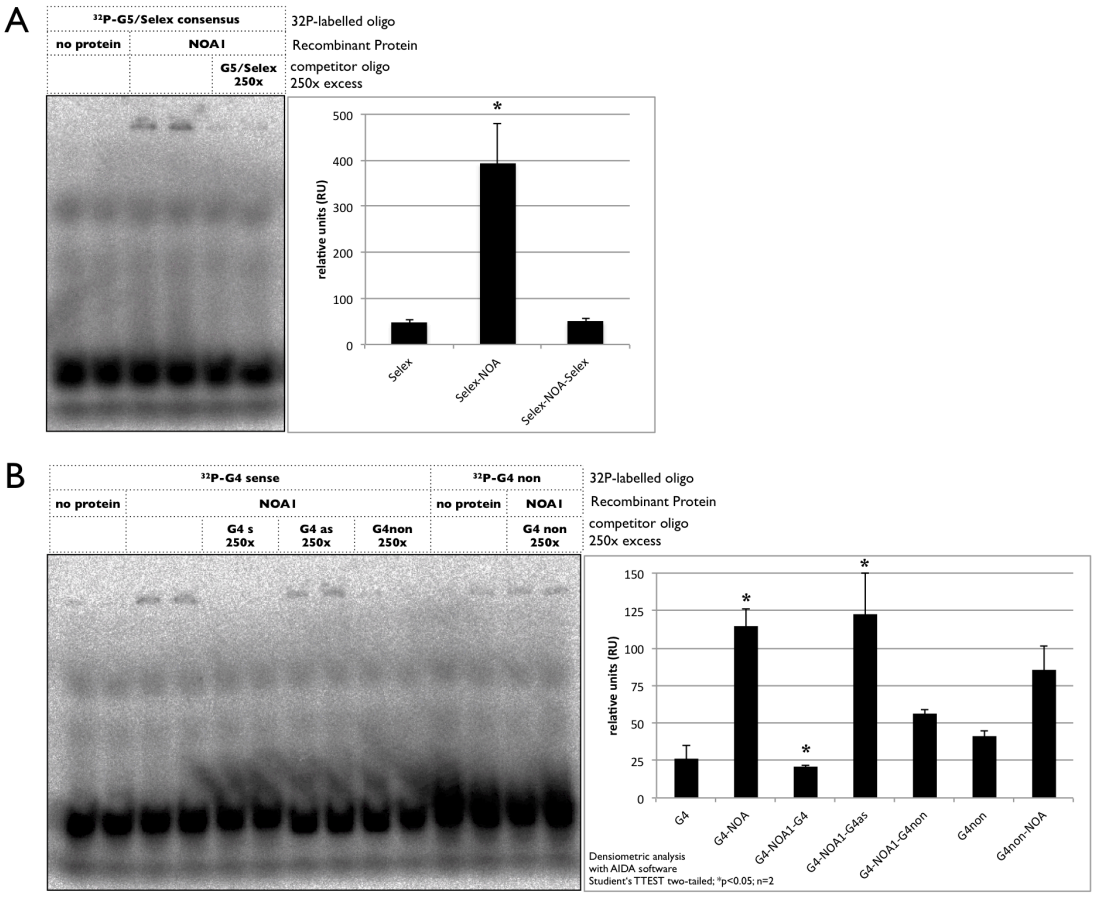

Figure 27 Competition experiments show specificity of quadruplex binding. A) NOA1 binds the G5/Selex consensus oligo and excess of non-labeled SELEX oligo competes for the binding site. B) NOA1 binds to quaduplexes. Competetion with quadruplex is successful whereas antisense oligo does not compete at all. The G-rich oligo that cannot form a quadruplex can compete partially for the quadruplex binding since NOA1 protein binds also to the G-rich sequence.

The specificity of the gel shift assays was confirmed by competition experiments using a 250x excess of unlabeled oligonucleotide to compete for the binding with the ^{32}P-end-labeled oligos. Figure 27A shows the binding to ^{32}P-labelled SELEX consensus quadruplex and a complete competition by the addition of 250x unlabeled oligo. As shown before NOA1-His$_6$ binds to the G4 sense G-quadruplex (Figure 27B). The binding can be competed by addition of excess of unlabeled G4 sense G-quadruplex to the reaction. The G4 antisense oligo not forming G-quadruplexes nor containing guanines does not compete for the NOA1-bindings site. The G-rich "G4 non" oligonucleotide not forming G-quadruplexes does compete partially with the G4 sense G-quadruplex due to the fact that the G-rich G4 non oligo is bound by

NOA1-His_6 although to a lesser extent than the G-quadruplexes. This showed that NOA1 has a moderate ability to bind to G-rich sequences *per se*.

L. G-quadruplex binding stimulates the GTPase activity of NOA1-His_6

Ligand binding can alter enzymatic activity. Therefore, the GTPase activity of NOA1-His_6 was measured in the presence of the ligand G-quadruplexes by ^{32}P-γGTP supported GTPase assay. A serial dilution of NOA1-His_6 in comparison with the GTPase mutant showed that NOA1 is a functional GTPase while mutation of Lysin353 to Arginine lead to disruption of the GTPase function (Figure 28A). The basic GTPase activitiy (copy of the wildtype GTPase assay panel from Figure 28A) was significantly increased by the addition of G4 sense G-quadruplex oligos (Figure 28B, C).

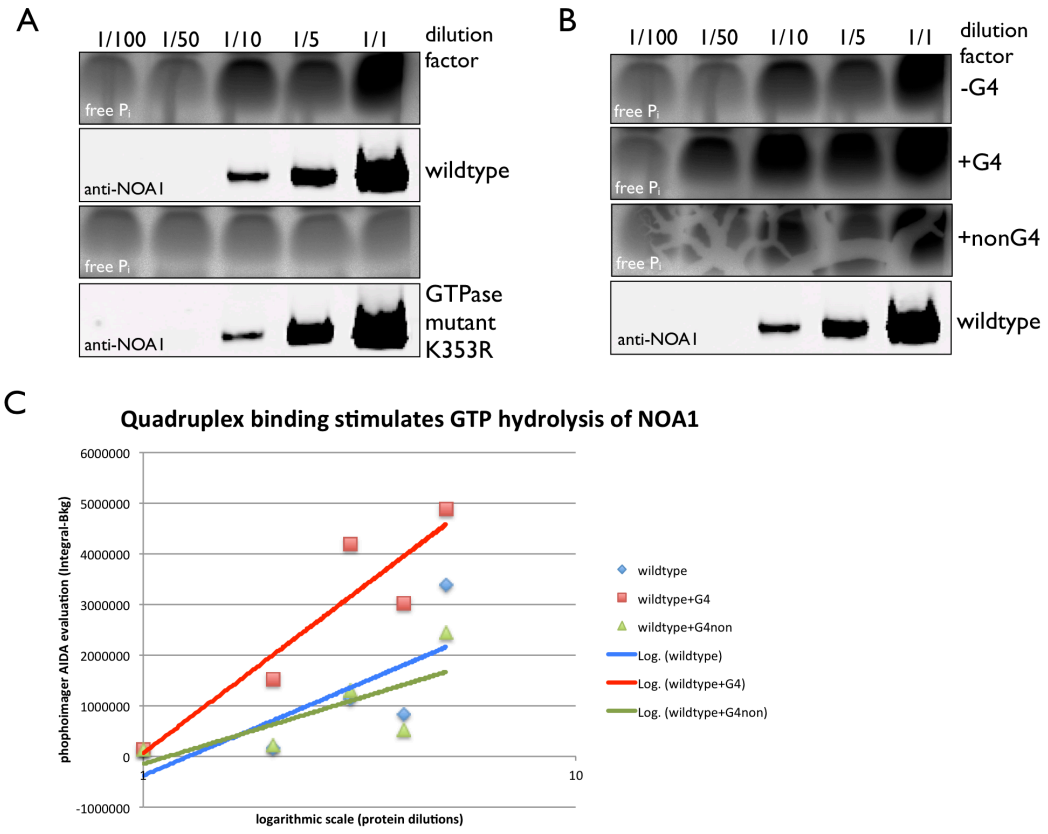

Figure 28 G-quadruplex binding activates GTPase activity of NOA1. A) GTPase activity of NOA compared to enzymatic dead GTPase mutant K353R. B) Quadruplex binding stimulated the GTP hydrolysis whereas the G-rich non-quadruplex oligo was not influencing the enzymatic function. C) Graphic evaluation of the GTP hydrolysis. G4 sense G-quadruplex elevated the GTP hydrolysis rate.

Although NOA1 showed the tendency of binding to G-rich sequences that cannot form G-quadruplexes, the GTPase activity was not affected by these non-quadruplexes

In summary, NOA1 binds G-rich sequences with a higher affinity for G-quadruplexes. The binding of NOA1 to a G-quadruplex increases the GTP hydrolysis activity.

M. RNA-Immunoprecipiation (RIP) and ^{32}P-dCTP supported RT-PCR shows random enrichment of RNA in NOA1-immunoprecipitated samples.

To identify the natural target of NOA1 RNA-immunoprecipitation experiments were established to identify the RNA-ligand.

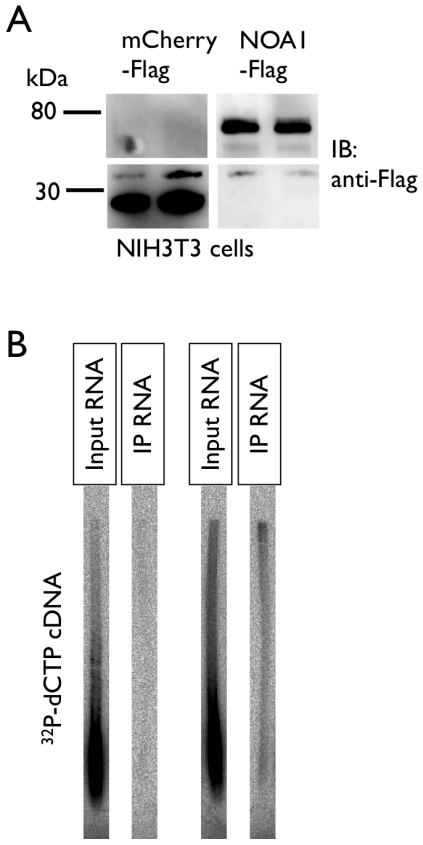

Figure 29 RNA-Immunoprecipiation (RIP) of NOA1-Flag overexpressing cells. The proteins were isolated in parallel to the RNA isolation. A) Cherry-Flag control and NOA1-Flag protein complexes precipitated robustly B) The NOA1-Flag RIP pulled down RNA of all sizes whereas control RIP did not contain any RNA.

NOA1-Flag and cherry-Flag were transiently overexpressed in cells and immunoprecipitated. The co-precipitated RNA's were extracted, radioactively

reverse-transcribed and visualized on agarose gels. While the control showed no signal a smear of cDNA was detected in the NOA1-Flag RIP indicating that NOA1 is binding to RNA *in vivo*. Unfortunately, no distinct bands were observed indicating multiple targets of NOA1 in whole cell RNA (Figure 29B).

In conclusion NOA1 binds to cellular RNA *in vivo* but the RIP is rather unspecific. Therefore, it was decided to refrain from RIP-seq until the method would be improved.

N. Oligomerization of NOA1 correlates with G-quadruplex binding.

NOA1 has a basic leucine zipper that is involved in the dimerization of NOA1[4]. Ligand binding can influence the oligomerization status of proteins and protein complexes. Crosslinking experiments with glutaraldehyde were done to test if G-quadruplex binding influences dimerization or oligomerization of NOA1 monomers.

Based on serial dilutions 0.0005% of glutaraldehyde was chosen as a concentration where residual monomeric NOA1 was detected but also higher molecular weight complexes were formed (Figure 30A). The samples were separated on a 3-8% Tris-Acetate SDS-PAGE to ensure separation of larger complexes. (Figure 30B). The detected bands corresponded with the sizes for monomeric, dimeric, trimeric and tetrameric NOA1 complexes.

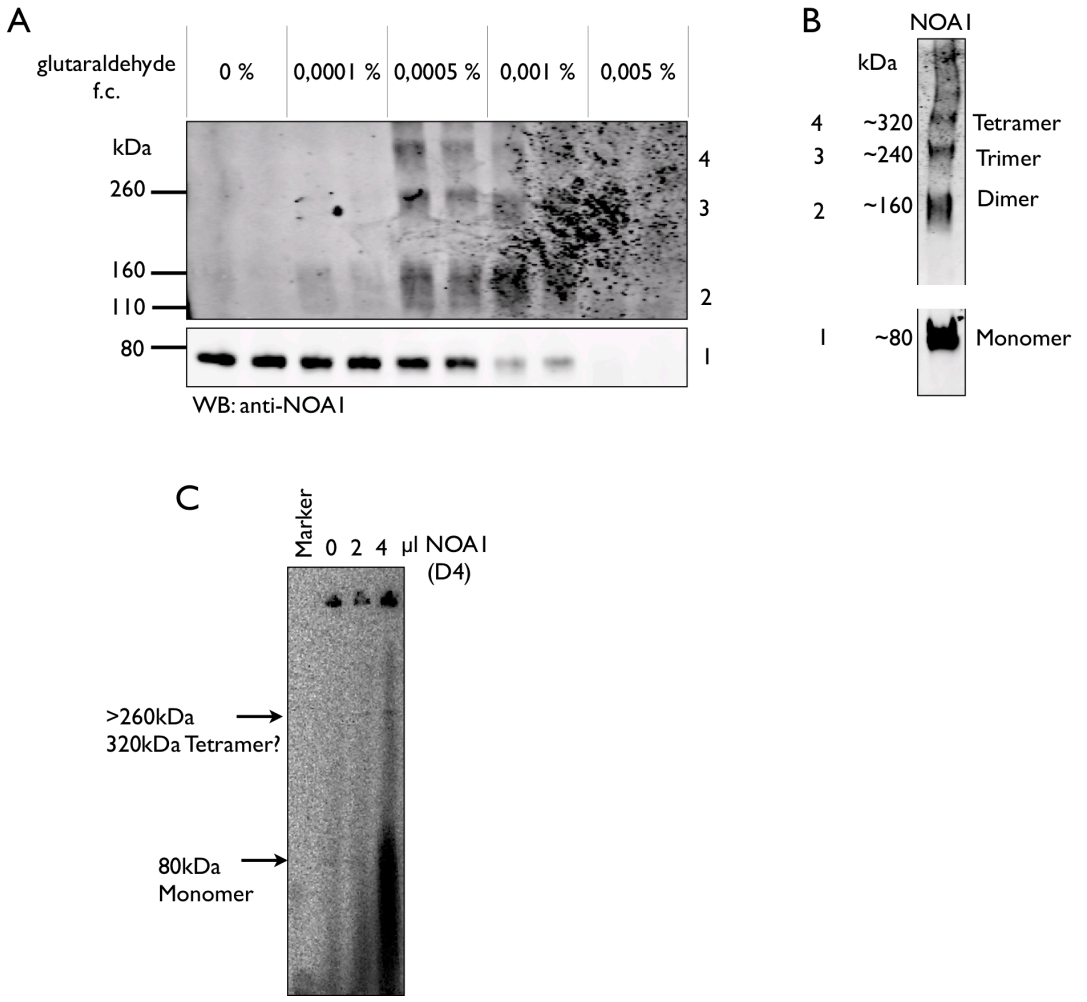

Figure 30 Oligomerization of NOA1. A) Recombinant NOA1 was crosslinked with different concentrations of glutaraldehyde and the complexes were resolved on a Tris-Acetate 3-8% gel. B) Assignment of the four different bands to oligomers. C) Oligomers bind quadruplexes. The crosslinking was performed in the presence of ^{32}P-SELEX oligo and 0.0005% glutaraldehyde. The unspecific signals in the wells most likely originate from unspecific crosslinking of oligonucleotides.

To assess if such oligomers incorporate G-quadruplexes, different concentrations of NOA1-His$_6$ protein and ^{32}P-labeled G-quadruplex were crosslinked and separated by 3-8% Tris-Acetate SDS-PAGE (Figure 30C). Although faint, a slight band was detected at the size of NOA1 monomer and tetramer. The more NOA1-His$_6$ was added the more radioactive signal was shifted upward indicating a proportional binding of G-quadruplexes independent of the oligomeric state of NOA1.

O. G-quadruplexes analysis of mtDNA and mitochondrial transcripts

The bacterial homologue of NOA1, YqeH, was shown to play a role in the assembly of the small subunit of the ribosome and an interaction between YqeH and 16S rRNA[2,8] was hypothesized. Therefore, 16S rRNA and 12S rRNA are putative candidates for NOA1 binding partners and were subjected to a G-quadruplex analysis. The mitochondrial genome (NCBI NC_005089.1) of the laboratory mouse (*mus musculus*) was analyzed with the QGRS-quadruplex mapper[74]. Guanines that participate in the formation of the G-quadruplex are underlined. The G-score is a measure of the stability of the G-quadruplexes and a value of 15-20 is a standard stability for G-quadruplexes with duplets of guanines spaced by a variability of alternative nucleotides.

The heavy strand of the mtDNA contains five G-quadruplexes. Two G-quadruplexes are in the 12S rRNA gene and the genes of ND2, COX1 and ND5 each contain one G-quadruplex (Table 5).

Assuming that NOA1 binds to RNA, the mtDNA transcripts were also subjected to G-quadruplex analysis. The major part of mitochondrial transcripts is generated with the heavy strand template. These G-quadruplexes might have functions in the regulation of transcription or replication at the level of DNA.

Table 5 QGRS quadruplex analysis of mouse mtDNA

rRNA/tRNA/Gene	Position	Length	QGRS	G-Score
12S rRNA	2248	17	GGTTGGGGTGACCTCGG	14
12S rRNA	2672	24	GGTTATTAGGGTGGCAGAGCCAGG	15
ND2	4406	14	GGGGCATGAGGAGG	16
COX1	5997	10	GGAGGAGGGG	20
ND5	12168	16	GGCTGAGAAGGGGTGG	14

The analysis of mtDNA transcripts contained 79 G-quadruplexes (Table 6). The 12S ribosomal RNA contained seven G-quadruplexes and the 16S ribosomal RNA contained four G-quadruplexes. The other 68 G-quadruplexes are distributed over the mitochondrial transcripts.

Table 6 QGRS quadruplex analysis of the mtDNA transcripts. Yellow boxes mark light strand transcripts, green boxes mark the region of the D-loop.

rRNA/tRNA/Gene	Position	Length	QGRS	G-Score
12S rRNA	123	24	GGAGGTATCTGGCCACATTTTAGG	12
12S rRNA	208	17	GGAACGGATCGGTGTGG	21
12S rRNA	309	27	GGTCGGTGGCGCCAGTATGCTAATTGG	6
12S rRNA	501	24	GGGGTGATACGAATCGGTATTTGG	10
12S rRNA	642	17	GGGGCGAGATGGAGTGG	15
12S rRNA	676	27	GGATATATGGCGGTAGAAGTCGTTTGG	10
12S rRNA	906	16	GGCGGGCAGTGGGAGG	19
16S rRNA	1330	22	GGGGCTTTGGTTTGCTCGATGG	11
16S rRNA	1598	26	GGTAACATCCGGATTTTCGTCGGTGG	13
16S rRNA	1864	30	GGTTGTGGCCTTACGGATTTCCTTTCTAGG	13
16S rRNA	1925	15	GGGGCGGACAAATGG	15
tRNA-Leu L1	2716	30	GGAACAAGGGTCTCCAAGTTTAGGAGAGGG	13
tRNA-Ile I	2777	28	GGAGCAGGGGTAAGATTAGCGGTATCGG	15
ND1	2928	30	GGTTATGCGGGAAATTGTTGGAGATATAGG	20
ND1	3012	20	GGGGATGGTTATGGTGTGGG	21
ND1	3279	18	GGTCGGACTGGGTATCGG	19
ND1	3332	17	GGCCCGGGGGAAGCTGG	17
ND1	3458	29	GGATTGTTGATAATAGAAGGATCCTGGGG	5
tRNA-Gln Q	3817	24	GGCACGATGGATTTGTGGAATAGG	19
tRNA-Met M	3873	30	GGGTATGGGGCTTTTGCAACCAAATTTAGG	3
tRNA-Met M	3906	29	GGCATGATTATTTAGGATAGTGGGAACGG	13
ND2	3962	28	GGACATTAGTGTTATAGGTCGTGGTTGG	9
ND2	4110	23	GGAGTTATTAATAGGAGGACCGG	11
ND2	4234	14	GGAGCGGGGTAAGG	18
ND2	4663	18	GGATCCTCCGGAAGGTGG	15
ND2	4877	22	GGGTTGGATTATAAAAGGTGGG	14
ND2	4920	18	GGGATGGGGATCGGGGGG	39
COX1	5639	26	GGATGGTGGTAGTAAAGAGGAAGAGG	16
COX1	5714	25	GGGTGGAGATCGGCCTTTAGATCGG	13
COX1	5844	29	GGGGGTCGGTATTGTGTCATAGTTTGAGG	4
COX1	6821	30	GGGAGGTGGTATAGTGTGTAAGCTCCTTGG	3
COX2	7027	30	GGTTGAACCAGATGTTCTGCGGTGTAGGGG	3
COX2	7290	30	GGCATAATTGGCAATTTTGGTATCCCGTGG	20
COX2	7489	25	GGAGGTGAGTACTCGTCAGGGGAGG	9
ATP6	8005	21	GGAAGTTAGGATAAGGGTAGG	18
ATP6	8034	29	GGATTAGTTGTTGGCAGAGGTAAGAAAGG	15
ATP6	8178	30	GGATCCGGAAAATGGTGTATGTAAATGTGG	12
ATP6	8304	24	GGTGAAGGAAGGTGTTCCTTGAGG	13
ATP6	8558	27	GGATGCATAAGTGGGAGGATCATTCGG	13
COX3	8649	30	GGTACTGGTAATTGACCTCGGAAAAGTCGG	14
COX3	8737	24	GGGAACCGGATGAGTGGTTATAGG	20
COX3	8803	15	GGATGGTTCCGGTGG	18
COX3	8955	28	GGAGGTTGTCCTTAAAGTGGTGAATTGG	9
tRNA-Arg R	9872	27	GGTTATACGGTAGATGGAAGAAGTTGG	18
ND4L	10034	29	GGTATTCGAGGTATGGTTAGGGGTAGTGG	19
ND4	10343	15	GGGGGATAGGTGTGG	19
ND4	10667	26	GGTTTTGGTACATCCTTGGGATTTGG	16
ND4	10943	19	GGGGAAGTAGGAAGAGAGG	15
ND4	11425	25	GGTTGGTATATTAATTGGAGGTTGG	13
ND5	11791	27	GGGGTTAGGATTAAAGTTATAGTTTGG	5
ND5	11869	24	GGAAGTAATAATCGGAGAATGGGG	10
ND5	12121	23	GGTACGAATAGGAGTGGAGTCGG	16
ND5	12425	18	GGAGGTGGGTACTGATGG	15
ND5	12515	23	GGATGACCAGGCTAAGGTGGGGG	18
ND5	12701	20	GGTTGGTGTGGATCGTAAGG	16
ND5	12872	26	GGAGCGGGAGTGTCCTTATGGTAAGG	13
ND5	12943	23	GGACGTTGTGGTTGCGGACTCGG	18
ND5	13044	24	GGCGCAAAAGGGGGGGATTAGAGG	17
ND5	13082	29	GGGTCTGGAGTATTTGGGTTAGTTTGCGG	16
ND5	13158	22	GGTGGTTGGTCGTAAGGTCAGG	18
ND5	13370	29	GGATTCGGATTTTTGTAGGGATTGAGAGG	16
ND5	13423	17	GGTAGGGTTTTAGGTGG	17
ND6	13644	23	GGCGATGGGGTTAGGGAGGAAGG	21
ND6	13689	28	GGAGTATGTAGTTGGTTAGAGGGTTTGG	14
ND6	13868	23	GGTTTGTGTTGGTTGTAGGGGGG	15
ND6	13928	29	GGTGGTTTGGGATTTTGGTAATTTGTTGG	18
ND6	13964	26	GGTGATTGTTAATTTGGATTTGGAGG	9
CYTB	14204	16	GGATGGACGGGTAGG	20
CYTB	14588	17	GGAGGATAGTCGGTAGG	16
CYTB	14662	27	GGTGGAACTGGGCTAAGAAGCGAAAGG	9
CYTB	14732	14	GGAGGAGAAGGAGG	18
CYTB	14916	28	GGTCGATTAGGTGATTTGTGGGGTGGGG	18
CYTB	14996	28	GGGGTTATTTGATCCTCCACAGGATCGG	4
CYTB	15049	23	GGGATTATGGAAAGGAAGTATGG	18
CYTB	15151	30	GGACTTAACCCCCGGTTGGTCATCTTGTGG	12
tRNA-Pro P	15375	10	GGGGTGGTGG	20
Non coding	15652	20	GGTATACTGATAGGGGAAGG	11
region of the	15672	29	GGTAAACCAGATAATTAGATGGTAGGAGG	4
D-loop with	15707	25	GGTTGTTGGGCGGGTGGTTACGGGG	20
the CSBI-III	16088	20	GGTTTGGGGGTGGGGAGG	21
plus strand				
minus strand				

Recently, a tool was developed to compare nucleotide sequences for the homology of their G-quadruplexes. Mitochondrial 12s rRNA and 16S rRNA contained several G-quadruplexes. Comparison of the two ribosomal RNAs with the QGRS-H-predictor[76] showed that there is only one G-quadruplex conserved in both ribosomal RNAs indicating that the G-quadruplexes listed in Table 6 are very different in their properties (Table 7).

Table 7 QGRS-H Homology score of 12S rRNA and 16S rRNA

RNA	Position	Tetrads	G-Score	QGRS Homology Score
12S rRNA	573-589	2	30	0.862
16S rRNA	832-858	2	26	

This variability of the detected G-quadruplexes in mtDNA transcripts leads to the assumption that the binding of NOA1 to its yet not identified target RNA is very specific, although in principle there are very many other G-quadruplexes available in the mitochondrion.

P. Phosphorylation of Casein Kinase II influences nuclear export of NOA1

NOA1 is a dual targeted protein with localization in the nucleus and the mitochondria. Nuclear import and export of proteins can be modulated by phosphorylation. *In silico* analysis of putative NOA1 phospho-sites indicated multiple phosphorylation by Casein Kinase II (CKII).

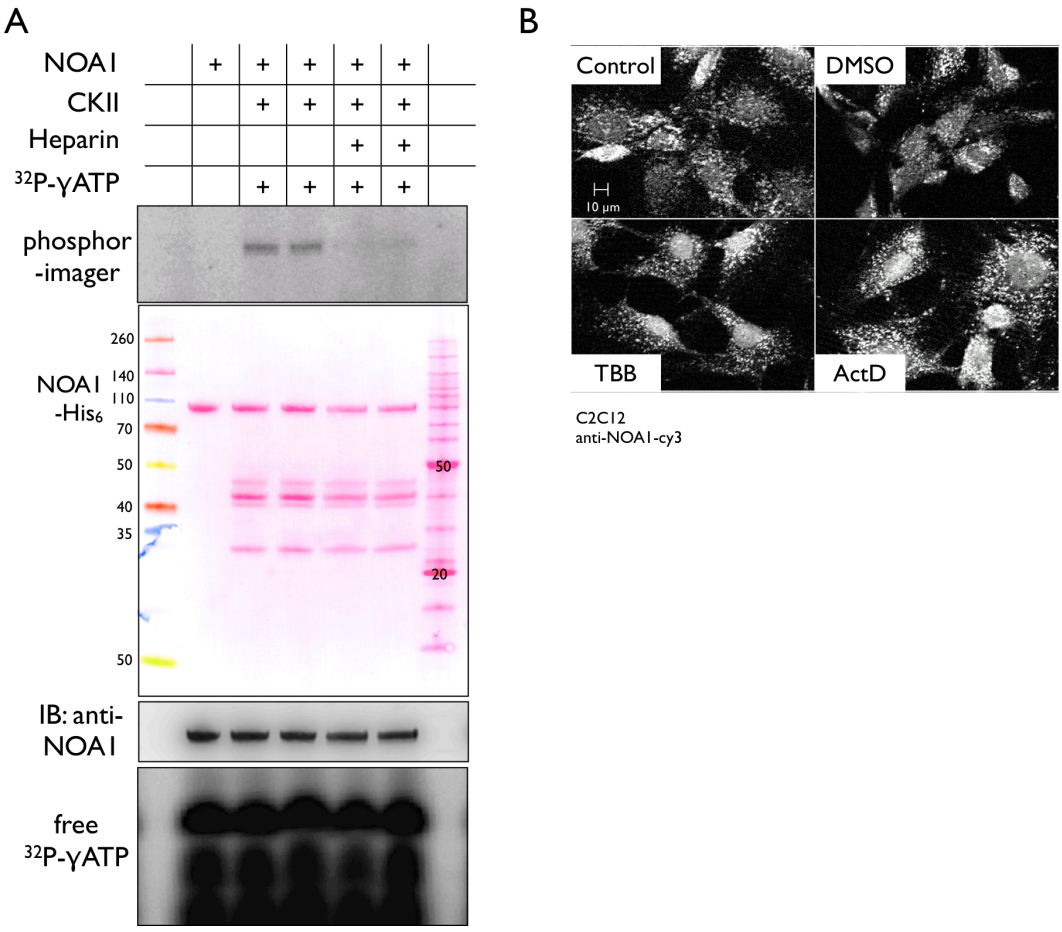

Figure 31 Casein Kinase II phosphorylates NOA1. A) An *in vitro* assay with ^{32}P-γATP showed phosphorylation of NOA1 by CKII. B) The specific CKII inhibitor TBB lead to nuclear accumulation of endogenous NOA1 in C2C12 cells stained for NOA1. The impairment of nuclear export by TBB was similar to the effect of the nuclear export blockers Actinomycin D and Leptomycin B.

In an *in vitro* assay using recombinant NOA1-His$_6$ and recombinant CKII the phosphorylation of NOA1-His$_6$ was detected. Addition of heparin, an inhibitor of CKII, blocked the transfer of phosphate to NOA1-His$_6$ (Figure 31A). Recently, it was shown that the nucleo-cytoplasmic shuttling of the transcription factor PPARγ is dependent on CKII phosphorylation[77]. To test the correlation of CKII phosphorylation and NOA1 subcellular localization *in vivo*, cells were stained for endogenous NOA1 after treatment with 4,5,6,7-tetrabromobenzotriazole (TBB) a selective CKII inhibitor. Cells treated with TBB accumulated endogenous NOA1 in the nucleus comparable to treatment with Leptomycin B (Figure 31B, Figure 21). Therefore, Casein Kinase II phosphorylation triggers the nuclear export of NOAI.

Q. NOA1 is cleaved by Caspase-1 dependent on the phosphorylation status of serine 421

Beside the modulation of subcellular localization, CKII is involved in the caspase-dependent pathways of apoptosis[64]. CKII can phosphorylate serine and threonine residues of its substrates. NOA1 contains eight putative CKII phosphorylation sites of which 7 are threonine sites and one is a serine sites (Figure 32A).

As one predicted phosphorylation site of NOA1, serine421, is in close proximity to a predicted caspase-1 celavage site the cleavage of NOA1 by caspase-1 and the effect of CKII phosphorylation were investigated in an *in vitro* assay. Recombinant NOA1-His6 was subjected to CKII phosphorylation for 10 and 20 minutes. Western blot analysis with an anti-phospho-serine antibody showed the increase in serine phosphorylation of NOA1 (Figure 32B). Serine421 is in close proximity of the predicted caspase-1 cleavage site and both sites are highly conserved. *In vitro* cleavage assay with recombinant caspase-1 showed the processing of NOA1 into the predicted ~52 kDa and 25 kDa fragments (Figure 32D). The phosphorylation of NOA1 by CKII prior to caspase-1 cleavage assay inhibited the processing (Figure 32E). It is excluded that CKII inhibits caspase-1 directly since caspase-1 is a substrate for CK1 but not CKII[78,79].

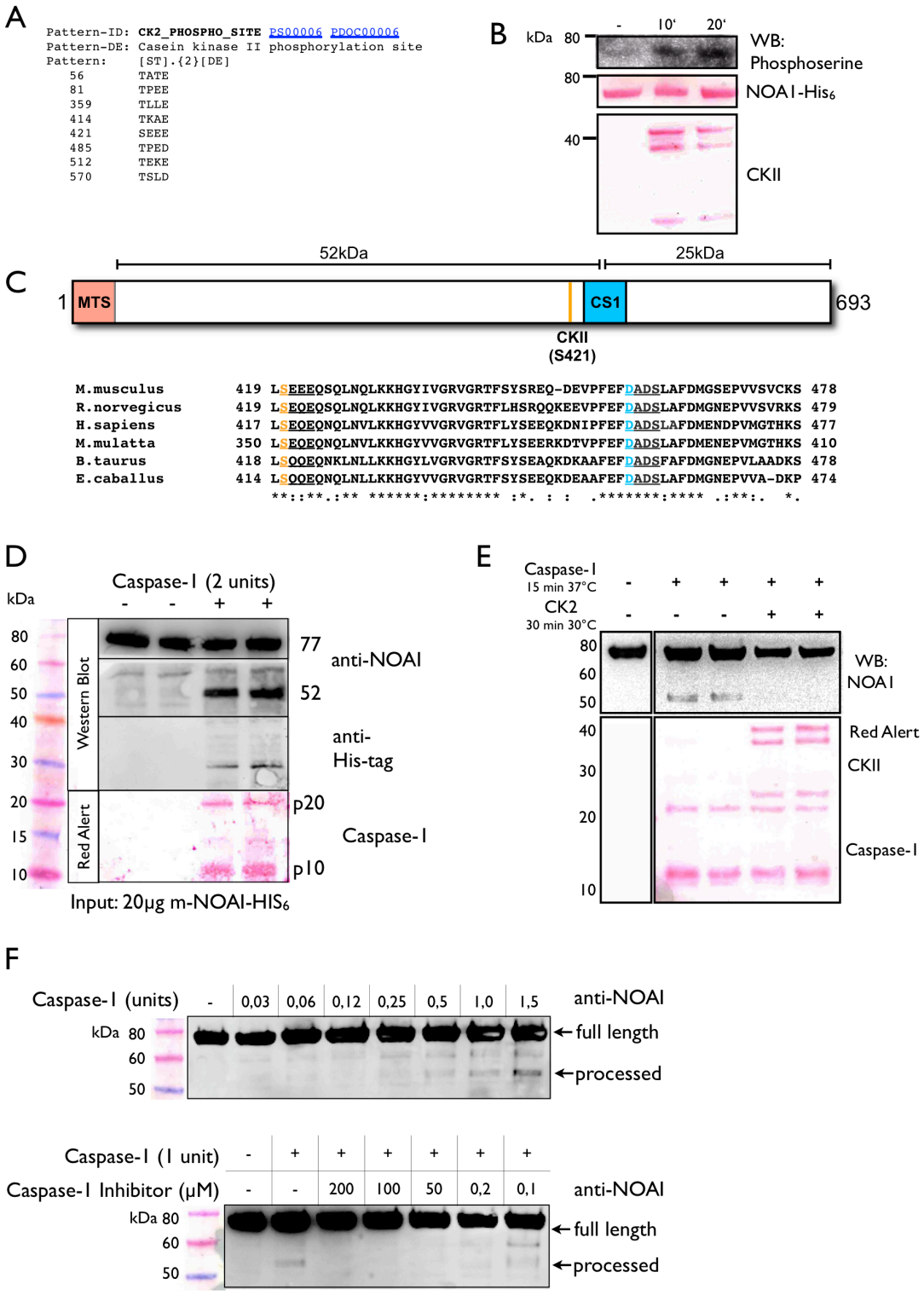

Figure 32 NOA1 is serine-phosphorylated by Casein Kinase II (CKII). A) Besides seven threonine sites, NOA1 has one predicted serine-phosphorylation site specific for CKII at serine 421, which is in close proximity to the caspase-1 cleavage site. B) Increased serine phosphorylation after CKII addition was detected. C) NOA1 has a conserved caspase-1 cleavage site (blue F*DADS). Species alignment showed a high degree of conservation. D) *In vitro* caspase-1 cleavage assays results in the expected fragment sizes of 52 and 25 kDa. E)

CKII phosphorylation of NOA1 inhibited processing by caspase-1. F) Caspase-1 cleavage is concentration dependent and can be specifically inhibited by Caspase-1 inhibitor.

The processing of NOA1 by caspase-1 was dependent on the amount of proteolytic enzyme and was specifically inhibited by casapse-1 inhibitor in a concentration dependent manner (Figure 32F).

As final proof of the specificity of caspase-1 cleavage, the predicted caspase-1 recognition site „F'DADS" was mutated into „F'DGDS" and the recombinant NOA1A460G mutant protein was produced. This form was not processed by caspase-1 (Figure 33).

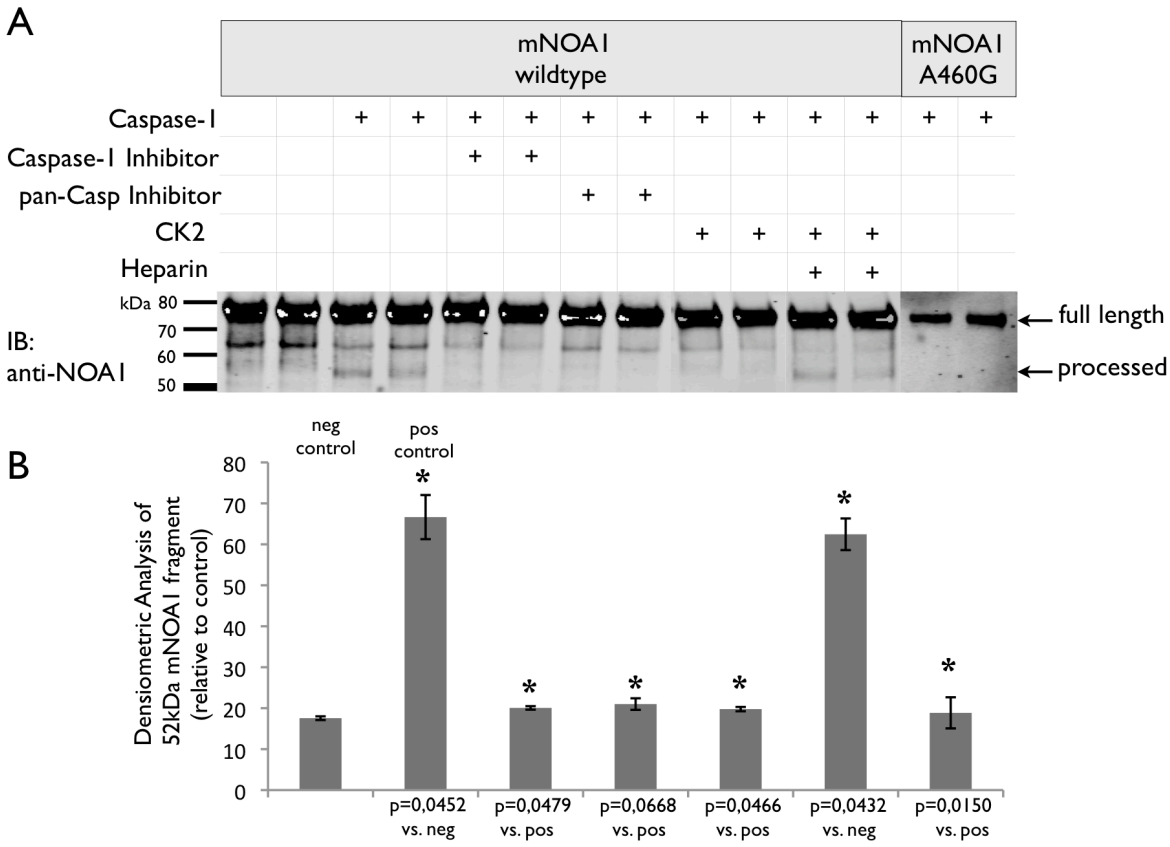

Figure 33 Identification of Serine421 as the Caspase-1 specific cleavage site. Phosphorylation by CKII inhibits the processing. Heparin inhibits phosphorylation by CKII and facilitates cleavage by Caspase-1. The A460G mutation in recombinant NOA1 abolishes the Caspase-1 recognition site. The mutant is not cleaved by Caspase-1. The cleavage is a specific process that can be inhibited by pan-Caspase-Inhibitor and specific Caspase-1 inhibitor.

Experiments with recombinant caspase-3 and caspase-8 did not show any processing of wild type NOA1 supporting the uniqueness of NOA1 as caspase-1 substrate.

In conclusion, NOA1 has a single recognition site for caspases specific for caspase-1 (458 F'DADS 462). Caspase-1 cleaves NOA1 into two fragments, the 52 kDa N-terminus and a 25 kDa C-terminal fragment *in vitro*. The physiological meaning of this site remains unclear, as stimulation of cells with the classical caspase-1 activator lipopolysaccharide (LPS) was not sufficient to process endogenous NOA1 *in vivo* although the cells used in this assay express Toll-like receptor 4 (TLR4) which is responsible for the LPS response. Probably the intrinsic pathway inducing this proteolysis is more complex and has to be analyzed with various cell types and apoptotic stimuli. However, the cleavage of NOA1 by caspase-1 is certainly linked to protein function and/or localization since the truncation of the 25 kDa C-terminal fragment alters mitochondrial import as shown with the NOA1ΔC-terminus variant (Figure 12A, C).

R. NOA1 is a substrate of the mitochondrial ClpXP protease

Degradation is as important for protein function as are subcellular dynamics and posttranslational modifications. Regulatory proteins often have short half-lives and are regulated by degradation[80]. Mitochondria contain a variety of peptidases with different functions[81,82]. The matrix metallo-proteases are processing proteases that cleave the mitochondrial presequence after proteins are imported to the mitochondrial matrix. For protein quality control and degradation the matrix contains three major ATP-dependent proteases. The AAA+ protease m-AAA is an innermembrane protein that faces the matrix. Lon protease and the heterodimeric ClpXP are soluble matrix proteases. Therefore the degradation of NOA1 inside the mitochondrion was investigated.

The mitochondrial proteases as well as NOA1 were ubiquitously expressed in all tissue (Figure 34A) and the mitochondrial proteins NOA1 and ClpX were colocalized (Figure 34B). NOA1 was stabilized upon knockdown of the catalytical subunit ClpX of the ClpXP protease (Figure 34C) suggesting that NOA1 is a substrate of the mitochondrial ClpXP protease.

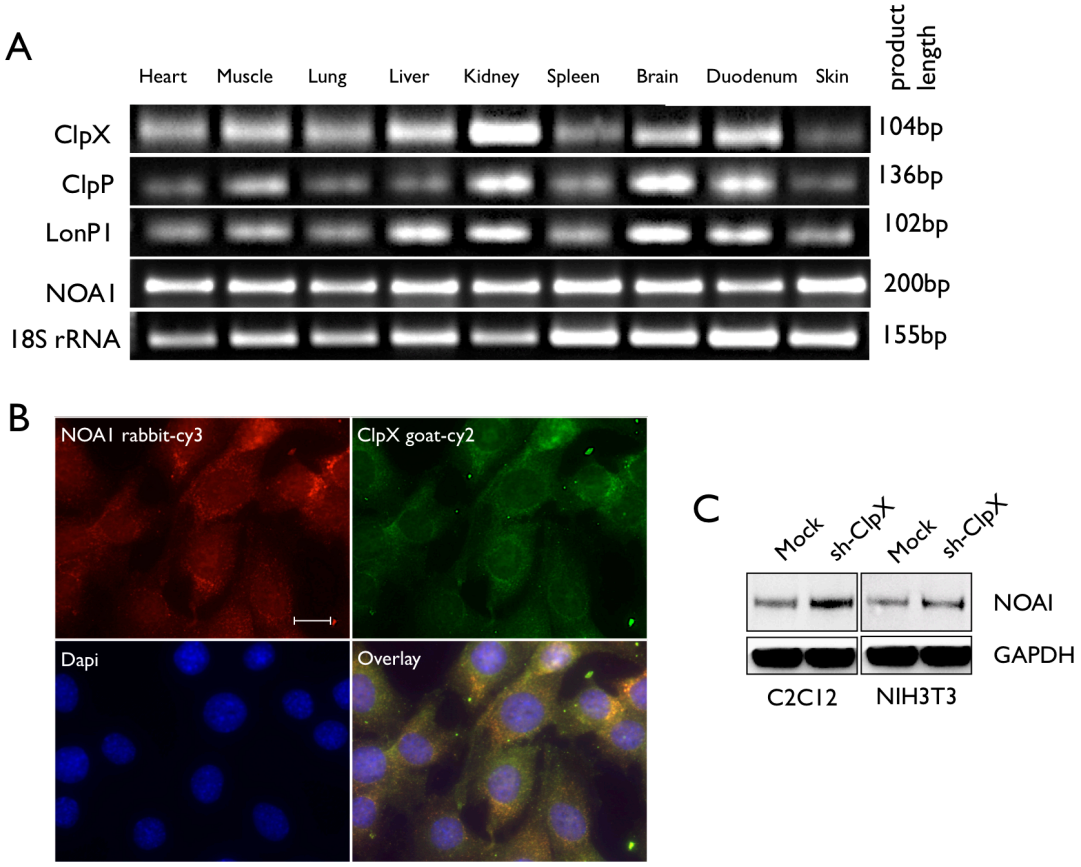

Figure 34 Expression of ClpX. A) Ubiquitous transcript expression of mitochondrial matrix proteases ClpX, ClpP and LonP1 in mouse tissue. B) Colocalization of ClpX and NOA1 in mouse myoblasts (scale bar 10µm) Knockdown of ClpX in leads to the accumulation of NOA1 protein in C2C12 myoblasts and NIH3T3 fibroblasts. GAPDH shows the equivalent protein loading

To prove that NOA1 is a substrate for ClpXP the amino acid sequence of NOA1 was screened for ClpXP recognition sites. The C-terminus of NOA1 contains three motifs that are aligning to the C-motif 2 that is a known recognition motif for ClpX in *E. coli*[53] (Figure 35A). Alanine mutation of the most C-terminal lysines K690 and K691 was sufficient to significantly stabilize NOA1 compared to wild type NOA1 (Figure 35B).

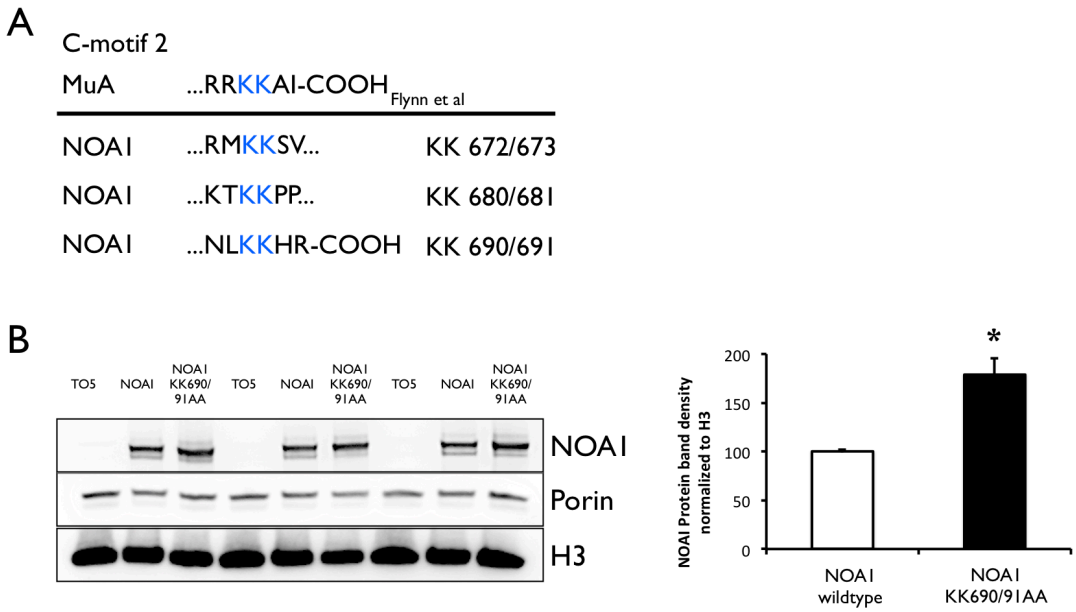

Figure 35 The C-terminus of NOA1 contains sequences similar to the ClpX recognition motif. A) Alignment of the ClpX consensus motifs from the C-terminus of NOA1 with C-motif 2[53]. B) Alanine mutation of the lysine 690 and lysin 691 is sufficient to stabilize NOA1 in C2C12 cells.

While ClpX could be detected by Western blot in mouse liver mitochondria (Figure 36A) in whole cell lysates of C2C12 it was only detected after overexpression mitochondria (Figure 36B). ClpX expression reduced tagged and unmodified NOA1 protein *in vivo* (Figure 36C). This shows that the increase of ClpX was sufficient to increase the activity of the whole ClpXP complex.

Based on the study by Santagata et al[83] a mutant mouse ClpXK300A defective in ATP hydrolysis was generated by site-directed mutagenesis. As reviewed by Baker and Sauer[52] ClpX is an ATPase that uses the energy derived from ATP hydrolysis for substrate recognition an transporting the unfolded peptide to ClpP. Surprisingly, the ClpXK300A mutant still degraded co-expressed NOA1 (Figure 36D) to the same degree as wild type ClpX although the mutation was properly introduced (Figure 36E). One reason for the persisting activity of dominant negative ClpXK300A mutant might be the oligomeric state of ClpX. Since up to four ATPs can be bound by the ClpX hexamer at a time, the overexpression of ClpXK300A could result in chimeric hexamers that maintained residual enzymatic activity.

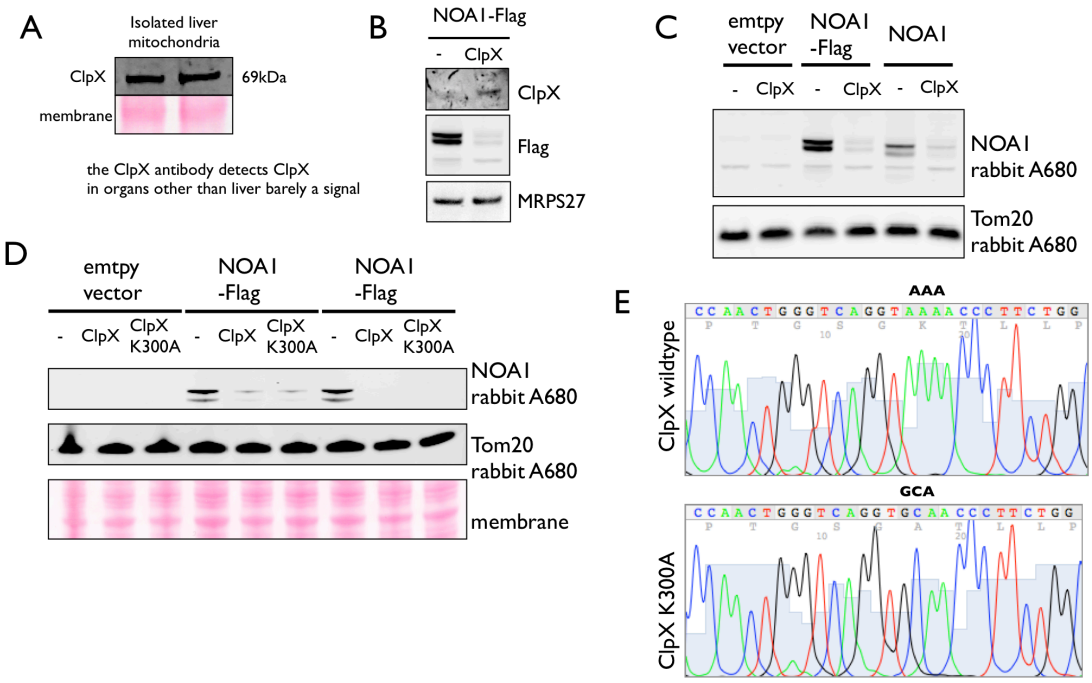

Figure 36 ClpXP degrades NOA1 in cells. A) The ClpX antibody correctly recognizes the 69kDa ClpX in lysates from liver mitochondria. B) Overexpression of ClpX in C2C12 cells leads to degradation of simultaneously expressed NOA1-Flag. C) ClpX coexpression dramatically reduces coexpresed tagged and untagged NOA1. D) A mutation of lysine 300 in the ClpX coding sequence was described to be enzymatic dead and unable to process substrates. In our case no inactivity occurs. E) Comparison of the original sequencing files of the wildtype and the Clpx K300A expression construct.

In collaboration with Dr. Julia Kardon from the laboratory of Prof. Dr.Tania Baker NOA1 was subjected to *in vitro* degradation assays with recombinant *S. cerevisiae* and *E. coli* ClpXP. A mixture of ClpX and ClpP degraded NOA1 within a time <3 minutes. ClpP alone was not able to degrade NOA1 (Figure 37).

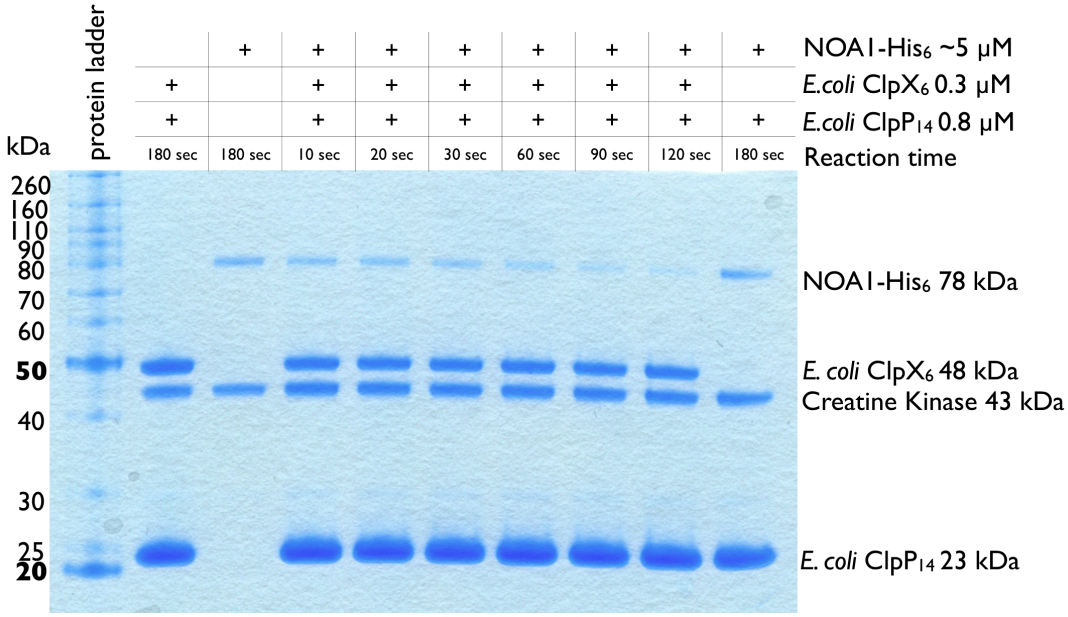

Figure 37 ClpXP *in vitro* degradation of NOA1. Coomassie stained 10% Bis-Tris SDS-PAGE gel showed that *E. coli* ClpXP degraded recombinant NOA1-His$_6$. The degradation was dependent on ClpX. ClpP alone does not degrade NOA1.

Upon substrate binding the ATPase rate of ClpX is stimulated[84]. This was the case when NOA1-His$_6$ protein was added to *E. coli (*Ec) or *S. cerevisiae* (Sc) ClpX protein. In both cases the ATPase rate of ClpX increased about 2 fold (Figure 38; data provided by Dr. Julia Kardon).

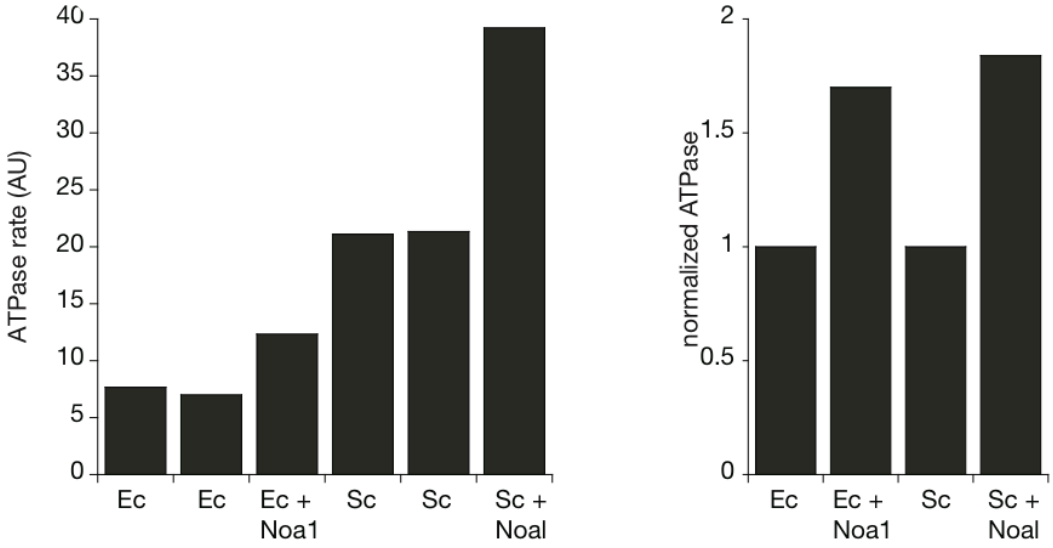

Figure 38 NOA1 stimulated the ATPase activity of *E. coli (*Ec) and *S. cerevisiae* (Sc) ClpX ~2 fold.

In summary, ClpX modulates NOA1 protein levels. The C-terminus of NOA1 contains recognition motifs for ClpX and mutation of these motifs is sufficient to stabilize NOA1 *in vivo*. Substrate binding stimulates the ATPase rate of ClpX. NOA1 induces a 2-fold increase of the ATP hydrolysis rate of ClpX.
In summary, NOA1 is hereby identified as the first mammalian substrate of the mitochondrial ClpXP protease.

S. GTP hydrolysis and the availability of the nascent chain are essential for the interaction of NOA1 with the mitochondrial ribosome.

Previous studies have suggested that NOA1 is a ribosome assembly factor and is involved in the regulation of mitochondrial protein synthesis[4,5,7]. Although quite some data are published, the exact molecular function of NOA1 during mitochondrial protein synthesis remains unknown.
To investigate the interaction of NOA1 with the mitochondrial ribosome comigration studies using sucrose gradient fractionation of whole cell lysates were performed. To ensure the stability of mitochondrial ribosomes conditions with high potassium salt concentrations were chosen. Western blot analysis showed the presence of NOA1 in those fractions that contained either the small ribosomal subunit 28S or assembled 55S ribosomes (Figure 39A).
To analyze the effect of GTP and the nascent protein chain of this interaction of NOA1 with the ribosome the comigration sutides were repeated with GTP, GTPγS or Puromycin. Puromycin is a bacterial nucleoside analog of the peptidyl-tRNAs and induces premature termination of translation with subsequent release of the nascent protein chain.
Figure 39B compares the 55S fraction under these different conditions. GTP alone did not alter the amount of NOA1 protein comigrating with the mitoribosome compared to the untreated sample. Non-hydrolysable GTPγS increased the amount of NOA1 at the mitoribosome. Thus GTP hydrolysis is required for the release of NOA1 from the mitoribosome *in vivo*. Furthermore, the addition of puromycin removes NOA1 from the ribosome showing that the nascent peptide chain is essential for the interaction of NOA1 with the ribosome (Figure 39B).

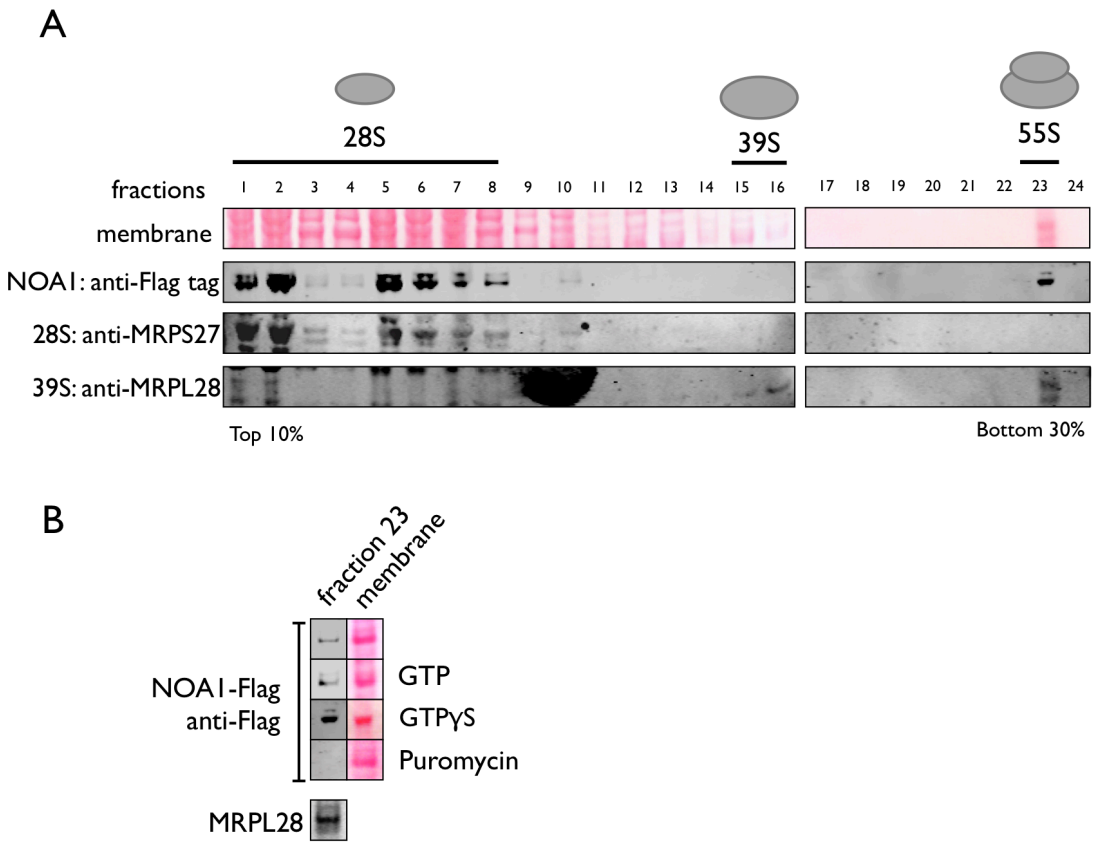

Figure 39 Sucrose gradient fractionation of NOA1 and the mitoribosome. A) Representative sucrose gradient with sucrose concentrations from 30% (bottom) to 10% (top). The small mitoribosomal subunit was detected by anti-MRPS27 antibody and the large mitoribosomal subunit by anti-MRPL28 antibody. B) Addition of GTPγS increased the amount of NOA1 protein comigrating with the 55S mitoribosome. Puromycin treatment of the cells removed NOA1 from the mitoribosome. This is representative data from two independent experiments.

In summary, the interaction of NOA1 with the mitoribosome seems dependent on the nascent protein chain while the release of NOA1 from the mitoribosome is dependent on GTP hydrolysis. This was also shown by others[7] with an *in vitro* experimental setup.

T. NOA1 enhances membrane insertion of in vitro translated mitochondrial transcripts into inverted vesicles of the mitochondrial inner membrane

To test the influence of NOA1 on mitochondrial translation and membrane insertion an *in vitro* mitochondrial protein synthesis approach was set up. To date no mitochondrial *in vitro* translation system is available. The basic mitochondrial *in vitro* translation mixture used contained mitochondrial inverted inner membrane vesicles,

mitochondrial matrix fraction, and mitochondrial RNA, an ATP regeneration system based on creatine kinase and ^{35}S-radiolabeled amino acids methionine and cysteine. Rat liver was used for the preparations of the single components (performed by Dr. Steffi Goffart). The components were mixed and either recombinant NOA1-His_6 protein or the mitoribosomal translation inhibitor chloramphenicol was added. After *in vitro* translation the samples were separated into a pellet fraction consisting of the inverted vesicles and a supernatant fraction containing the soluble matrix proteins. Both fractions were precipitated and the proteins were separated over a high percentage acrylamide gel.

The majority of radioactive signal was unspecific (*) and probably caused by binding of radioactive amino acids to high molecular weight protein complexes, e.g. tRNA-aminoacyltransferases or ribosomes. Only two bands of approximately 15 and 10 kDa size (i and ii) were chloramphenicol sensitive and therefore specific mitochondrial translation products (Figure 40B). The abundance of these products in the membrane fraction was increased by addition of NOA1, suggesting a simulation of membrane insertion of freshly translated proteins by NOA1 (lane 3). The positive effect on membrane insertion is independent of the GTPase function of NOA1 (lane 4). A densitometric analysis of the membrane insertion of the basic translation with and without NOAI shows the two specific peaks (i and ii) (Figure 40C).

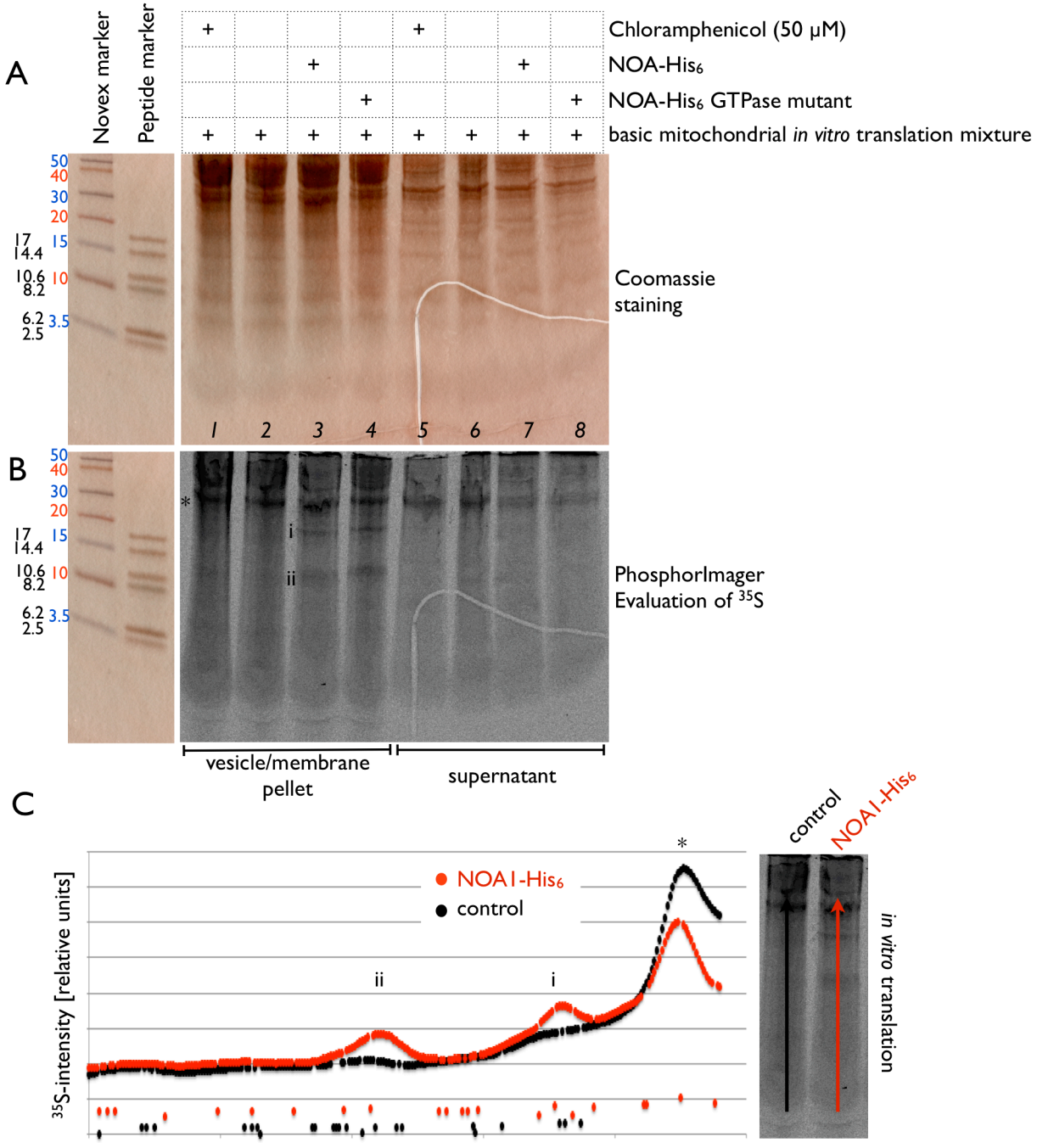

Figure 40 *In vitro* translation of mitochondrial proteins in the presence of ^{35}S-radiolabeled methionine and cysteine and inverted inner membrane vesicles A) The coomassie staining of the dried gel served as loading control. B) The phosphorimager screen showed the bands of ^{35}S-radiolabeled proteins. C) Intensity plots of translation products with and without recombinant NOA1-His$_6$ protein.

In summary, these results lead to the conclusion that NOA1 positively influences membrane insertion of mtDNA encoded proteins.

VII. Summary of results

- NOA1 has dual localization. It is first targeted to the nucleus where it associates to the nucleolus and then imported into mitochondria where the targeting presequence is processed. (VI.B-VI.J, VI.P)
- The NOA1 binds to G-quadruplexes in a GTPase independent manner. G-quadruplex binding stimulates the GTP hydrolysis rate (VI.K-VI.O).
- $NOA1_{Serine\ 421}$ phosphorylation by CKII influcences the cleavage by caspase-1 *in vitro* and nuclear shuttling *in vivo* (VI.P, VI.Q).
- NOA1 is a substrate of mitochondrial ClpXP protease (VI.R)
- NOA1 binds to the ribosome in a GTP and nascent chain dependent manner and stimualtes the membrane insertion of mitochondrial translation products (VI.S, VI.T).

VIII. Discussion

A. A Detour through the Nucleus before Mitochondrial Import – is this the right Route?

The structure and function of the mitochondrial protein synthesis machinery is different from the cytosolic translation apparatus in eukaryotic cells. A variety of mitoribosome associated proteins contribute to different steps of protein synthesis like mitoribosome assembly, rRNA folding, ribosome stability and support membrane targeting of the translated protein products.

The bacterial NOA1 protein homolog YqeH was described to act as "ribosome assembly factor" and "rRNA chaperone"[6,8,9,57,85,86]. Although comprehensive studies with mammalian NOA1 in cells[4,58] and the generation of knockout mice[5] verified the major impact of NOA1 on cellular survival in general and on mitochondrial metabolism specifically, no concise picture of the underlying molecular mechanism was obtained. This study concentrates on the molecular characteristics of mouse NOA1 protein by analyzing the features of conserved domains and motifs.

Dual Localization in the Nucleus and the Mitochondria

Differential targeting of proteins might play a key role in the regulation of cellular functions. Targeting of proteins to different locations can be based on multiple mechanisms. A gene can be duplicated resulting in two separate isoforms of a protein. Alternative splicing of a single gene transcript can generate two translation products, or downstream of transcription, posttranslational processes can modulate protein targeting. Folding, ligand binding and/or conformational and various posttranslational modifications can mask a targeting signal. Such considerations are especially important when two targeting signals compete with each other. The biophysical characteristics of different N-terminal targeting signals are almost identical and to date the parameters that regulate the distribution of such proteins is essentially unknown.[87,88] Some mitochondrial proteins are targeted to different locations thereby maintaining different functions dependent on cellular needs and act as signaling switches to guarantee fast adaptation to cellular signals.

NOA1 contains a classical bipartite nuclear localization signal (NLS), which targets NOA1 to the nucleus. This was already described when NOA1 was identified in

plants[56]. The simultaneous staining of endogenous and overexpressed NOA1 protein shows that both subcellular localizations, mitochondrial and nuclear, are characteristic for NOA1. Comprehensive analysis of the NOA1 transcript demonstrates that NOA1 is encoded by a single messenger RNA with is no evidence for alternative splicing. The analysis of the NOA1 protein supported the finding that under standard conditions the NOAI polypeptide is not modified or cleaved. Only the N-terminus is processed after mitochondrial import.

Nuclear Localization is accompanied by C-Terminal Toxicity

When this work started all published data about NOA1 concerned its mitochondrial function. Hence, studying the nuclear localization and function of NOA1 was considered pivotal to understand the dual localization of NOA1 in general. Surprisingly, the nuclear accumulation of N-terminally truncated NOA1 lead to immediate cell death. This made it impossible to work with the nuclear mutant (NOA1ΔMTS). The C-terminal domain contains a conserved TRAP-like RNA-binding motif, which is responsible for the induction of caspase dependent apoptosis. The functional impact of the C-terminal RNA-binding motif is similar in the bacterial homolog YqeH[57]. The C-terminus carries toxicity when the NOA1 protein is accumulating in the nucleus. The intrinsic toxicity of the RNA-binding domain was ascertained by removal of the C-terminus, which rescued nuclear lethality.

To overcome the lethal effects of overexpression of nuclear NOA1 the experimental setting was revised. Also the focus of the investigation changed and treatment of cells with numerous chemical drugs was employed to analyze the dynamics of NOA1 localization. Some compounds induced nuclear accumulation of NOA1-EGFP fusion protein without affecting mitochondrial integrity. However, a dose-dependent cell death occurred after drug stimulation comparable to the lethality induced by NOA1ΔMTS. The initial observation that NOA1 localizes to the nucleus was confirmed and refined. Drugs that induced nuclear accumulation of NOA-EGFP were applied on non-transfected cells and uncovered that some foci of endogenous nuclear NOA1 are co-localizing with nucleoli. Furthermore, NOA1 is spread in speckles throughout the nucleus.

NOA1 in the Nucleolus

Nuclear speckles are partitions within the nucleus that are localized to inter-chromatin areas. They are dynamic compartments that contain factors involved in RNA storage, processing, modification or assembly into complexes[89]. Due to this role in RNA biogenesis and maintenance nuclear speckles mainly contain RNA-binding proteins like heterogenous nuclear RNPs (hnRNPs), small nucleolar RNPs (snRNPs), splicing factors and pre-mRNA binding proteins.

Studies on NOA1 interacting proteins involved isotopic labeling and immunoprecipitation of target proteins bound to NOA1. One such interaction study was published from our group[4]. Candidates were considered interaction partners if they were enriched >3-fold in the NOA1 precipitate. Mitochondrial ribsosomal proteins, subunits of OXPHOS complexes and the prohibitins were found to interact with mitochondrial NOA1[4]. A multiplicity of such interaction studies was performed during the work with the NOA1 protein. Interestingly, if proteins that enriched to a lower degree (>1.5-fold and <3-fold) were analyzed a battery of nuclear localized RNA-binding proteins was identified. The list of results contains hnRNPs, snRNPs, splicing factors, poly-A-binding proteins, pre-mRNA binding proteins and helicases. Estimating from the immunofluorescence staining more than 90% of the NOA1 protein is mitochondrial and only a minor portion is nuclear, therefore it cannot be expected that nuclear interacting proteins are enriched to the same degree as mitochondrial ones. Considering the localization of endogenous NOA1 to nuclear speckles it will be an important duty to validate these interaction partners in the future. Since the characterization of nuclear speckles is weak no further analysis of the localization of NOA1 to this compartment was made.

The nucleolar association was verified by co-staining with UBF1, the main marker for nucleoli. Interaction studies in the presence of RNAses and DNAse exclude that NOA1 and UBF1 interact via RNA or DNA bridges. This strengthens the hypothesis that NOA1 is imported into the nucleus and physically interacts with UBF1, a protein that is abundant at transcriptional start sites of ribosomal RNAs. The site of rRNA transcription is the place where cytosolic ribosomal particles get assembled. This is a noticeable thematic connection of the sub-nuclear localization and the suggested mitoribosomal function of NOA1.

Active Nuclear Import and Crm1-dependent Nuclear Export

To avoid artifacts it was crucial to show that NOA1 is actively imported into and exported from the nucleus. Proteins carrying a classical NLS are normally imported by the importin α/β system. Indeed, recombinant NOA1 protein is actively imported into isolated nuclei *in vitro* resulting in the described speckled distribution. The application of GTPγS, a non-hydrolysable equivalent of GTP, inhibits the G-protein dependent importin α/β system and as a consequence inhibits the import of NOA1. The transcript and protein analysis revealed that NOA1 is a dual localized protein with two subcellular signals within the same peptide chain. This suggests that the nuclear localization of NOA1 and mitochondrial import is related. To address the sequence of events nuclear export blocking and fractionation assays were used. The data demonstrates that the nuclear localization occurs prior to the mitochondrial localization. The Crm1/exportin1 pathway is the main nuclear export machinery. NOA1 is accumulating in the nucleus when Crm1 is inhibited. The responsible nuclear export signal (NES) was identified within the NOA1 amino acid sequence. The functionality of the manually identified NES was validated by fusion of NLS and NES to EGFP in combination with the inhibition of nuclear export. The identification of the nuclear export signal proofs that the nuclear import/export of NOA1 is an essential mechanism of this protein. The NOA1-NES is encoded in opposite direction overlapping with the leucine-zipper domain. Nuclear export signals that overlap with leucine zippers are regulated by protein dimerization[71]. As long as the protein is dimerized the nuclear export signal is masked. This offers a lot of regulatory options for NOA1 since it is known that NOA1 can form dimers. A regulation by hetero-dimerization with other proteins is conceivable as well as ligand binding induced conformational change.

Sequence of Events: First Nucleus, Second Mitochondria

Two independent approaches confirm that NOA1 is first targeted to the nucleus and subsequently directed to the mitochondria. In a screen, chemical compounds were identified that induced nuclear accumulation of NOA1. No nuclear accumulation could be induced in the presence of the translation inhibitor cycloheximide showing clearly that only newly translated NOA1 protein is targeted to the nucleus. The mitochondrial population of NOA1 is not affected by the drugs and retains mitochondrial localization. Subcellular fractionation verified the nucleo-mitochondrial

pathway by showing that the nuclear fraction contains the longer, unprocessed NOA1 whereas the short, N-terminally processed NOA1 is exclusively detected in the mitochondrial fraction.

Taken together, these experiments support the proposed sequence of events, namely that NOA1 is (1) synthesized at cytosolic ribosomes, (2) targeted to the nucleus via importinα/β, (3) associating to nucleolar structures and nuclear speckles, (4) exported from the nucleus via Crm1 and finally (5) targeted to the mitochondria (Figure 41).

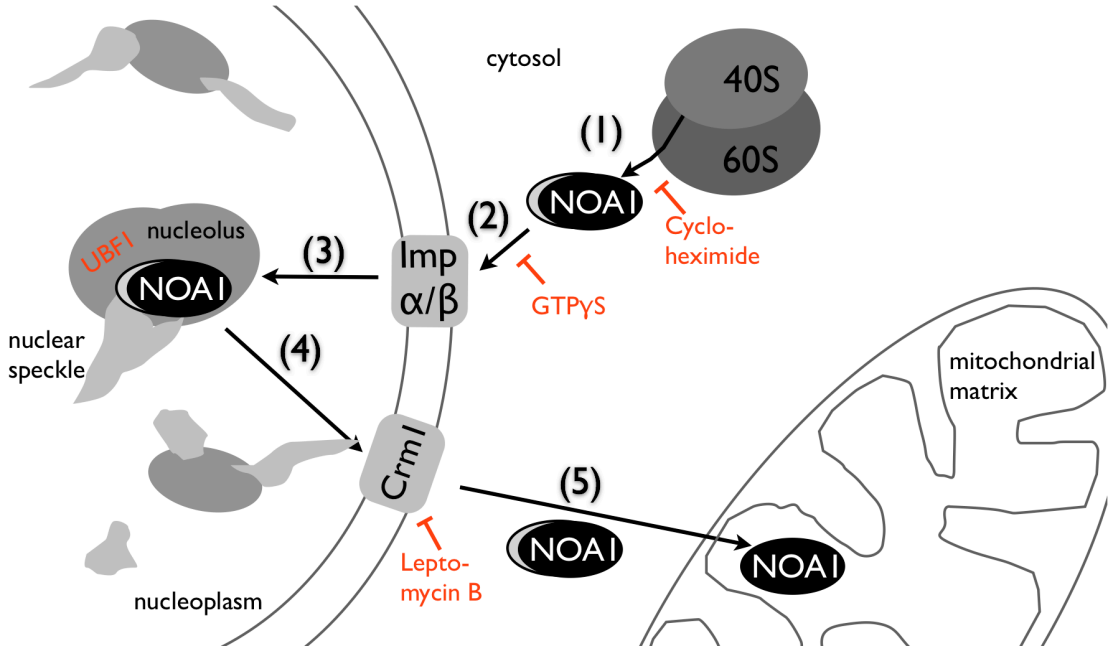

Figure 41 Schematic overview of the detour of NOA1 through the nucleus. Red marks the specific inhibitors and markers for each step. (1) Nuclear encoded NOA1 is translated by cytosolic ribosomes. (2) The nuclear importinα/β complex mediates NOA1' nuclear import. (3) NOA1 associates to the nucleolus and nuclear speckles. (4) Crm1 exports NOA1 from the nucleus. (5) Mitochondrial targeting is accompanied by the cleavage of the mitochondrial presequence.

Recently, the mitochondrial protein CRIF1 was shown to take the same route within the cell as shown here for NOA1[90]. Strikingly, another set of publications showed that functionally NOA1 and CRIF1 both act in the context of mitochondrial protein synthesis[7,91]. Importantly, NOA1 and CRIF1 probably share the same nuclear compartment as the family of nuclear factors that interact with CRIF1[92] is localized to nuclear speckles[89]. Hence, two independent sources provide evidence that proteins involved in mitochondrial protein synthesis, CRIF1 and NOA1, take this

specific detour route through the nucleus. The question remains what the functional relevance of this detour is. It might involve maturation and assembly events. However, further experiments dealing with the RNA-binding characteristics of NOA1 suggested a putative role of this unique nuclear targeting.

B. The G-Quadruplex binding NOA1 Protein – a Model for Mitochondrial Ribonucleoprotein Import?

The C-terminus of NOA1 contains a conserved RNA-binding domain. At the beginning of this study nothing was known about the characteristics of RNA-binding. Recently, NOA1 was described to have an affininty for DNA and RNA and especially for mitoribosomal RNAs[7]. However, no data regarding a consensus binding motif or a specific RNA ligand was shown.

Here, the "Selected Evolution of Ligands by EXponential Enrichment" (SELEX) approach was used to identify the main binding motif of the NOA1 protein. SELEX has the advantage that a specific core consensus is enriched independent of concentration differences or accessibility issues within a cell.

SELEX showed that NOA1 has high affinity for guanine rich (G-rich) sequences. Moreover, all G-rich sequences bound to NOA1 in the SELEX experiment were identified as G-quadruplexes.

G-Quadruplexes

G-quadruplexes are formed by single stranded G-rich DNA and RNA sequences[93] (Figure 42). In a G-quadruplex four guanines are forming planar sheets or even three-dimensional stacks that are stabilized by Hoogsten base pairing, that is the association of a third base to an existing classical Watson-Crick base pair by forming two additional hydrogen bonds. Such Hoogsten base pairings do not exist in double stranded DNA but they occur in triple helices, in RNAs[94] and the telomeres. Not every G-rich sequence can form a G-quadruplex. RNA G-quadruplexes are even more stable than DNA quadruplexes[75]. The formation of G-quadruplex depends on the presence of a cation ($K^+ > Na^+ > Li^+$) that organizes the guanine sheets and stabilizes the whole structure[95].

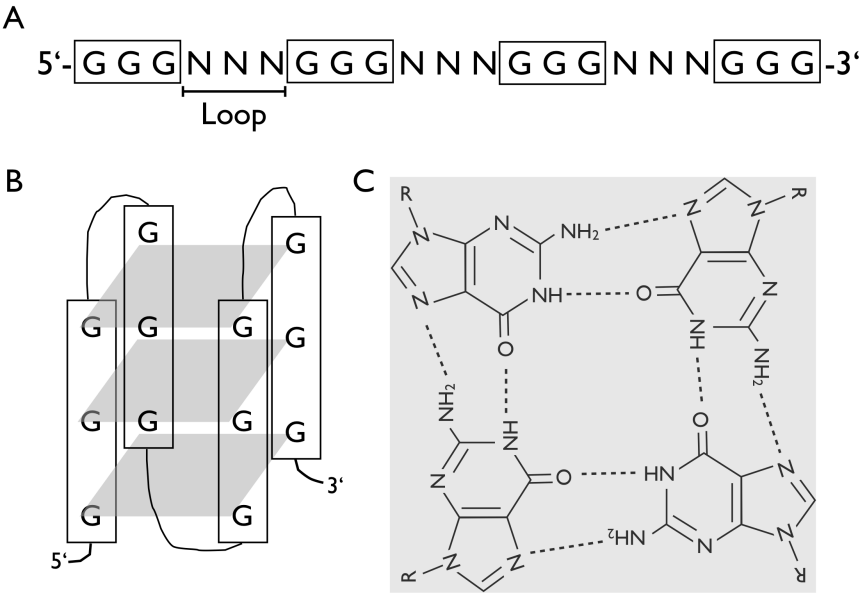

Figure 42 Schematic representations of G-quadruplexes. A) Three guanines form a G-quadruplex tetrad flanked by loop regions that contain random nucleotides. B) The guanines align in sheets and form C) hydrogen bonds by Hoogsteen base pairing as can be seen in the top view.

Reports about the functional relevance of G-quadruplexes in RNA biology literally exploded during the last five years. Many proteins binding to G-quadruplexes are resolving helicases for DNA or RNA G-quadruplexes[96,97], transcriptional[98] or translational[99] regulators. Therefore, G-quadruplexes are three-dimensional molecular regulators comparable to stem-loops in tRNA, miRNA and ribozymes. Both nuclear and mitochondrial genome contain G-rich stretches and there is some degree of conservation of functional G-quadruplexes[100]. Ribosomal RNAs are exceptionally G-rich and form G-quadruplexes that might play a role in the initiation of translation[94]. G-quadruplexes appear highly similar but their folding is not identical[101]. The variability of the number of guanines in a G-stretch and the number and probably the kind of the spacing nuclotides generate unique binding sites that are currently under investigation for the generation of highly selective and therapeutic drug design[102,103].

NOA1 couples G-Quadruplex Binding and GTP Hydrolysis

NOA1 binds to G-rich sequences in general, but solely the G-quadruplex stimulates the GTP hydrolysis rate. The work on YqeH provided evidence that the protein likely couples molecular recognition and GTP hydrolysis, but it was unclear if protein

or DNA/RNA-binding mediated the stimulation of the GTPase function. The herein demonstrated functional relationship of G-quadruplex binding and GTPase activity answers that question. Hence, NOA1 couples molecular recognition of G-quadruplexes to its enzymatic GTPase function. Earlier studies demonstrated that mature, mitochondrial NOA1 protein forms dimers in cell culture[4]. The incorporation of labeled G-quadruplexes into NOA1 oligomers seemed rather independent of the oligomeric state of NOA1. It has to be considered that crosslinking experiments are always prone to generate artifacts and further validation is needed whether G-quadruplex binding and oligomerization of NOA1 influence eath other. Others claimed that NOA1 is a RNA chaperone and that the ligand RNA would be a ribosomal RNA species[2,6,7]. Consequently, an extensive G-quadruplex prediction analysis of the mouse mitochondrial DNA and RNA was performed. As expected, the mitochondrial RNA contains a lot of G-quadruplexes. At this point an estimation of the G-quadruplex binding specificity of single transcripts cannot be made. However, this analysis explains why mitochondrial rRNAs and other mitochondrial transcripts have been amplified from RNA-immunoprecipitations and pulldown experiments[7]. As shown here, NOA1 binds G-rich sequences if they are available. As long as no further information about the NOA1 ligand RNA is given, it will be difficult to screen for it in such a setup.

Ribonucleoproteins and Mitochondrial RNA Import

The identification of a G-quadruplex as a core consensus feature of the NOA1 ligand RNA, and the subcellular localization of NOA1 also in the nucleus, opens up the field for further hypotheses. NOA1 was shown to make a detour through the nucleus before entering the mitochondria. There, NOA1 localizes to the nucleolus, the place of rRNA transcription, and to nuclear speckles. Therefore, NOA1 could be a ribonucleoprotein (RNP) and some place in the nucleus (nucleolus, nuclear speckle) is the origin of the binding RNA. Noteworthy, the hnRNP proteins, a family of interaction partners of nuclear NOA1, are involved in G-quadruplex recognition, binding and unwinding[104]. The NOA1/G-quadruplex RNP would then have to be exported from the nucleus and be imported into mitochondria. It is attractive to build a model based on these facts by utilizing the work of Ivan Tarassov' group that deals with the import of tRNAs and 5S rRNA into mitochondria.

In *Saccharomyces cerevisiae* one out of two cytoplasmic $tRNA^{Lys}$ is partially imported into mitochondria. The enzyme enolase acts as import chaperone for $tRNA^{Lys105}$.
Whereas cytosolic ribosomes contain 5S rRNA, preparations of mitoribosomes lack this type of rRNA. Normally, 5S rRNA is transcribed in the nucleus and exported to the cytoplasm where ribosomal protein L5 binds to 5S rRNA. The L5/5S rRNA RNP complex then returns to the nucleus and assembles with other ribosomal RNAs and proteins in the nucleolus. A portion of 5S rRNA is imported into mitochondria dependent on rhodanese sharing this chaperone function with the already mentioned enolase. Rhodanese binds 5SrRNA in an unfolded state and then the RNP complex is targeted to mitochondria[23].
Of course the obvious question is how these RNP complexes are transported across two mitochondrial membranes into the matrix. To date none of the known import pathways was shown to contribute to the import of chaperone/RNA complexes to mitochondria. Based on interaction partners of NOA1[4] and published data a pathway for mitochondrial RNP import is suggested in the following paragraph.

Model for Ribonucleoprotein Import into Mitochondria

Porin is an evolutionary conserved multimeric protein that forms a pore in the mitochondrial outer membrane. The exact function of porin within the cell is not clearly answered. It was shown that porin is indispensable for import of the RNP complex rhodanese/5S rRNA. Although the specific channel composition has not been unraveled yet, the RNP import channel of the outer membrane is likely to contain porin in association with the central import pore of the TOM complex. The requirement for the core TOM complex was shown for RNA import in *Neurospora crassa*[106]. *N. crassa* mutants that lack porin have respiratory and growth defects. However, facultative aerobic *N. crassa* can survive in contrast to mammals where the knockout of porins is lethal. The study furthermore demonstrated that a portion of the core TOM complex protein, the monomeric Tom40 might form a complex with porin. This is similar to the insertion pathway of Min1, which acts independently but still recruits components of the TOM complex for chaperone function.
For the inner membrane it is tempting to assign an import function to the prohibitin (PHB) complex. The PHB complex consists of alternating subunits of PHB1 and PHB2 isoforms. It forms a large ring-shaped complex in the inner membrane. The exact function of the PHB complex is not known. However, the work of Thomas

Langers and Leo Nijtmans' groups showed that the PHB complex is essential for cellular survival and is involved in membrane stabilization[107,108], mitochondrial morphology[109,110] and respiration[111]. Moreover, the PHB complex acts as chaperone for the assembly of OXPHOS subunits. It was hypothesized that the influence on cristae morphology is the link to OXPHOS assembly and dysfunction as a consequence of PHB loss. Alternatively, one might argue that the OXPHOS dysfunction would be similarly severe if PHB would act upstream of the import of RNPs that are essential for mitochondrial protein synthesis. Respiratory dysfunction might be an indirect effect that is primarily considered since the mechanisms of translation and insertion of mtDNA-encoded subunits of the OXPHOS complexes is not fully understood.

Studies of tRNA import in *Trypanosoma brucei* pointed to a contribution of parts of the TIM23 complex as candidate for the mitochondrial inner membrane RNP channel. *T. brucei* has to import all tRNAs from the cytosol to the mitochondrial compartment. Therefore, trypanosomes are considered as perfect model organisms for the search for the RNP import pore. It was shown that knockout of Tim17 a core protein subunit of the TIM23 complex completely abolishes mitochondrial tRNA import[112,113].

Figure 43 shows a model for a putative RNP import pathway based on the studies of RNA import in plants, *N.crassa* and *T.brucei*. Supporting this model, interaction studies of NOA1 by mass-spectrometric analysis contain porin and the prohibitin complex as well as heat shock proteins associated to the TOM complex[4]. The exact mechanism of mammalian mitochondrial RNP import must be addressed separately to obtain experimental information. However, this model and the underlying data illustrates that it cannot be completely ignored that there are more than five import pathways to mitochondria. The putative RNP import pore could consist of the central pore of the TOM complex associated with the porin complex in the outer membrane. The inner membrane part of the channel is probably a combination of central members of the prohibitin complex and the TIM23 complex. This theory is strongly supported by the recent publication describing the direct involvement of a TIM23 subunit in the assembly of OXPHOS complexes including the insertion of mitochondria-encoded proteins[114].

The m-AAA protease could act as maturation chaperone as shown for MrpL32 that is uncommonly N-terminally processed by the m-AAA protease dependent on a

conserved CxxCNCxxC cysteine motif that coordinates zinc[50]. NOA1 also contains such a conserved zinc-binding motif[57,115] close to its N-terminus that could serve as recognition element for m-AAA (Figure 43). A very recent study showed the significance of m-AAA/AFG3L2 heterooligomers for mitochondrial protein synthesis[116].

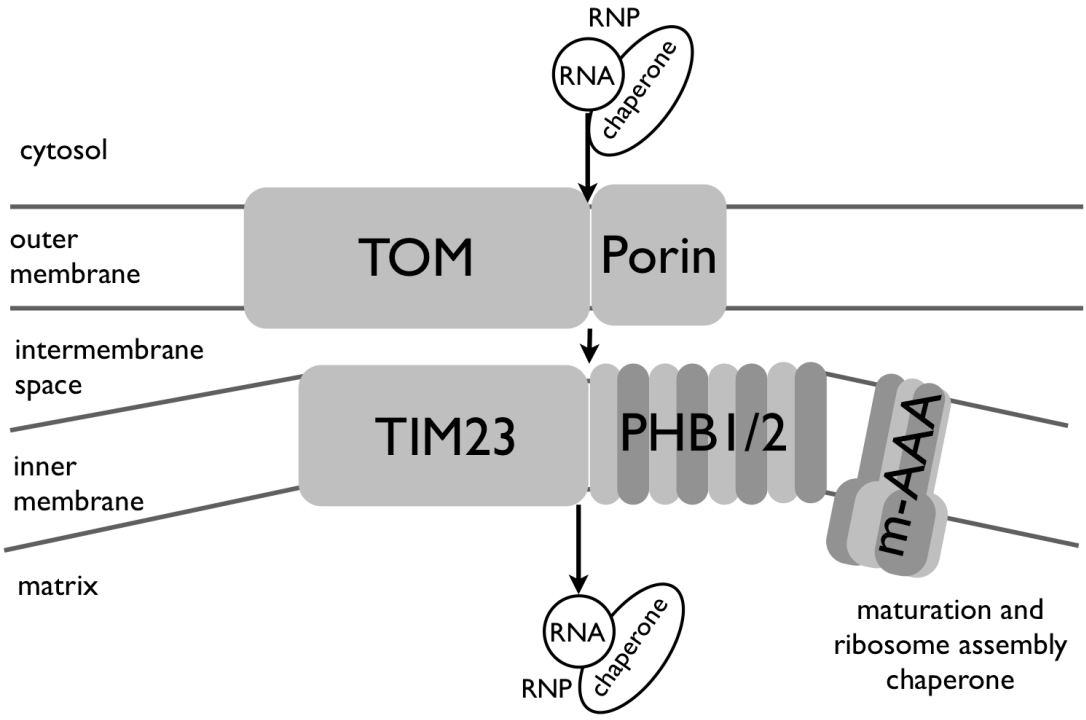

Figure 43 Suggestion for a mitochondrial import model for RNPs. Import is dependent on a RNP complex consisting of the RNA and a specific protein chaperone. Examples: $tRNA^{Lys}$-enolase[105]; 5S rRNA-rhodanese[23]. m-AAA protease could act as maturation and assembly chaperone[50].

Role of the C-Terminus: Caspase-1 Processing

The lack of the C-terminus in NOA1 hinders the mitochondrial import. The C-terminal domain of NOA1 binds the G-quadruplex containing RNA component. Assuming this NOA1/G-quadruplex RNP complex would take the here suggested import pathway (Figure 43) this might explain the impaired mitochondrial import of NOA1 lacking its C-terminus. Certainly more detailed analyses are needed to identify the role of the NOA1 C-terminus during mitochondrial import.

Nevertheless, the *in vitro* degradation studies of NOA1 by caspase-1 emphasizes that the C-terminal domain has potential for a multiple regulatory function. The C-terminus of NOA1 can be detached from the protein by specific Caspase-1 cleavage.

Unfortunately, the treatment of cells with classical caspase-1 activators like LPS was not sufficient to induce a cleavage of NOA1. Therefore the studies of caspase-1 mediated processing of NOA1 are pure *in vitro* studies that need validation in a cellular context in forthcoming experiments. Caspase-1 is an inflammatory caspase and has several less characterized substrates and one well-known substrate, the pro-inflammatory protein interleukin-1β. The processing of interleukin-1β leads to the release of the signaling molecule and the induction of programmed cell death mediated by the inflammasome. Caspase-1 cleavage of NOA1 would assure that mitochondrial protein synthesis is shut down immediately following inflammasome activation. That goes in line with the notion that mitochondrial function including protein translation is shut down at the onset of severe inflammation e.g in sepsis. Another point to mention is that there are reports of a homolog of caspase-1 that uniquely recognizes and processes the identical cleavage site and is sensitive to caspase-1 inhibitors. However substrate specificity is different from caspase-1[117]. It is possible that *in vivo* NOA1 is a substrate for this alternative caspase that was named protease resembling interleukin-1β-converting enzyme (prICE). Since no sequence information about prICE is available this hypothesis cannot be tested specifically to date.

Role of the C-Terminus: Casein Kinase II Phosphorylation

The caspase-1 processing of NOA1 is regulated by phosphorylation of casein kinase II (CKII), an ubiquitous kinase that has plenty of target proteins. CRIF1[90], the protein taking potentially the same mitochondrial import route as NOA1, is also modified by CKII. CKII can phosphorylate threonine, tyrosine and serine residues. NOA1 and CRIF1 have in common that both are serine phosphorylated. CKII is a main regulator of nuclear shuttling proteins especially a regulator of the nuclear export[77] and it regulates the mitochondrial import machinery[118]. Here, CKII phosphorylation of NOA1 is critical for *in vitro* processing by caspase-1 and for nuclear export. Such a post-translational enzymatic regulation that is situated upstream of mitochondrial import would allow the cell to control mitochondrial protein synthesis by cutting low the amount of an essential protein. It needs to be addressed in further experiments to what degree differential phosphorylation of CKII plays a role in the regulation of mammalian NOA1.

C. The mitochondrial sink: NOA1 is the first reported mammalian substrate for the ClpXP protease

NOA1 is a short-lived protein[119]. A main question was how the NOA1 protein is degraded and whether the mode of degradation influences NOA1's function.

It was assumed that NOA1 degradation takes place within the mitochondrial matrix. In the introduction the three major mitochondrial matrix protease systems Lon, m-AAA and ClpXP were described. After extensive studies of putative protease recognition elements a C-terminal ClpXP degradation motif was identified in the NOA1 amino acid sequence. Degradation studies with recombinant proteins and double overexpression studies clearly demonstrated *in vitro* and *in vivo* that NOA1 is a substrate for the mitochondrial ClpXP protease. This is a remarkable finding since to date no mammalian endogenous substrate for ClpXP was identified.

ClpXP is comprised of the catalytical subunit ClpX that recognizes, binds and transfers the substrate and the proteolytic subunit ClpP that finally degrades the substrate. This study gives evidence that ClpXP degrades NOA1 and likewise shows that increasing the amount of the catalytical subunit ClpX is sufficient to augment the degradation of ClpXP substrates *in vivo*. This indicates that substrate protein stability is mainly regulated by the amount of ClpX protein.

Transcriptional Upregulation of ClpX during Heart Growth

Not much is known about the functions of ClpXP in mammals. Mammalian heart and muscle growth are accompanied by a massive increase in mitochondrial mass. Therefore, these model systems are often used to get insight in the transcriptional regulation of proteins during mitochondrial biogenesis. Although, transcriptional data cannot automatically be correlated with protein function they at least highlight tendencies. Recently, a dataset about the transcriptomic changes during postnatal rat heart growth was published[120]. While Lon protease and the proteolytic ClpXP subunit ClpP show unchanged expression levels, the ClpX transcript is upregulated ~1.4 fold in the first 10 days after birth. This tendency is followed by a 3-fold upregulation of the ClpX transcript during hypertrophic heart growth until adulthood. On the contrary, the transcript levels of the ClpXP substrate NOA1 and the highly abundant mitochondrial matrix protein Tfam rather stay unchanged.

The transcriptional upregulation of ClpX could be related to an increased impact of the ClpX protein during heart growth. As seen in the overexpression experiments,

higher levels of ClpX are sufficient to increase the degradation of its substrate NOA1. By pinpointing NOA1 as ClpXP substrate, it becomes evident that the ClpXP protease plays a key role in the regulation of mitochondrial biogenesis and the regulation of OXPHOS. It is known for long that proteases play more complex roles than just degrading substrates. Many proteases act as chaperones assisting the maturation, folding or assembly of substrate proteins. However, the direct regulation of mitochondrial protein synthesis or OXPHOS by an evolutionary conserved protease like ClpXP is unique and has to be further characterized.

ClpXP tightly regulates the protein level of NOA1 by keeping it constantly low. In mammalian heart, the NOA1 protein levels are below threshold for the identification by a mass-spectrometric analysis of heart tissue samples. On the contrary, ClpXP protein fingerprints showed that these proteins have a relatively long half-life in heart tissue. The high abundance of the stable protease ClpXP and the low abundance of the substrate NOA1 in the same organelle lead to the assumption that mitochondria are a sink for NOA1. Further unraveling the mechanism of NOA1 function during translational regulation will clarify the role of ClpXP in the mammalian system.

How could the Degradation of NOA1 by ClpXP be regulated?

Interestingly, in bacteria ClpXP substrates modulate their own degradation via the accessibility of their degradation tags by oligomerisation or by conformational changes through substrate binding[121]. NOA1 forms dimers in cells[4] and oligomers *in vitro*. Since these oligomers incorporate G-quadruplex ligands to a degree this offers a possible regulatory mechanism. It could also be the case that GTP binding, hydrolysis and release of GDP induces conformational changes that regulate accessibility of NOA1 for ClpXP. These options have to be studied separately by using biophysical methods. At this point it is very clear that ClpXP degrades mammalian NOA1 specifically. In the future an extensive analysis of the enzyme kinetic of the degradation process needs to be performed. It seems that the turnover of free NOA1 in solution is very high. This mitochondrial sink categorizes the nucleo-mitochondrial pathway of NOA1 as one-way road.

D. NOA – the Mitochondrial SRP?

The main aim of this thesis was to develop a comprehensive model of NOA1's mitochondrial function. The strategy involved the analysis of the properties of single domains. Is NOA1 a ribosome assembly factor for the small mitoribosomal subunit? Is NOA1 a RNA chaperone or even a RNA processing enzyme as suggested for the bacterial homolog YqeH? NOA1 might not necessarily act as an assembly factor because ribosome integrity changes in response to NOA1 knockdown and there is no evidence that mammalian NOA1 has any RNA processing function. Two research groups confirmed that NOA1 is essential for OXPHOS assembly and supercomplex formation[4,5] dependent on the GTPase function. Both publications discuss putative mechanisms. Either a role in the stabilization of mitoribosomes[5] or a role in the stabilization of respiratory complexes[4] was proposed by the authors. However, none of this experimental evidence allows a specific description of the function of NOA1.

The Cytosolic Signal Recognition Particle

As described in the introduction no signal recognition particle (SRP)-like protein or protein complex was identified in mitochondria, yet. SRP is a cytosolic ribonucleoprotein (RNP) complex and the main mediator of Sec-translocon dependent membrane insertion of newly translated proteins. The SRP consists of several proteins and a specific ribosomal RNA component and is assembled in the nucleolus and then exported via Crm1 to the cytoplasm. SRP recognizes ribosomes carrying the nascent chain of a membrane protein and retards translation until the ribosome/nascent chain/SRP complex is docking to the membrane by interaction with the SRP-receptor. This interaction stimulates GTP-hydrolysis in SRP and SRP-receptor and leads to the release of SRP from the ribosome. The specific construction of SRP with its SRP-RNA scaffold and the GTPase activities of the participants are essential for this process.

Similarities of Signal Recognition Particle and NOA1

There are several indications that NOA1 could act as a SRP-like protein in the mitochondrial matrix. It was shown before that mutation of the GTPase domain of NOA1 alters the co-sedimentation properties relative to the small mitoribosomal subunit. In co-sedimentation assays the buffer composition and salt concentration is critical for the maintenance of intact mitoribosomes. There is not much data

available about the stability of mitoribosomes under conditions of impaired protein synthesis. Therefore, it is not entirely clear if the disassembly of the mitoribosome is a cause or a consequence of impaired translation. The bacterial nucleoside puromycin is an analog to peptidyl-tRNAs and therefore induces premature translation termination and the release of the nascent protein chain from the intact ribosome. By adding puromycin it is possible to address whether the interaction of a protein with the mitoribosome is dependent on active translation and the availability of a nascent chain. As demonstrated here, puromycin treatment deleted NOA1 from the fraction containing the mitoribosome, indicating that the association of NOA1 and the mitoribosome takes place after the assembly process when protein synthesis already started. The exploration of such spatiotemporal aspects of the association of accessory proteins with the mitoribosome is challenging. The here performed co-migration studies under high salt conditions, that protected the mitoribosomes from disassembly, also show that GTP is involved in the release of NOA1 from the mitoribosome, as the non-hydrolysable analogue GTPγS stalls NOA1 at the mitoribosome. A similar assay was performed by others showing that GTPase mutant NOA1 is unable to pulldown ribosomal particles *in vitro*[7]. These fascinating findings stimulate speculations about NOA1's function. Thinking about protein synthesis, striking similarities of the properties of NOA1 and facts about the signal recognition particle (SRP) can be drawn. Table 8 summarizes the parallels of NOA1 and SRP and the corresponding references from the literature or this thesis.

Although NOA1 is no homolog nor anyhow related to the SRP family of proteins it shares numerous feature with SRP. It is possible that mitochondrial translational regulation diverged from other organelles and also from the related chloroplast system that kept a rudimentary SRP protein. The beneficiaries of a mitochondrial SRP-like system are a very tiny group including solely the 13 polypeptides encoded on the mtDNA.

Table 8 Similarities of SRP and NOA1

		SRP	NOA1
1	bipartite nuclear localization signal (NLS)[122]	[122]	Figure 10, Figure 19
2	Crm1 specific nuclear export signal (NES)	[122]	Figure 21
3	Nucleolar associated localization; interaction with UBF1	[123]	Figure 17, Figure 20
4	Ribonucleoprotein	[124]	Figure 26, Figure 29
5	RNA binding domain	[124]	[57]
6	RNA binding	[124]	Figure 29
7	RNA identity	4.5S rRNA plasma membrane[125] 7SL rRNA ER[126]	not yet identified
8	RNA characteristics	Alu and S domain[127, 128]	G-quadruplex Figure 26, Figure 28
9	Required for co-translational membrane targeting of a nascent protein chain	ER-membrane[129, 130]	Mitochondrial inner membrane (supercomplexes[4])
10	Association with the small subunit of the ribosome	40S cytosolic small subunit[131]	28S mitochondrial small subunit[5, 7]
11	Enzymatic function: GTPase	[132]	[3], Figure 18
12	GTPase activity essential for function	[133]	[4]
13	GTP hydrolysis leads to release from the ribosome	[134]	[7], Figure 39
13	Free protein is rapidly recycled/degraded (short in solution half-life)	[135]	Degradation by ClpXP Figure 36
14	Phosphoprotein (C-terminal serinephosphorylation distal to Caspase-1 cleavage site)	[136]	CKII - Figure 32
15	Cleavage by caspase-1	[136]	Figure 33
16	Caspase-1 cleavage is asymmetric: small c-terminal fragment and large n-terminal fragment	35 kDa[136]	25 kDa, Figure 33

NOA1 enables Mitochondrial Inner Membrane Insertion

To assess if NOA1 could act as mitochondrial SRP, meaning as a soluble RNP that facilitates co-translational insertion of newly translated products in the inner mitochondrial membrane, an *in vitro* system was set up. Inverted mitochondrial vesicles offered the possibility to access the site of insertion and modify the translational cocktail consisting of mitochondrial matrix solution and enriched mitochondrial RNAs. Another advantage is that the inverted inner mitochondrial membrane vesicles can be easily separated from the soluble supernatant by centrifugation to define the place of the newly translated proteins.

The unmodified translation mixture showed some basic translation activity in the soluble fraction. The addition of recombinant NOA1 protein shifted the isotopically

labeled bands to the membrane fraction. So did the GTPase mutant NOA1 protein indicating that the GTPase function is not necessary for the acceleration of membrane insertion. Protein availability was not a limiting factor since NOA1 was added in excess. It is possible that the rapid depletion of NOA1 from mitochondrial lysates by ClpXP is one of the reasons why *in vitro* translational mitochondrial systems do not work. It is shown here that the addition of NOA1 protein to a crude translational mixture is sufficient to induce membrane insertion of labeled translation products. The sizes of the two prominent membrane inserted proteins, ~12kDa and ~18kDa, indicate that they consist of more than two transmembrane domains supporting the idea that NOA1 acts as mitochondrial SRP to assist co-translational targeting of proteins with more than two transmembrane domains.

The OXA Complex is not enough

The ER-membrane and the plasma membrane of bacteria, the main targets for SRP-dependent protein insertion contain the Sec-translocon machinery. Many publications claim that there are no Sec-dependent membrane proteins in mitochondria. However, structural comparisons showed that a Oxa1/YidC dimeric pore of the inner mitochondrial membrane is highly similar to the pore of the Sec-translocon[48]. Although there is no known Sec-translocon in the inner membrane of mitochondria, there are numerous channel systems that were shown to be flexible in composition and function. The membrane proteins of the OXA complex assure the correct topological insertion of the mtDNA encoded membrane proteins and also of other inner membrane OXPHOS proteins that are encoded in the nucleus. Still it is not clear how membrane proteins with more than two transmembrane domains are entering the inner membrane. To define the function of the OXA complex model systems were used that involved only small proteins (1-2 transmembrane proteins). It is unclear how proteins with more than two transmembrane domains are co-translationally inserted. It is a theoretical possibility that bigger translation products are post-translationally inserted. However, there are several counter-arguments, e.g. the extreme hydrophobicity of mtDNA-encoded proteins. The existence of a modified SRP-like complex in mitochondria is supported by another argument. It was shown in yeast that the OXA complex alone is not the mediator of mitoribosome targeting to the membrane and also not entirely essential for survival. How mitoribosomes are targeted to the inner membrane is not entirely clear, although

some groups claim that mitoribosomes naturally stick to the inner mitochondrial membrane. The lack of synthetical *in vitro* systems makes it very difficult to produce clear experimental data to understand such problems. However, the analogies of NOA1 with SRP, especially NOA1 being a G-quadruplex binding RNP, supports the working model illustrated in Figure 44.

Of course such a statement needs to be supported by additional experimental evidence in the future. Still, the provided data indicates that NOA1 plays a key role in the organization of the membrane insertion process at the translating mitoribosome. Additionally, the NOA1-mitoSRP model harmonizes with published data on mammalian NOA1.

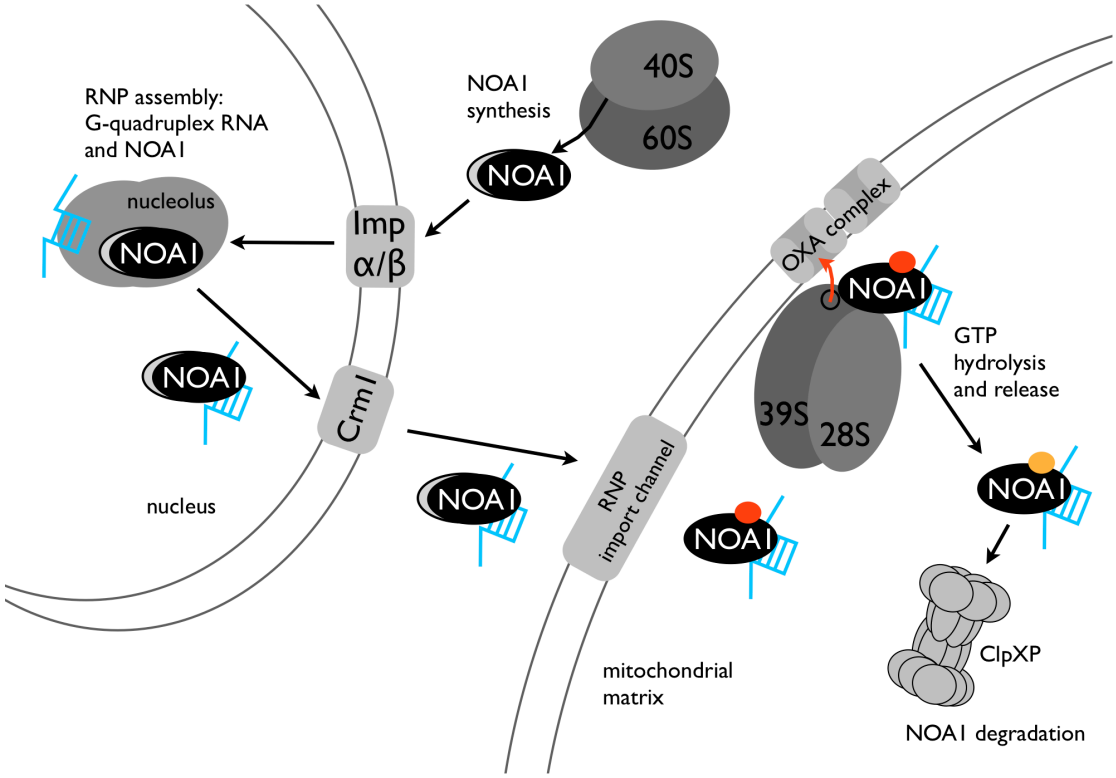

Figure 44 Working model for the maturation and function of NOA1. After synthesis of nuclear encoded NOA1 it is imported to the nucleus where it assembles in the nucleolus with the G-quadruplex RNA comoponent. Nuclear export is followed by import into the mitochondrial matrix where NOA1/G-quadruplex RNA acts as mitochondrial SRP. After GTP hydrolysis NOA1 is relased from the mitoribosome and degraded. Color legend: blue G-quadruplex RNA, red GTP, yellow GDP.

For refined analyses there is obviously need for detailed protein-protein interaction studies of NOA1 and inner mitochondrial membrane protein complexes. It is

assumed that the *in vivo* experimental outcome suffered from the probably transient nature of the interactions of NOA1 with other proteins and protein complexes. That might also be an explanation for lack of detection of members of the OXA complex in interaction studies. Different solubilization conditions and mild cross-linkers could make such transient interactions more accessible to detection. Other proteins might be associated to the NOA1-RNP complex. Thus, it will be interesting to analyze interactions of NOA1 and other nucleo-mitochondrial proteins like CRIF1.

IX. Methods

A. Molecular Biology

1. Concentration measurement of DNA and RNA

The concentration of nucleic acids was determined with the NanoDrop2000 photometer (PeqLab). Parameters: OD_{260} = 1 = 50 µg/ml dsDNA, OD_{260} = 1 = 40 µg/ml ssRNA. The photometer was calibrated with the sample solvent.

2. Enzymatic Digestion

One µg of Plasmid-DNA was incubated for 2–4 hours at 37°C with 10 units of each enzyme and the corresponding enzyme buffer provided by the company in a reaction volume of 50 µl. For the removal of enzymes and buffer the Macherey-Nagel Gel Extract II Kit was used following the standard protocol. Alternatively, the DNA can be extracted from and agarose gel.

3. Agarose Gel Electrophoresis

Agarose gel Electorphoresis uses the negative charge of DNA to separate it dependent on its size. Ethidiumbromide was added to the gels for visualization of the DNA under UV light. Gels were run in 1xTAE at 120-160 V. A DNA ladder was loaded for size comparisons. For analytical agarose gel electrophoresis of PCR products 1.5%-2% gels were used. For preparative gel electrophoresis 1% agarose was sufficient for a speparation of insert and backbone of enzymatic-digested plasmid DNA. The gel was barely exposed to UV light to prevent strand breaks. Bands were excised with a scalpel and extracted from the gel using the Macherey-Nagel Gel Extract II Kit following the manufacturers protocol.

4. TBE-Polyacrylamide Gel Electrophoresis (TBE-PAGE)

To analyze small DNA fragements like the Selex oligonucleotides TBE-PAGE was used. Ready-made 8% TBE gels were purchased from Invitrogen and run in 1x TBE running buffer at 120V. The gels were incubated in an ethidiumbromide containing 1xTBE bath to stain the DNA for visualization on a UV light table. The bands were excised and the oligonucleotides were extracted using the Macherey-Nagel Gel Extract II Kit following the manufacturers protocol.

5. Annealing of oligonucleotides

For the insertion of small linker DNA fragments (<200 bp) e.g to introduce new restriction sites to a plasmid the oligonucleotides were designed with enzymatic overhangs that fit into the enzymatic digested target plasmid DNA. 2 µl of sense and antisense oligonucleotide (100 µM) were phosphorylated at the 5' end by incubating them for 1 hour at 37°C with 2µl 10x T4 Kinase Buffer, 1 µl ATP (1 mM), 12 µl H_2O and 1 µl T4-Polynucleotide Kinase (10 u/µl). The annealing reaction was done in a PCR cycler to guarantee stepwise cooling from 95°C to 8°C. The following protocol was used: Annealing: 3 min at 95° C (cool down with 0.8 °C steps per cycle, 99 cycles); Program: 1 – T = 95°C – 03:00 – 2 – T = 95°C – 0:20 – R = 3.0 °/s – 3 – Go to – 2 – Rep – 99 – 4 – Hold – 8.0 °C. After phosphorylation and annealing the linker was diluted 1:200 in H_2O and 4 µl were used in the ligation reaction with 100 ng of target vector.

6. Ligation of DNA

The ligation reaction contained 50-100 ng enzymatic digested plasmid DNA backbone and insert DNA in a 3:1 insert:backbone molar ratio, for linker DNA 4µl of the phosphorylated, annealed and diluted DNA was used. The reaction was carried out overnight at 16°C in a volume of 50 µl with 5µl T4-Ligase (10u/µl) and the corresponding ligation buffer. 5µl were used for transformation of chemical competent bacteria.

7. Transformation of chemical competent bacteria

The transformation mixture contained 5 µl of the ligation reaction, 20 µl 5x KCM, 25 µl H_2O and 50 µl chemical competent *E.coli XI1Blue* bacteria. The transformation mixture was incubated for 10 min on ice. After 20 min at RT (25°C) 1 ml pre-warmed LB-medium without antibiotics was added and the transformation reaction was incubated for 1 h at 37°C with 700 rpm shaking. After centrifugation for 1 min at 3,000 g the supernatant was discarded leaving residual 50 µl medium for gentle resuspension of the bacterial pellet. The bacteria were plated on agar plates containing the appropriate antibiotic corresponding to the resistance cassete of the transformed vector backbone (Kanamycin 50 µg/ml, Ampicillin 100 µg/ml).

8. Chemical competent bacteria

1 ml LB-medium was inoculated with 10µl *E.coli XI1Blue* cryostock. After incubation for 1h at 37°C with 700 rpm shaking the cells were plated on a LB agar plate without antibiotics (LB-0). The plate was incubated over night at 37°C. The next day 5 ml LB-0 medium was inoculated with a single clone from the plate and incubated over night at 37°C in a shaker. 100 ml LB-0 were inoculated with the 5ml overnight culture and incubated for 1h at 37°C in the shaker until the OD_{600} reached a value of 0.5-0.6. Then the bacteria were harvested by gentle centrifugation at 2500 g with 4 °C for 15 min. The pellet was resuspended in 7.5 ml TSB and air bubbles were avoided. The suspension was incubated on ice for 1h. Aliquots of 110 µl bacteria suspension were shock frozen in liquid nitrogen and stored at -80°C. The chemical competence was controlled with a test transformation.

9. Analytic Plasmid isolation (Mini-prep) by Alkaline Extraction[137]

3 ml LB-medium (with appropriate antibiotics) were inoculated with a bacteria clone from an agar plate and incubated over night at 37 °C with shaking. 2 ml of the overnight culture were pelleted for 5 min at 10.000 g. Optional a glycerol stock was secured containing 225 µl glycerol/1x TE and 500 µl of the overnight culture wich can be stored at -80°C. The supernatant was removed and the pellet was resuspended in 150 µl Solution A containing RNase to break the cells and incubated for 10 min at RT. Then, 200 µl Solution B is added that induces alkaline lyses of the genomic DNA, the tube is inverted several times and incubated for another 10 min at RT. The solution was neutralized by the addition of 175 µl Solution C and incubation for 10 min on ice. Then, the preparation was centrifuged for 10 min at maximum speed g and 4°C. The supernatant was transferred into a new tube containing 500 µl isopropanol and the DNA was precipitated by centrifugation for 20 min at maximum speed and 4 °C. The pellet was washed with 500 µl ice-cold 70 % ethanol and pelleted again for 10 min at maximum speed and 4 °C. The pellet was air dried by putting the open tubes upside down in Styrofoam rack under the fume hood (faster evaporation of residual ethanol). The plasmid DNA pellet was resuspended in 80 µl 1x TE (concentration was ~200 µg/µl). 5 µl of the preparation was used for control digestion and visualization on an agarose gel.

10. Preparative Plasmid isolation (Maxi-prep) Alkaline Extraction[137]

100 ml LB-medium (with appropriate antibiotics) were inoculated with a clone or an overnight culture. After incubation overnight at 37 °C with shaking the bacteria were harvested by centrifugation for 15 min at 5,000 g and 4 °C. The pellet was resuspended in 5 ml Solution A to lyse the bacteria and transferred to new tube. 10 ml alkaline Solution B was added and the solution was gently inverted and incubated for 10 min on ice. After addition of 7.5 ml Solution C for neutralization and an additional incubation for 10 min on ice the bacterial debris is removed by centrifugation for 15 min at 5,000 g and 4°C. The supernatant was transferred into a new tube by filtering through a fluted filter. The solution appeared clear after filtering. Then 10 ml isopropanol was added and incubate for 15 min at RT on a roller platform. After centrifugation for 10 min at 5,000 g and 4 °C the pellet was resuspended in 2 ml H_2O and 2 ml 5 M LiCl solution. After an incubation of 20 min on ice, the salt was removed for 5 min at 3,000 g 4 °C. The supernatant was transferred into a tube containing 9 ml ice-ocld 100 % ethanol and incubated for 1 h at -20 °C to precipitate the DNA. The DNA was pelleted for 20 min at 10,000 g and 4 °C. The DNA was resuspended in 0.5 ml 1x TE and digested with 10 µl RNase A (10 mg/ml) for 1 h at 37°C and with 10 µl Proteinase K (10 mg/ml) for 1 h at 60°C. The DNA was purified by phenol-chloroform extraction.

11. Phenol-Chloroform-IAA-Extraction[138,139] & NaAc-EtOH Precipitation

1 Volume (500 µl) Rotiphorese-phenol was added to the RNase A and Proteinase K treated Maxi-Prep solution. After vortexing and centrifugation for 1 min at 12.000 g the upper phase containing the DNA was transferred in a new tube with 1 Volume (500 µl) chloroform / isoamylalcohol (IAA) (24:1) and vortexed. The upper phase after another centrifugation for 1 min at 12.000 g was transferred in a new tube containing 50 µl 3M NaAc and 1250 µl 100 % ethanol. The tube was incubated for 1 h at -20 °C to precipitate the DNA. The preparation is pelleted for 20 min at maximum speed and 4°C. The pellet contained pure DNA and was resuspended in 200-400 µl 1x TE. The purity of the plasmid-DNA was analyzed by digestion, gel electrophoresis and sequencing.

12. Sequencing of DNA

The company Seqlab performed the sequencing of DNA. 7 µl of a DNA solution with a concentration ~200µg/ml were mixed with 1 µl Sequencing-Primer (10 pmol/µl) and submitted for sequencing.

13. Isolation of RNA from eukaryotic cells and mouse tissue

For RNA isolation DEPC-treated solutions and filter tips were used. RNA was isolated using the Trizol Reagent (Ambion) following the standard protocol. Before adding the Trizol the cell layer was washed with 1x PBS. Mouse tissue was washed with PBS and chopped into small pieces and homogenized with a pestle. 1 ml Trizol Reagent was added and incubated for 5 min at RT. 0.2 ml Chloroform were added, the tube was inverted several times and incubated for 2 min at RT. Transfer the upper aqueous phase resulting from a centrifugation step spin at 12.000 g for 5 min and 4 °C contained the RNA and was mixed with 0.5 ml 100% isopropanol. After incubation for 10 min at RT the RNA was pelleted at maximum speed and 4 °C. The RNA was washed with 1ml 75% ethanol in DEPC-water and the pellet was air-dried. Then the RNA was resuspended in DEPC-Water (30 µl for RIP-RNAs, 50 µl for whole cell RNA) and incubate for 10 min at 60 °C in the heating block for better resuspension. The concentration and purity of the RNA was checked with the NanoDrop 2000 spectrophotometer. The RNA solution was stored at -80°C.

14. Protein isolation from Trizol-supernatants after RNA extraction

For parallel protein isolation from an RNA extraction sample, 1.5 ml isopropanol was added to the Trizol leftover and incubated for 10 min at RT. After centrifugation at 12.000 g, 10 min, 4 °C the protein pellet was washed three times with 0.3 M guanidine hydrochloride in 95% ethanol. 2 ml of the washing solution was incubated for 20 min at RT and removed by centrifugation at 7500 g for 5 min and 4 °C. Then the protein pellet was air dried and resuspended in Laemmli Cell Lysis Buffer and sonicated. In case the proteins were hard to solubilize, Protein Solubilization Buffer was added and the sonication was repeated. The solution was incubated at 50°C to dissolve the proteins (>1% SDS is needed here). The unsoluble debris was spun down at 12.000 g for 5 min. For SDS-PAGE analysis the protein solution was mixed with 5x Laemmli Sample buffer.

15. DNaseI digestion

1µg of TrizoI isolated RNA was incubated with 1 unit RNase-free DNase I, reaction buffer with MgCl2 and nuclease-free water for 30 min at 37 °C. To stop the reaction 1 µl 50 mM EDTA was added and incubated at 65°C for 10 min. The RNA was directly used for reverse transcription.

16. c-DNA Synthesis by reverse transcription

1 µg DNaseI digested RNA was mixed with 1 µl random hexamer primers for RIP-RNA or oligodT primer for whole cell RNA and incubated for 5 min at 65°C. Then the following components were added: 4 µl 5 x Reaction buffer, 1µl 10 mM dNTP mix (for radioactive visualization dNTPs were mixed freshly consisting of 10 mM dATP, dGTP, dTTP, 2 mM dCTP with the supplementation of ^{32}P-dCTP), 2 µl M-MuLV Reverse Transcriptase (20 u/µl). The components were mixed and incubated for 5 min at RT, 60 min at 37 °C. Heating the mixture to 70°C for 5 min terminated the reaction. The non-radioactive cDNA was tested by amplification of 18S rRNA by PCR. The radioactive samples were treated as follows. Excess of ^{32}P-dCTP was removed by using illustra Probe Quant G-50 Micro columns. The cDNA was separated on a 1 % agarose gel. The agaraose gel was dried on whatman papers with a gel drier at 60°C for 4 hours and read out with the PhospholmagerSystem.
cDNA was stored at -20°C.

17. Polymerase Chain Reaction

The polymerase chain reaction (PCR) was used to amplify DNA. Here, the RedTaq Ready Mix (Sigma Aldrich) was used according to the manufacturer's protocol. The principle of the reaction follows the scheme: denaturation of dsDNA, primer annealing (temperature was chosen for each primer pair), elongation and final elongation. The PCR products were visualized on an agarose gel and the data was saved with the BioDoc analyzer gel documentation system.

18. Overlap PCR

For the analysis of localization and function different truncation and point mutants of wild type NOA1 were generated. An overlap PCR approach was utilized where the middle primers introduced the desired mutation by mismatches. The proofreading Phusion Polymerase was used according to the manufacturers protocol. The 20µl volume reaction mixture contained 12.8 µl H_2O, 4 µl 5x Phusion HF buffer, 0.4 µl 10

mM dNTPs, 0.5 µl Primer A (10 pmol/µl), 0.5 µl Primer B (10 pmol/µl), 1 µl Template DNA (linear Plasmid DNA insert of 1µg digestion eluted in 50 µl H_2O after gel extraction), 0.6 µl DMSO and 0.2 µl Phusion Hot Start Polymerase. PCR was run according to the following protocol: 1– T = 98°C – 00:30 – 2 – T = 98°C – 00:10 – 3 – T = 68°C – 00:25 – 4 – T = 72°C – 00:30 – Go to – 2 – Rep – 24 – 5 – T = 72°C – 05:00 – Hold – 8.0 °C. The mutant PCR product was isolated from an agarose gel and eluted into 50 µl H_2O (Nucleospin Extract II Kit, Macherey-Nagel).

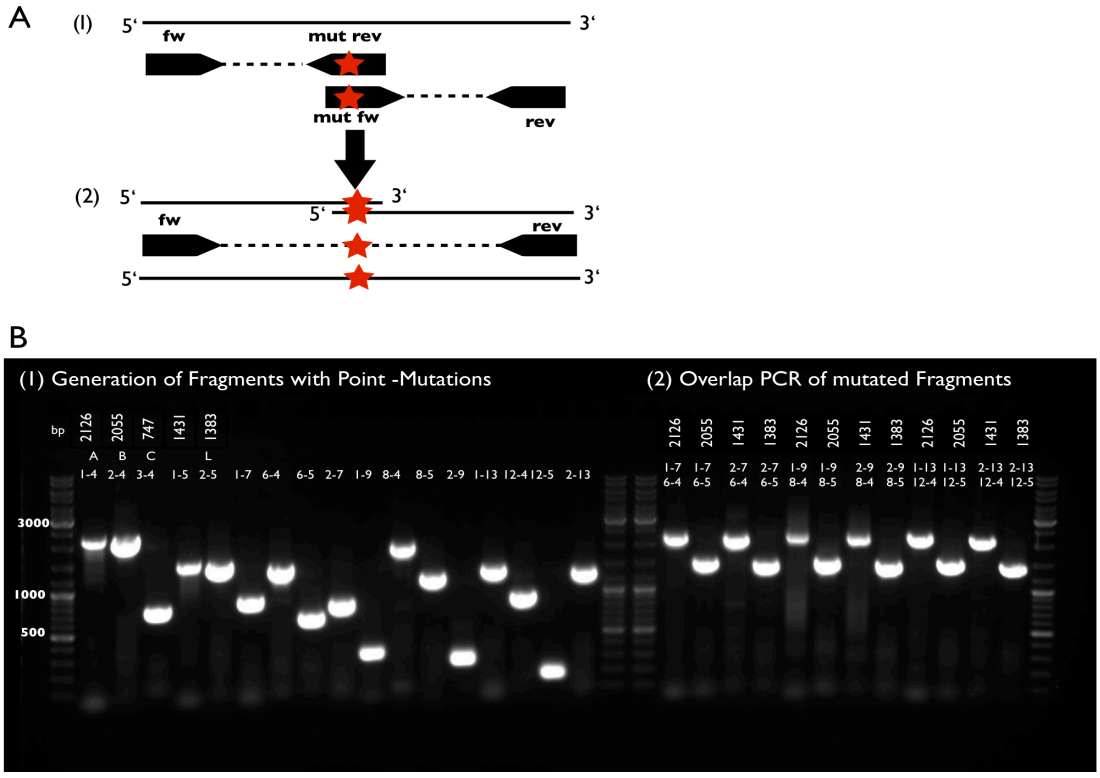

Figure 45 Generation of overexpression constructs for cell culture studies. A) Schematic representation of the method. B) Agarose gel of single fragments and overlapped products (1) Introduction of Point mutations by PCR of fragments containing the mutation (1) and subsequent overlap-PCR (2) of the fragments with Phusion Taq-Polymerase (Finnzymes). Also truncation mutants were generated this way.

The overlap PCR consisted of two steps. In a first step two fragments were generated containing the mutation at one end of the PCR product (Start-Primer/Mutation-Primer and Mutation-Primer/End-Primer) (Figure 45A). Since the mutation sites of the two fragments overlap a second PCR with 1µl of each fragment as template resulted in the mutated full length PCR product (Start-Primer/End-Primer). The mutated fragment was eluted from an agarose gel in 30 µl H_2O. Since Phusion Polymerase generated blunt products A-overhangs were introduced prior to

subcloning. The start-primer contained a BamHI restriction site and the start codon ATG while the end-primer contained a Flag-tag and stop codon followed by a SlaI restriction site. The A-tailed fragment cloned into the pGemTeasy vector. After insert analysis the mutants were digested with BamH1/SlaI and cloned into the pcDNA5/TO target expression vector. To avoid sequence mutation during the PCR the proofreading Phusion Polymerase from Finnzyme was used.

The nomenclature of the generated truncation variants of NOA1 was derived from the numbering of primer pairs:

A / 1-4	Full length NOA1
B / 2-4	NOA1ΔMTS
C / 3-4	NOA1 C-terminus alone (herein only a single motif: RNA binding domain)
1-5	NOA1ΔC-terminus
L / 2-5	NOA1ΔMTSΔC-terminus

19. Introduction of A-overhangs to Phusion PCR-products

For introduction of A-overhangs 10 µl of the purified PCR fragment generated by Phusion Polymerase were used. The reaction mixture contained 5 units Taq-DNA Polymerase (5PRIME), 5µl 10x Reaction Buffer and 5µl 25 mM $MgCl_2$. Then dATP to a final concentration of 0.2 mM (5 µl of 1mM stock) and water were added to a final reaction volume of 50 µl. The mix was incubated at 70 °C for 30 min and cleaned up with the PCR cleanup kit (Macherey-Nagel). The PCR product was thereafter used for ligation with the pGEM-TEasy Vector (Promega).

20. Sit-directed-mutagenesis PCR with Proofreading Polymerase (Agilent)

Reactions were performed with PfuUltra High-Fidelity DNA Polymerase AD (Agilent Technologies) according to the manufacturer's protocol. Primer design was performed with the online Stratagene mutagenesis tool. The vector template was diluted to 10 ng/µl. The mutagenesis PCR was setup as follows: 1 µl DNA (10 ng/µl), 2.5 µl 10x buffer, 0.65 µl Primer 1 (100 ng/µl), 0.65 µl Primer 2 (100 ng/µl), 0.5 µl dNTP mix (10 mM each), 19.2 µl H_2O, 0.5 µl Pfu Ultra Polymerase (2.5 u/µl). The PCR running parameters were 95°C 1min, 26 cycles of 95°C for 30 sec, 55°C for 1 min and 68°C for 1min/kb (here 8.0 min were used). A final elongation time of 10 min at 72°C was added. 5 µl of the PCR was mixed with 6x DNA Loading Buffer and visualized on an agarose gel. A single band showed that the PCR amplification was succesful (Figure 46).

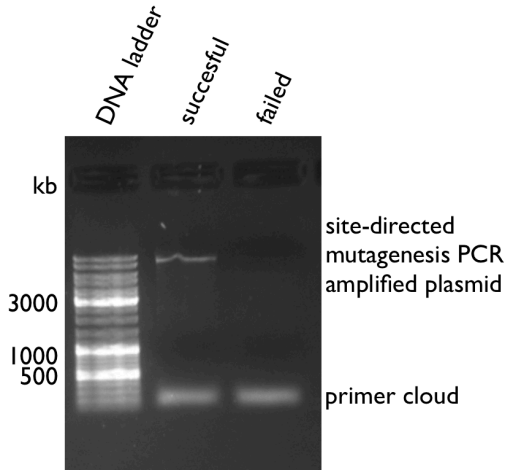

Figure 46 Example of an agarose gel with 5µl of a succesful and a failed site-directed mutagenesis PCR reaction mixture (here succesful ClpXR300A mutant).

The rest of the PCR mixture was precipitated. Therefore 20 µl PCR reaction was mixed with 80 µl H_2O, 100 µl 4M NH_4Acetate and 400 µl Isopropanol. The precipitation reaction was incubated 15 min at RT followed by 15 min centrifugation at max speed. The (invisible) pellet was washed with 70% Ethanol and centrifuged at max speed for 5 min. The DNA pellet was dissolved in 13 µl H_2O and mixed with 1.5µl NEB2 or B2 buffer and 0.5 µl DpnI enzyme to digest the template DNA. The digestion was incubated >4h to over night at 37°C. 5 µl of the DpnI treated mutagenesis PCR mix was transformed into *E.coli XI1Blue*. Transformants were analyzed for the mutation by sequencing.

21. SELEX analysis

SELEX is the "Selected Evolution of Ligands by Exponential Enrichment" and was used for enrichment of a consensus binding sequence for the NOA1 protein after the method published in Hyvärinen et al[140]. For amplification of the single stranded library into double strands the Klenow polymerase was used in combination with primers homologous to the flanking sites of the library (Figure 47B). The samples were visualized on a 14% TBE-PAGe gel to separate the double stranded library from the single stranded library by gel elution (Figure 47C). The eluted library was used for immunoprecipitation followed by PCR amplification. After six rounds of enrichment the bands were excised and cloned into the pGemTeasy vector and transformed into *E.coli XL1Blue*. Single clones were analyzed by sequencing.

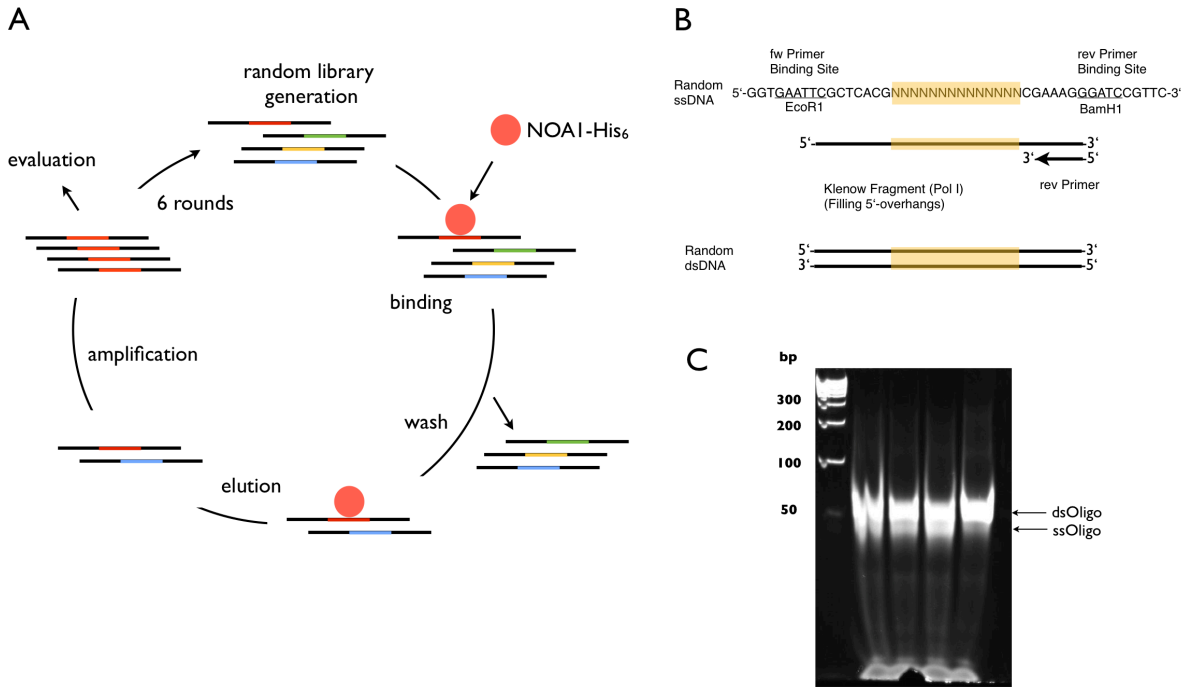

Figure 47 SELEX prodedure. A) Scheme of SELEX cycles. B) Generation of a random nucleotide library with Klenow polymerase and flanking primer. C) Purification of the double stranded library by extraction from a 14% TBE-PAGE gel.

22. Generation of knockdown vectors

The oligonucleotides coding for the shRNA have stemloop character and compatible overhangs for the BsmBI restriciton site. The oligos are annealed following the protocol 'Annealing of oligonucleotides'. The annealed oligos coding for the shRNAs are ligated into the BsmBI restriction site of the backbone of the pcDNA 3.1-derived U6i vector that was opened by enzymatic digestion.

23. End-labeling of oligonucleotides

For EMSA assays the oligos were end-labeled with ^{32}P-γATP. A reaction contained the following substances: 1 µl oligonucleotide (100 pmol/µl), 2.5 µl ^{32}P-γATP, 1 µl T4 Polynucleotide Kinase, 2.5 µl 10x T4 Polynucleotide Kinase buffer, 18 µl H_2O. The reaction was incubated for 30 min at 37 °C. the final concentration of oligonucleotides was 4 pmol/µl. The labelded oligos were cleaned-up by Millipore Amicon Ultra 3K Columns by washing three times by addition of 500 µl 1x TE and spinning at 12.000 g for 20 min. The excess ^{32}P-γATP was removed with the flow

through. 25 µl of labeled oligo was diluted up to 250 µl with 1x TE to obtain a final concentration of 0.4 pmol/µl labeled oligo in 250 µl solution.

24. G-Quadruplex folding

5 µl of 0.4 pmol/µl end-labeled oligos were boiled at 95°C for 5 min, then transfered on ice and incubated for 2 min. 5 µl of 2M KCl were added to get a final mix of 0.2 pmol/µl oligo in 10 µl of 1 M KCl solution. This folding reaction was incubated over night at 37°C. The quadruplexes were used directly. To check the folding a precast 8% TBE gel (Invitrogen) in 1xTBE at 200V 15 -20 min was run. The G-quadruplexes were loaded with 20% Ficoll/Orange G Loading Buffer.

25. Radioisotope Imaging

The imaging of radioisotope labeled samples was performed with the PhosphorImaging System Image ReaderV2.02 from Fuji Photo Film Co.,Ltd. and the data was evaluated with AIDA software package.

B. Cell culture

1. Growth conditions and transfection

C2C12/NIH3T3 cells were cultivated in DMEM 4.5 g/l glucose supplemented with 10% fetal calf serum (FCS), 100 U/ml penicillin, 100 µg/ml streptomycin, 1 mM sodium pyruvate, and 2 mM stable glutamine in an atmosphere of 5% CO_2 and 37°C. For propagation cells were detached with 1 x TE (here: 0.5 mg/ml Trypsin, 220 µg/ml EDTA). Transfection was performed with Lipofectamine2000 (Invitrogen) or Turbofect (Fermentas) as described in the manual. For cryo-storage, cells were trypsinized and centrifuged 500g for 5min at RT. The pellet of ½ 10cm petri dish was resuspended in growth medium supplemented with 5% DMSO. The cryo-stocks were stored for 2h at -20°C followed by over night storage at -80°C and long term storage in a liquid nitrogen cooled tank. For thawing cell stocks were thawed in a 37°C water bath and put into pre-warmed growth medium.

2. Isolation of primary muscle fibers from mouse feet

This protocol was provided by Dr. Günther, Dept Braun, MPI, Bad Nauheim.

The feet of a C57/B6 wild type mouse were cut off the body and fixed with the palms upwards with help of bent syringes. The skin was detached from leg to finger; skin and asymmetric filament were removed. When palm muscles were mounted

free, the muscle fibers were detached from the bone by rubbing with a scissors tip between finger muscles and bones. Then the muscles were cut at the finger-roots and the whole palm muscle was removed by cutting at the wrist. The muscle was transferred into DMEM high glucose 4.5 g/l medium with 10 % FCS and 0.2 % collagenase P (Sigma) and incubated for 1.5 h at 37°C and 10 % CO_2 atmosphere. Vigorous pipetting separated the fibers. A FACS tube was coated with concentrated FCS. The fibers were transferred into the tube and washed 3 times with 1x PBS until the supernatant was clear. The myofibers were fixed by incubation in 4% PFA for 10 min at RT and then washed again 3 times with 1x PBS. The myofibers were stored at 4°C until they were stained in solution with antibodies. The stained fibers were mixed with some drops of mowiol and directly mounted by putting drops of fibers in mowiol on glass slides.

C. Protein biochemistry and Immune Histology

1. Protein Isolation

For cells, the medium was removed and the cell layer was washed twice with 1x PBS. The Laemmli Cell Lysis Buffer was added directly to the cell layer and incubated for 1 min at RT. The slimy cell lysate was scraped down with a cell scraper and transferred into a tube. The sample was sonicated for 10 sec (cycle 5 intensity 40% amplitude) and the cellular debris was removed by centrifugation for 1 min at maximum speed. The protein concentration was determined by the lowry method with the DC Protein Assay Kit (BioRad) using the Nanodrop2000 spectrophotometer. The favored amount of protein was mixed with 5x Laemmli Sample Buffer and boiled for 5 min 95°C. The samples were analyzed by Bis-Tris SDS-PAGE or they were stored at -20°C.

2. bis-Tris SDS-PAGE[141-143]

Sodium dodecylsulfate polyacrylamide gel electrophoresis (bis-Tris SDS-PAGE) that is based on the bis-Tris / MES buffersystem was used to analyze protein samples. Precast 4-12% gradient gels with 17 wells and 10 wells were purchased from Invitrogen. Linear bis-Tris SDS-PAGE gels were casted into 1 mm casting cassettes purchased from Invitrogen according to the following scheme:

	4 % stacking gel	10% separating gel	12% separating gel	15% separating gel
Volume for 1 gel	1.5 ml	7 ml	7 ml	7 ml
3.5x bis-Tris SDS-PAGE Gel Buffer	0.45 ml	2.1 ml	2.1 ml	2.1 ml
AA/BAA 40 % w/v 29:1	1.15 ml	1.75 ml	2.1 ml	2.6 ml
H_2O	0.9 ml	3.15 ml	2.8 ml	2.3 ml
APS 10 %	15 µl	70 µl	70 µl	70 µl
Temed	1.5 µl	7 µl	7 µl	7 µl

Gels were run at 140 V in 1x MES-SDS Running Buffer or in 1x MOPS-SDS Running Buffer.

3. Coomassie staining of bis-tris SDS-PAGE gels

For coomassie staining the Colloidal Coomassie Staining Kit (Invitrogen) was used following the manufacturer's manual. Alternatively, the fast InstantBlue coomassie staining solution from Expedeon was used.

4. Western Blotting

Bis-Tris SDS-PAGE gels were transferred on a whatman paper soaked in 1x Transfer Buffer. A nitrocellulose membrane was placed on the gel and blotting was performed with the NuPAGE Blotting System from Invitrogen. After 1.5 h at 30 V the sandwich was disassembled and the membrane was rinsed in water to remove residual SDS. Proteins were fixed and visualized by staining of the membrane with 1x Red Alert Staining Solution (Novagen). The blots were scanned and incubated in 1x TBS-T to remove the Red Alert staining. Prior to primary antibody incubation the membrane was blocked for 30 min in 5% Milk TBS-T solution at RT under gentle shaking. The first antibody was diluted in 3% Milk TBS-T solution and incubation occurred over night in the cold room. The blot was washed three times with TBS-T and incubated with secondary antibody diluted in 3 % Skim milk powder TBS-T solution for 1 hour at room temperature. After washing three times for 10 min the blot was evaluated with the ECL reagent and documented with the BioRad Versadoc system or alternatively with the LICOR Odyssey System.

5. Mitochondria Isolation and Nuclear Extract Protocol

The solutions and the homogenizer were pre-cooled on ice. Preparation of Mitochondria and Nuclei: The cells of a 10 cm dish (or more) were harvested by use of Trypsin and EDTA (2 min, 300 g, 4°C). The pellet was washed with cold 1x PBS to remove traces of medium. The cells were resuspended in 1 ml 0.1x Homogenization Buffer (1 ml for a 10 cm dish, 5 ml for a 15 cm dish) and incubated

for 5 min on ice to allow the cells to swell. Then the cells were transferred into a Wheaton Glass Homogenizer and were disrupted with 8 strokes. The cells were transferred into a fresh tube and 125 µl / 625 µl 2M Sucrose/TE solution was added. Inverting several times mixed the homogenate and neutralized the tonicity. After pelleting the nuclei for 3 min at 1200 g and 4°C the supernatant containing the mitochondria was transferred into a fresh tube (continued*). In case of incomplete cell lysis the homogenization step was repeated with the pellet and the supernatant was combined with the other supernatant. Mitochondria were pelleted at 10.000 g for 10 min at 4°C and washed with 1 ml Wash Buffer. The mitochondrial pellet was either stored at -20 °C or directly lysed in 6x Laemmli Sample Buffer.

Preparation of Nuclear Extract: * the nuclear pellet was resuspended in 1.5ml Wash Buffer and and washed twice with spinning at 1200 g for 3 min and 4 °C. Then 980 µl Wash Buffer and 20 µl (1/20 vol) 5 % NP-40 were added to lyse residual intact cells. After incubation for 10 min on ice and centrifugation at 1200 g for 3 min and 4 ° the pellet contained pure nuclei. Thee nuclei preparation was checked by trypan blue staining with a light microscope. The nuclei were extracted for 30 min on ice by resuspending the pellet in Nuclear Extraction Buffer. Debris was removed for 30 min at maximum speed and 4 °C.

6. Subcellular fractionation of eukaryotic cells

Subcellular fractionation of eukaryotic cells was performed with the ProteoExtract Subcellular Protein Extraction Kit from Calbiochem following the manufacturer's instructions. Dependent on the cell type the mitochondrial matrix fraction was not necessarily enriched in the Organelle/Membrane fraction but more in the Cytosol fraction. Enrichment was checked by western blot with compartment specific antibodies.

7. Isolation of nucleoli from C2C12 myoblasts

Nucleoli Isolation Buffer A:

Nucleoli Buffer S1

All steps were performed on ice since Nucleoli of cultures mammalian cells disassemble at 37°C under hypotonic conditions[144]. Cells of 10 x 10cm dishes were harvested by trypsinization and pooled into 2x 50ml tubes (300g 3 min). The pellet was resuspended in 5ml of Nucleoli Isolation Buffer A and incubate on ice for 5min to swell. The swelling was checked under the microscope. The suspension was

transferred to a pre-cooled Homogenizer (Wheaton 0.0010" - 0.0030" clearance) and homogenized by intervals of 10 strokes. Every 10 strokes the sample was checked under the light microscope. Homogenization was stopped when 90% of the cells were burst leaving intact nuclei with various amounts of cytoplasmic material attached. The pellet (200g for 5min at 4°C) contained enriched, but not highly pure nuclei that were resuspended in 3 ml Nucleoli Buffer S1 and layered over 3 ml of Nucleoli Buffer S2 solution. After spinning at 1430 g for 5 min at 4°C the nuclear pellet became cleaner. Nuclei were resuspended in 3ml Nucleoli Buffer S2 and then disrupted by sonication for 6x10 second bursts with 10 sec intervals between each burst. The sonicated nuclei were checked under the microscope. When there were no intact cells left and the nucleoli were radially observed as dense refractive bodies the sonication was finished. The sonicated sample was layered over 3 ml of Nucleoli Buffer S3 and spun at 3000 g for 10 min at 4°C. The pellet contained the nucleoli and the supernatant the nucleoplasm fraction. Nucleoli were suspended in 0.5 ml Nucleoli Buffer S2 followed by centrifugation at 1430 g for 5min at 4°C. The pellet contained the highly purified nucleoli. The Nucleoli preparation was disolved in 50µl Nucleoli Buffer S2 and store at -80°C or lysed in RIPA buffer for pull-down assay.

8. Immunoprecipitation

All steps were performed on ice. The cell monolayer of a 15 cm dish was washed with 1x PBS and 5 ml RIPA buffer was added and incubated 10 min for lysis in the cold room. The cells were scraped into the buffer and the debris was pelleted for 5 min at 10.000 g and 4 °C. The supernatant was used as immunoprecipitation (IP) lysate and separated in 500 µl aliquots that served for one IP.

The IP lysate was incubated with 1-10 µg antibody of interest for 1 h in the cold room on a rotating wheel. Protein G Sepharose 4 Fast Flow slurry was washed with RIPA buffer several times to remove the ethanol. 30 µl beads were used for each IP. 30 µl Protein G Sepharose 4 Fast Flow slurry was added to the lysate/antibody IP and incubated for 1 h at 4 °C on a rotating wheel. The beads were washed 3x with 500 µl RIPA buffer (10,000 g, 4 °C, 30 sec) and resuspended in 50 µl 5x Laemmli Sample Buffer and eluted at 70°C for 5 min. Alternatively 4% SDS, 100mM Tris pH6.8 was used for elution. The sample was stored at -20°C or directly analyzed by bis-Tris SDS-PAGE and western blot.

9. NOA1-His_6 pull-down assay

All steps were performed on ice. The bait, 30µl NOA1-His_6 (e.g. fraction D1) was bound to 0.1ml Ni-NTA agarose beads that were before washed three times with 1 ml Pulldown Lysis Buffer. The beads were incubated for 1h at 4°C on a rotating wheel. Then the unbound protein was washed out with 3x 1ml Pulldown Lysis Buffer. The prey (either 500µl RIPA-IP lysate or 1.3 ml nucleoli fraction) was added to the 0.1ml Ni-NTA agarose beads with NOA1-His_6 and incubate another 1 h at 4 °C on rotating wheel for binding. The beads were washed with 3x 1 ml Pulldown Lysis Buffer. Then the bound proteins were eluted with 50 µl Pulldown Lysis Buffer that contained 100 mM Imidazol. The imidazole elution solution was incubated for 10 min at 4 °C and was mixed from time to time by finger snipping. The eluate was harvested by centrifugation at 10.000g for 1 min at 4°C and was mixed with 5x Laemmli Sample Buffer and boiled for 5 min at 70°C. The pulldown was stored at -20°C until bis-Tris SDS-PAGE.

10. Sucrose gradient fractionation

The sucrose gradient was generated using the Sucrose Gradient KCl Buffer supplemented with 10% or 30% sucrose. Using a mini pump and a gradient mixer device 8 ml gradient was casted into ultracentrifugation tubes for the TST41.14 rotor. A 10 cm dish of confluent C2C12 cells was treated with the following substance: 20 ng/ml Leptomycin B, 10 µM GTP or GTPγS, 10 µg/ml puromycin. After incubation the dish was washed 2 times with ice-cold 1x PBS and the cells were scraped in 1 ml RIPA modified buffer. The lysate was incubated 15 min on ice. After centrifugation (10,000 g 4 °C 5 min) the lysate was overlaid on the sucrose gradient (bottom < 30 %, top 10%-lysate). The tube weight was balanced with 0 % Sucrose Gradient KCl Buffer. Ultracentrifugation was performed over night for ~14 hours at 25.000 rpm. 0.5 ml fractions were harvested. The fractions were stored at -20°C. The sucrose gradient fractions were thawed on ice and precipitated by TCA precipitation. The following steps were done at room temperature. 500 µl 10%TCA/50%Aceton Solution was added to each 500 µl sucrose gradient fractions, vortexed and centrifuged at 14.000 g for 5 min and RT. The precipitated protein appeared as a shiny pellet with white disc. The TCA solution was aspirated and the pellet was washed with 90% Aceton. He protein pellet was air dried and lysed directly in 5x Laemmli Sample Buffer. In case solubilization was poor some drops

Solubilization Buffer were added. In case residual TCA acidified the solution 1 M Tris-HCl pH8.0 was added. The samples were boiled at 95°C for 5 min and analyzed by a bis-Tris SDS-PAGE gel or stored at -20°C.

11. RNA-Immunoprecipitation (RIP)

The RNA-Immunoprecipitation was performed with the same protocol as the normal IP with the exception that the buffers were prepared in DEPC-treated water and after washing the beads were mixed with 1 ml TRZIOL solution. The RNA isolation was performed following the standard protocol. The TRIZOL supernatant was retained and proteins were isolated also following the standard protocol.

12. Recombinant NOA1-His_6 protein production in insect cells

For recombinant protein production Spodoptera frugiperda (Sf9) were cultivated in suspension in SFM 900 medium (Invitrogen) with 5% fetal calf serum at 27°C (this was done in the Falkenberg lab in Gothenburg, Sweden by Emily Hoberg). The coding region of NOA1 was PCR-amplified from mouse cDNA and cloned into pBacPAK9 vector (Clontech) without the MTS (1-17 amino acids) and with a His_6-tag attached to the N-terminus (the vector was cloned and provided by Dr. Szibor, Dept. Braun). *Autographa californica* nuclear polyhedrosis viruses were prepared as described in the BacPAK™ manual (Clontech) to produce virus recombinant for the NOA1 expression constructs. For protein expression 400 ml Sf9 cells were grown until a density of 2 x 10^6 cells/ml in suspension. Cells were infected with 10 plaque-forming units/cell of recombinant baculovirus and harvested 72 h after infection. The cell pellet was shock frozen in liquid nitrogen and stored. This was done in collaboration with the laboratory of Prof. Dr. Maria Falkenberg at the University of Gothenburg, Sweden and performed by Emily Hoberg.

13. Purification of recombinant NOA1-His_6

Adding 20 ml Purification High Salt Lysis Buffer and incubation for 20 min on ice lysed the insect cell pellet. The DNA was sheared using a needle and syringe by pipetting 5x up and down on ice. The extract was cleared by ultracentrifugation at 20.000 rpm for 45 min at 4°C (Beckman TLA100.3 rotor). For purification the cleared lysate was diluted with equal volume (20ml) of Purification Buffer A containing 20 mM Imidazole. The 40 ml extract were added to 5 ml of equilibrated HIS-select HF Nickel affinity gel (Sigma) and incubated for 1 hour at 4°C on rotating

wheel. The Nickel gel was collected by centrifugation (JA-17, 2500 rpm, 10 min, 4°C). The gel was washed with 15 ml Purification Buffer A containing 40 mM Imidazole and again collected by centrifugation. Then the affinity gel with the bound protein was loaded into a plastic column. The column was washed with 10 column volumes Purification Buffer A containing 40 mM Imidazole. Elution was performed with 15 columns volumes Purification Buffer A containing 250 mM Imidazole. Peak fractions were identified by SDS-PAGE and visualized immediately by the Criterion Stain Free Imaging System (Bio-Rad). Peak fractions were pooled and desalted by a) Econo-Pac 10DG Desalting Columns (Bio-Rad) following the manufacturers instructions; elution with buffer C containing 0.2M NaCl or b) diluted 1:4 in Purification Buffer C containing 0.2 M NaCl. The 5-ml HiTrap Heparin-Sepharose column (Amersham Biosciences) was equilibrated with Purification Buffer C containing 0.2 M NaCl. Fractions were loaded on the heparin column and the flow through was collected. The column was washed with 5 column volumes Purification Buffer C containing 0.2 M NaCl (= wash fraction). Elution was performed with a linear gradient (10 column volumes = 50 ml) of Purification Buffer C with 0.2-1.2 M NaCl starting at 30% of the gradient mix concentration. NOA1-His_6 eluted at ~700 mM NaCl. The peak fractions were collected and analyzed by SDS-PAGE (Criterion Stain Free Imaging System (Bio-Rad)). The aliquots were shock frozen in liquid nitrogen and stored at -80°C.

14. GTPase activity assay

The GTPase Assay Buffer was mixed with 1, 2, 3 or 4 µl recombinant NOA1 protein and incubated for 60 min at 37°C. After addtion of 5 µl GTPase Assay Stop Buffer the samples were frozen at -20°C or directly separated by 15% TBE-PAGE in 1x TBE Running Buffer for 2h at 200 V. Then the gel was dried for 2 h at 80°C and evaluated with the PhosphorImager system.

15. Gel shift assay with G-quadruplexes

For electromobility shift assays of recombinant protein and G-quadruplex folded oligos, the following composition was used: 2 µl 10x EMSA Binding Buffer, 2 µl 25 mM $MgCl_2$, 2 µl 1 µg/ml poly dIdC, 0.5 µl oligo (folded & ^{32}P-ATP labeled), ad 20 µl H_2O. The recombinant NOA1-His_6 protein (1-4 µl) was added and the reaction was incubated for 30 min at 37°C. 6 µl KCl-Glycerol Loading Dye was added and the

samples were analyzed on 6% TBE-PAGE run in 0.5x TBE with 10 mM KCl at 150 V for 2h. the gel was dried and analyzed by PhosphorImager.

16. Glutaraldehyde crosslinking of recombinant NOA1-His_6

10 µl recombinant protein (3 µg/µl) with 0.5 µl end labeled G-quadruplex oligo () were crosslinked for 2 min at RT in a buffer and salt composition identical to the EMSA setup. The crosslinking was performed with glutaraldehyde solutions of different final concentrations. The crosslinking reaction was incubated for 5 min at 37 °C. The reaction was stopped by adding 3 µl 1M Tris-HCl pH 8.0 and 5 µl 5x Laemmli Sample Buffer. After boiling the sample at 95 °C for 5 min, 15 µl were separated on a 3-8% Tris-Acetate SDS-PAGE gel (Invitrogen). The gel was run in 1x Tris-Acetate Running Buffer (Invitrogen) at 200 V for 1 h. The gel was analyzed by PhosphorImager analysis or immunoblot.

17. Import of recombinant NOA1-His_6 into isolated nuclei

The nuclei isolation protocol was adapted from[145] and[146]. In short, nuclei isolated from RAW264.7 mouse macrophages were used in combination with recombinant mouse NOA1-His_6 protein. The cells were pelleted from a dense 10 cm dish and incubated in 200 µl Hypotonic Nuclei Lysis Buffer for 10 min on ice. The nuclei isolation was supported by 2-4 gentle strokes in a dounce homogenizer. The purity of the nuclei was checked under the microscope by mixing 10 µl nuclei solution with 10 µl trypan blue solution. The nuclei were pelleted at 500 g for 30 min at 4°C. The nuclear pellet was resuspended in 150 µl Nuclei Storage Buffer. For the nuclear import assay the 50µl Transport buffer was mixed with 50 µl Nuclei Solution, 5 µl 100 mM ATP, 5 µl 81 mg/ml Creatine phosphate, 2 µl 2000 u/ml Creatine phosphate kinase, 5 µl ~3mg/ml recombinant NOA1-His_6, 2 ml 22 ng/µl Leptomycin B, 5 µl 10 mM GTP or GTPγS. The import reaction was mixed by gentle pipetting and incubated for 30 min at RT. The nuclei were pelleted at 500 g for 10 min and washed quickly with 1x PBS. After pelleting the nuclei again they were incubated in 4% PFA for 10 min and washed again with 1x PBS. The antibody staining occurred in solution with 100 µl antibody diluted 1:100 in 1x PBS solution. The stained nuclei were mounted with Mowiol were dried at RT before microscope analysis.

18. Preparation of 4% PFA Fixing Solution

450 ml of H_2O was heated to 60°C using a hot plate with stirring. While stirring 20 g of paraformaldehyde powder (Fisher #04042) were added to the heated water. The mixture was covered and maintained at 60°C. After the addtion of 5 drops of 2N NaOH (1drop per 100 ml) the solution appeared clear within a couple of minutes. The solution must not be heated above 70°C because PFA breaks down at temperatures above 70°C. 50 ml of 10x PBS were added to the solution and cooled. The pH was adjusted to pH7.2 and the volume to 500 ml. The PFA solution was filtered, placed on ice and covered with foil to protect from light. Aliquots were frozen at -20°C and thawed as needed.

19. Fixation and Mounting

For fixation cells were washed twice with 1x PBS and incubated for 10-15 min in 4% PFA Solution. Mounting was performed with Mowiol Solution that was applied on the fixed and washed cell layers.

20. Antibody staining of cells

Antibody staining was performed after PFA fixation. Staining was done overnight in a humid chamber. The cells were permeabilized with 0.3% TX-100 in 1xPBS for 10 min at RT. In chamber slides, the cells were overlaid with the antibody solution. When cells were seeded on coverslips a drop of antibody solution was put on a piece of parafilm and the coverslip was put upside down on the solution. For washing the coverslips were dipped several times in a glass of 1x PBS. The primary antibody was incubated over night at 4°C in the cold room. The secondary antibody was incubated for 1 hour at RT. Addition of DAPI to the first washing step stained the nuclei. For Mitotracker staining the cells were incubated with a 1:10.000 dilution of the 1 mM Mitotracker stock solution.

21. FACS analysis of cells

Cells were harvested by trypsin/EDTA and centrifugation. Then, the cells were fixed with 4% PFA solution followed by staining with Annexin V / PI of JC-1 in solution following standard protocols for one hour on ice. The cells were washed with 1x PBS and resuspended in 1x PBS. Phosphatidylserine is normally oriented towards the inside of the cell membrane. During apoptosis the phosphatidylserine is translocated to the outside of the cell and becomes accessible for Annexin V. Necrotic cells have

permeable cell membranes and the propidiumiodide can penetrate the cells whereas apoptotic cells are not permeable for propidiumiodide. Therefore, cells that are Annexin V-FITC positive and propidiumiodide negative are considered apoptotic. Measuring was done on a FACS Diva device.

22. LOPAC library screen

C2C12 cells were transfected with TO5 NOA1-EGFP. A stable cell line was obtained by selection with Hygromycin B (200µg/ml) for 2 weeks. Cells overexpressing NOA1-EGFP were seeded into 16 well Lab-Tek Chamber Slides. Cells were treated with an end concentration of 100 µM of each of the 1280 LOPAC substances per well for 6 hours at 37°C and 5% CO_2. Cells were washed in 1x HBSS (PAA), fixed with 4% PFA and mounted with Mowiol Solution. Analysis of the localization of EGFP-fluorescence occurred with the Zeiss Axioimager Z1 microscope. Positive hits were further validated by treatment of untransfected cells and antibody staining for NOA1.

23. Preparation of inverted mitochondrial vesicles

Mitochondria were isolated from 1-2 rat livers according to Protocol 5 and were resuspended in 2 ml 20 mM KH_2PO_4 solution containing RNase inihibitors. After sonication on ice (settings: 50%, 3x, 15 sec on, 15 s off) large clumps were spun down at 6500 g for 7 min at 4°C. The supernatant was transferred into a fresh tube and the pellet was resuspended in 2 ml 20 mM KH_2PO_4 solution containing RNase inihibitors. Sonication and centrifugation were repeated and the two supernatants were combined in an ultracentrifuge tube and centrifuged for 1h at 105.000 g (29.000 rpm in TST41.14 rotor) at 4°C. The supernatant was the matrix fraction. The resulting pellet was resuspended in 10 ml 20 mM KH_2PO_4 solution containing RNase inihibitors and the ultracentrifugation was repeated. The resulting pellet was resuspended in 300 µl 20 mM Tris pH 7.5 containing RNase inihibitors, aliquoted, snap-frozen and stored at -80°C.

24. In vitro translation with inverted vesicles

For each sample an *in vitro* translation mixture containing 110 µl H_2O, 20 µl 10x Translation Buffer, 10 µl mitochondrial RNA preparations, 10 µl mitochondrial inverted vesicle fraction and 40 µl mitochondrial matrix fraction was prepared. Then 5 mM chloramphenicol in 20 mM Tris pH 7.5 and and recombinant NOA1-His_6

protein were added and the mixture was incubated for 5 min on ice. After addition of 10 µl ^{35}S-Methionine/^{35}S-Cysteine (Easy-tag ExpreSS, Perkin Elmer, ~100 µCi) the assay was incubated for 45 min at 37°C. To avoid pelleting of vesicles the sample was vortexed every 10 min. The sample was separated into the membrane contaning pellet and the matrix contining supernatant fraction by centrifugation for 5 min at 14.000g and 4°C. The pellet was resuspended in 100 µl 4% SDS, 50 mM Tris pH 7.5. Both fractions were precipitated by methanol/chloroform (Wessel & Flügge). 4 vol methanol were added. After vortexing, 2 vol chloroform were added and the sample was vortexed again. Then 1.5 vol H_2O were added the samples were spun for 5 min. The upper water phase was removed leaving the interphase untouched and 1.5 vol methanol was added, the samples were vortexed and spun again for 5 min. The liquid was removed and the pellet was air dried, briefly. The sample was resuspended in Sample Buffer and was incubated for 60 min at 37°C. The samples were separated on large 17% Bis-Tris SDS-PAGE gels and run at 70V in 1x MES Running Buffer. The gel was stained with InstantBlue and dried slowly onto Whatman paper. The imaging was evaluated after PhosphorImager exposure.

X. Materials

A. *Software*

Name	Company	Purpose
4Peaks	Mekentosj.com	Viewing and editing sequencing files
Adobe Acrobat 9 Pro	Adobe Systems	pdf dokument handling
AIDA 1D Evaluation 2D Densiometry	Raytest, Straubenhardt	Evaluation of phosphorimager data
ApE (A plasmid Editor)	M. Wayne Davis	Vector information filing
Endnote X4	Thomson Reuters	Reference Management
EnzymeX	Mekentosj.com	Restriction enzyme tool
Epson Scan	Epson Meerbusch	Scanning Software
Firefox	Mozilla	Internet Browser
Image Reader V2.02	Fuji Photo Film Co.,Ltd.	Phosphorimager screen readout
iWork 2009 (Keynote)	Apple	presentation
NEBcutter V2.0	New England Biolabs Inc.	Restriction enzyme tool
Odyssey Software	LI-COR Biosciences	1-D 2-Color Analysis Software
Office for Mac 2011 (Word, Excel, PowerPoint)	Microsoft	Text processing, data evaluation and poster design
Quantity One	BIO-RAD	1-D Analysis Software
Sophos Anti-Virus	Sophos Ltd	Antivirus Software

B. *Lab equipment*

Device	Distributor
3M1440 Ear Muff	VWR
Agarose gel chambers various sizes	peqlab
Bacterial incubator B5060E	Heraeus
Balance Max 4800g Min 0.5g LC4800P-OD2	Sartorius
Balance Pioneer PA214	OHAUS
Biofuge fresco	Heraeus
Biofuge stratos	Heraeus Instruments
BioDoc Analyze	Biometra
BioImage Analyzer BAS-2500	Fujifilm
Cell culture microscope: Leica Mikroscope DM1L with DFC400C Camera	Leica
Centrifuge 4-16K	Sartorius
Centrifuge 5417C	Eppendorf
Centrifuge 5417R (Refrigerating)	Eppendorf
Centrifuge Evolution RC	Sorvall
Concentrator plus 5305	Eppendorf
Contamination Monitor LB147	Berthold Technologies
Eraser	Raytest
Flake Ice Machine AF200	Scotsman
Gel dryer Model 583 with membrane vacuum pump	BIO-RAD
Hand-held Contamination monitor LB122	Berthold Technologies
Heating Block	HLC
HERA cell 150i incubator	Heraeus
HERA SAFE KS sterile bench	Heraeus
iCycler Basis System & iCycler Optical System	BIO-RAD
INNOVA 44 Incubator Shaker Series	New Brunswick Scientific
LI-COR Odyssey Infrared Imager	LI-COR
Magnetic Stirrer RCT	IKAMAG
Microwave Express Cook&Defrost	SHARP

MilliQ Device Advantage A10	Millipore
Mithras LB940 Multilabel Reader	Berthold Technologies
Novex Mini Cell Gel Running Chamber	Invitrogen
PCR machine Eppendorf Mastercycler	Eppendorf
PCR machine Sensquest Labcycler Gradient + Thermoblock 96	Sensquest
Perfection 4990 Photo Scanner	Epson
Peristaltic Pump P-1	Amersham Biosciences
pH Meter Five Easy FE20/EL20	Mettler Toledo
Phosphorimager Cassettes Fujifilm BAS Cassette 2040	Fujifilm
Pipet Aid	Drummond
Power Pack P25	Biometra
Power Supply 500V-500mA	CONSORT
Power Supply EPS 2A200	Hoefer
Power Supply Power Ease 500	Invitrogen Life Technologies
PROTEAN IIXi Cell with inner & outer plate, spacer 1.0mm; casting device 26S/5135 and 10well comb 1.0mm Teflon	BIO-RAD
Rocking Platform 348/1	Assistant
Rocking Platform PROMAx1020	Heidolph
Rotator neo Lab	neoLab
Rotor: SLA-1500	Sorvall
Rotor: SS-34	Sorvall
Rotor: TST41.14	Beckmann Coulter
Sonicator Sonoplus HD2070 with SM70G Sonotrode	Bandelin
Table Mini centrifuge sprout	Heathrow Scientific LLC
Thermomixer 5436	Eppendorf
Thermomixer compact	Eppendorf
Ultracentrifuge Optima L-90K	Beckmann Coulter
Versadoc Imaging System	BIO-RAD
Vortexer	Janke&Kunkel, IKA Labortechnik VFZ
Waterbath Type 1003	GFL Gesellschaft für Labrotechnik mbH Burgwedel
X Cell II Blot Module E19051	Invitrogen

C. Consumables

Name	Company
0.02, 0.5, 1.5, 2 ml PCR-Tubes	Variable supplier
10cm dish (bacteria)	Roth
10ml Tube - BDFalcon cell star	Greiner bio-one
50ml Tube – BDFalcon cell star	Greiner bio-one
Amicon Ultra 3K Columns	Millipore
Barrier Food Wrap	Roth
Cell culture dish 145, 100, 60, 35 mm dish	Greiner bio-one
Cell Scraper 25cm	Sarstedt
Cellstar Microplate plates 96 Well	Nunc
Cellstar Multiwell plates 6, 12 Well	Nunc
Chamber Slides LabTek	Nunc
Combitips advanced 0.5, 1, 2, 5 ml	Eppendorf
Cryotube 1ml	Nunc
Filter tips	Fisher Scientific
Gel casting cassettes 1.0 mm	Invitrogen
Glas objective slides superfrost	Thermo Scientific
Glass coverslips 18mm round	Marienfeld
Glass coverslips rectangle	Roth
Gloves Rotiprotect Latex & Soft Nitril Blue	Roth
Illustra Probe Quant G-50 Micro Columns	GE Healthcare

Inoculation spatels	Roth
Lab Alu Foil	Roth
Nitrocellulose membrane	Millipore
Parafilm M	Roth
Pipette tips	Variable supplier
Plastic Pipets sterile 5, 10, 25, 50 ml	Greiner bio-one
Polystyrene cuvettes	Sarstedt
Scalpel	B.Braun
Sterile Filter	Heinemann Labortechnik GmbH
Syringe	B.Braun
Tissue	Roth
Ultracentrifuge Tubes 344059 9/16x3 ½	Beckman Coulter
Ultracentrifuge Tubes 344059 9/16x3 ½	Beckman Coulter
Waste bags	Roth
Whatman Paper	Millipore

D. Chemicals, Kits and Ready-made Solutions

Name	Company
Ac-YVAD-cmk (Caspase-1-Inhibitor)	Sigma Aldrich
Acrylamide/Bisacrylamid Solution 19:1	Roth
Acrylamide/Bisacrylamid Solution 29:1	Roth
Caspase-1 inhibitor	Sigma Aldrich
Colloidal Coomassie Staining Kit	Invitrogen
DC Protein Assay Kit	BioRad
Easy-tag ExpreSS ^{35}S-Met/^{35}S-Cys	Perkin Elmer
Ethidiumbromide	AppliChem
Hygromycin B	PAA
Instant Blue	Expedon
JC-1	Sigma Aldrich
Lipofectamine 2000	Invitrogen
Mitotracker Red 580	Invitrogen
PCR clean up and gel extraction kit (Nucleosplin Extract II)	Macherey-Nagel
Propidium Iodide	Sigma Aldrich
Protein G Sepharose 4 Fast Flow	GE Healthcare
Red Alert	Novagen
Trizol	Invitrogen
Turbofect	Fermentas
Western Lightning Ultra	Perkin Elmer
Z-vad-fmk (Pan-Caspase-Inhibitor)	Sigma Aldrich

E. Antibodies

Name	Order Number	Company	Source	Dilution for Western Blot	Dilution for IHC
Primary antibodies:					
Annexin V	A13201	Invitrogen			
Anti- Tom20	Sc-11415	Santa Cruz	Rabbit	1:1000	1:100
Anti-His_6-tag	34660	Qiagen	Mouse	1:2000	
anti-phosphoserine	05-1000X	Millipore	Mouse	1:1000	
c-jun (60A8)	9165	Cell Signalling	Rabbit	1:1000	
calnexin	610523	BD Bioscience	Mouse	1:1000	
ClpX (S-14)	Sc-162692	Sigma Aldrich	Goat	1:500	1:50
Fibrillarin	Sc-166001	Santa Cruz	Mouse	1:1000	
Flag M2	F1804	Sigma Aldrich	Mouse	1:5000	1:500
GAPDH	2118	Cell Signalling	Rabbit	1:4000	
GFP	Ab6556	Abcam	Rabbit	1:5000	1:250
MEK1/2	9121	Cell Signalling	Rabbit	1:1000	
MRPL28	HPA030594	Sigma Aldrich	Rabbit	1:1000	

MRPS27	SAB1404954	Sigma Aldrich	Mouse	1:1000	
NOA1		Eurogentic	Rabbit	1:1000	1:100
PDHE1	MA5-14805	Pierce	Rabbit	1:1000	
Phalloidin, FITC	P5282	Sigma			1:200
Porin/VDAC	MSA03	Mitosciences	Mouse	1:10000	
S6RP	2211	Cell Signalling	Rabbit	1:1000	
UBF1	Sc-13125	Santa Cruz	Mouse	1:5000	1:100
Secondary antibodies:					
Anti-goat Alexa 488	A21467	Invitrogen	Chicken		1:200
Anti-mouse Alexa 594	A11005	Invitrogen	Goat		1:200
Anti-mouse Alexa 680	A21057	Invitrogen	Goat	1:10000	
Anti-mouse cy2	715-225-151	Dianova	Donkey		1:200
Anti-mouse cy3	715-165-151	Dianova	Donkey		1:200
Anti-mouse cy5	715-175-150	Dianova	Donkey		1:200
anti-mouse HRP	31430	Pierce	Goat	1:1000	
Anti-rabbit cy3	711-165-152	Dianova	Donkey		1:200
Anti-rabbit Alexa 488	A11070	Invitrogen	Goat		1:200
Anti-rabbit Alexa 680	A21076	Invitrogen	Goat	1:10000	
Anti-rabbit cy2	711-225-152	Dianova	Donkey		1:200
Anti-rabbit cy5	711-175-150	Dianova	Donkey		1:200
anti-rabbit HRP	31460	Pierce	Goat	1:1000	
anti-rat HRP	612-9302	Rockland	Goat	1:500	
Goat IgG IRD 800	605-732-125	Rockland	Donkey	1:10,000	
Mouse IgG IRDye 800	610-132-121	Rockland	Goat	1:10,000	
Rabbit IgG IRD 800	611-132-122	Rockland	Goat	1:10,000	
Rat IgG IRDye 800	612-132-121	Rockland	Goat	1:10,000	

F. Enzymes

Name	Company
BamH1	Jena Bioscience
BsmBI	New England Biolabs
Caspase-1	PromoKine
Caspase-8	PromoKine
Caspase-9	PromoKine
Collagenase P	Sigma Aldrich
Creatine Kinase	Sigma Aldrich
DNase I	Promega
Eco RI	Jena Bioscience
EcoRV	Jena Bioscience
Klenow Polymerase	Promega
NdeI	Jena Bioscience
Pfu High Fidelity Ultra Polymerase AD	Agilent
Phusion Polymerase	Finnzymes
RedTaq Mix	Sigma Aldrich
RNAse I	Sigma Aldrich
SlaI	Jena Bioscience
T4 DNA Ligase	Promega
T4 Polynucleotid Kinase	New England Biolabs
Taq DNA Polymerase	Promega
XbaI	New England Biolabs

G. Bacteria and eukaryotic cell lines

Bacteria:	
E.coli XI1Blue	Stock provided by Dr. M. Szibor (Dept. Braun)

Cell lines:	
C2C12 mouse myoblasts	ATCC CRL-1772
NIH3T3 mouse myoblasts	ATCC CRL-1658
RAW264.7 mouse macrophages	ATCC TIB-71

H. Buffer and Stock Solutions

Protease inhibitors are added directly before use.

0.1x Homogenization Buffer
1:100 10x Homogenization Buffer, 0.1 mM PMSF, in ddH_2O; storage at 4°C
0.5 M EDTA Stock
186.1 g Na-EDTA*$2H_2O$, 20 g NaOH pellets, pH 8.0, in ddH_2O (for a volume of 1000 ml)
0.5x TBE
1:20 10x TBE, in ddH_2O
10% APS
1 g APS in 10 ml ddH_2O, storage in aliquots at -20°C
Mowiol
2.4 g Mowiol 4-88, 6 g Glycerin, 6 ml ddH_2O, 12 ml Tris-HCl pH 8.5
10% NaDOC
1g Sodium-Deoxycholate in 10 ml ddH_2O, storage in aliquots at -20°C
100x Amp
100 mg/ml Ampicillin in ddH_2O, storage in aliquots at -20°C
100x Kan
100 mg/ml Kanamycin in ddH_2O, storage in aliquots at -20°C
100x Protease Inhibitor Mixture
100 mM PMSF, 200 mM Peptstatin, 60 mM Leupeptin, 200 mM Benzamidine, in 100% Ethanol; storage at -20°C
10x EMSA Binding Buffer
100 mM Tris-HCl pH 7.4, 1 M KCl, 10 mM EDTA, 0.1 mg/ml BSA, 5% Glycerol, 1% NP-40, in ddH_2O
10x Homogenization Buffer[147]
400 mM Tris-HCl, 250 mM NaCl, 50 mM $MgCl_2$, in ddH_2O; storage at 4°C
10x PBS
14.4 g Na_2HPO_4, 2.4 g KH_2PO_4, 2 g KCl, 80 g NaCl, pH 7.4, in ddH_2O; storage at 4°C
10x TBE
108 g Tris, 55 g Boric Acid, 40 ml 0.5M EDTA, for a volume of 1000 ml, in ddH_2O
10x TBE
108 g Tris Base, 55 g Boric Acid, 40 ml 0.5M EDTA in ddH_2O, (for a volume of 1000 ml)
10x TBS
2 M Tris-HCl pH 6.7, 1.4 M NaCl, in ddH_2O
10x Translation Buffer
15 mM Tris-HCl pH 7.5, 2 mM MgAc, 50 mM KCl, 0.5 mM ATP, 0.05 mM GTP, 5 mM creatine phosphate, 80 µM creatine kinase, 100µM amino acids, 1.5 mM β-mercaptoethanol, in ddH_2O; storage at 4°C
1x EMSA Binding Buffer
2µl 10x EMSA Binding Buffer, 2µl 1µg/µl 1poly dIdC, 2µl 25 mM $MgCl_2$, in ddH_2O (for a volume of 20 µl), must be prepared freshly
1x LB-0
LB medium in ddH_2O; sterilized by autocalving and storage at 4°C
1x MES-SDS Running Buffer
dilution of 20x MES-SDS Concentrate (Invitrogen) in ddH_2O
1x MOPS-SDS Running Buffer
dilution of 20x MOPS-SDS Concentrate (Invitrogen) in ddH_2O
1x TAE
1:50 50x TAE, in ddH_2O
1x TBE
1:10 10x TBE, in ddH_2O
1x TBS
1:10 10x TBS, in ddH_2O

1x TBS-T
1:10 10x TBS, 0.001 % Tween-20, in ddH_2O
1x TE
10 mM Tris-HCl pH 7.5, 1 mM EDTA, in ddH_2O
1x Transfer Buffer
1:20 20x Transfer buffer, 20% Methanol, in ddH_2O
20x MES native
1M Tris pH7.3, 1M MES, 20 mM EDTA
20x Transfer Buffer
0.5 M (163.2 g) Bicine, 0.5 M (209.3 g) Bis Tris, 20 mM EDTA, in ddH_2O (for a volume of 2 l)
2M Sucrose/TE
20 mM HEPES-KOH pH 7.5, 10 mM KCl, 1 mM EGTA, 1 mM EDTA, 0.25 M Sucrose, 0.1 % Fatty Acid Free BSA, 0.1 mM PMSF, in ddH_2O; storage at 4°C
2x LB-0
double concentrated LB medium in ddH_2O; sterilized by autocalving and storage at 4°C
2x LB-0
25 g ready-mix LB medium in 1000 ml ddH_2O; composition: 10 g/l Trypton, 5 g/l Yeast extract, 10 g/l NaCl, pH7.0; sterilized by autocalving and storage at 4°C
3.5x (Bis-Tris) SDS-PAGE gel buffer
1.25 M Bis-Tris pH 6.5-6.8, in ddH_2O
3% Milk TBS-T
3 g Skim Milk Powder, 1x TBS-T, storage at 4°C
5% Milk TBS-T
5 g Skim Milk Powder, 1x TBS-T, storage at 4°C
50x TAE
2M (242.28 g) Tris pH 8.5, 1M (60.05 g) Acetic Acid, 0.05 M EDTA, in ddH_2O (for a volume of 1 l)
5x KCM
500 mM KCl, 150 mM $CaCl_2$, 250 mM $MgCl_2$, in ddH_2O
5x Laemmli Sample Buffer[148]
3 ml 1M Tris-HCl pH 6.8, 10 ml 10% SDS, 32 ml H_2O, 5ml 100 % Glyerol, a few grains Bromphenol Blue, 100 mM DTT
6x DNA Loading Buffer
18.8 ml 80% glycerol, 30.6 ml ddH_2O, 600 µl EDTA, 60 mg Bromephenol Blue, 60 mg Xylene cyanol Blue
6x Ficoll Loading Buffer
50% Glycerol, 50% H_2O, with a spatle tip of Orange G
EMSA-KCl-Glycerol Loading Buffer
10 mM KCl, 25% Glycerol with a few grains Bromphenol Blue, in ddH_2O
GTPase Assay buffer
20 mM HEPES-KOH pH8.0, 4.5 mM MgAc, 150 mM KAc, 2 mM Spermidine, 0.05 mM Spermine, 4 mM β-mercaptoethanol, 2.5 nM GTP (including 5% ^{32}P-γGTP), in ddH_2O
GTPase Assay Stop Buffer
25% Glycerol with a few grains Bromphenol Blue, in ddH_2O
Hypotonic nuclei lysis buffer[145]
10 mM HEPES-KOH pH7.9, 0.1 mM EDTA, 2 mM $MgCl_2$, 10 mM KCl, 1 mM DTT, 5 mM PMSF, in ddH_2O; storage at 4°C
Laemmli Cell Lysis Buffer
3 ml 1M Tris-HCl pH 6.8, 10 ml 10% SDS, 32 ml H_2O
Mowiol Solution
6 g Glycerol, 2.4 g Mowiol, 6 ml H_2O,12 ml 0.2M Tris-HCl pH 8.5; storage at 4°C
Nuclear Extraction Buffer
20 mM Tris-HCl pH7.9, 25% Glycerol, 420 mM NaCl, 1.5 mM $MgCl_2$, 0.2 mM EDTA, 0.1 mM PMSF, 0.5mM DTT, in ddH_2O, storage at 4°C
Nuclei Import Mixture[146]
50 µl Transport buffer, 50 µl isolated Nuclei in Nuclei Storage Buffer, 5µl 100 mM ATP, 5µl 81 mg/ml Creatine phosphate, 2µl 2000u/ml Creatine phosphate kinase, 2 µl 22ng/µl Leptomycin B, 5 µl 10 mM GTP or GTPγS, must be prepared freshly, 5µl recombinant NOA1 protein
Nuclei Storage Buffer[145]
50 mM HEPES-KOH pH 8.3, 0.1 mM EDTA, 5 mM $MgCl_2$, 40 % Glycerol, in ddH_2O
Nucleoli Buffer S1

0.25M Sucrose, 10mM $MgCl_2$
Nucleoli Buffer S2
0.35M Sucrose, 0.5mM $MgCl_2$
Nucleoli Buffer S3
0.88M Sucrose, 0.5mM $MgCl_2$
Nucleoli Isolation Buffer A
10mM HEPES pH7.9, 10mM KCl, 1.5mM $MgCl_2$, 0.5mM DTT
Permeabilization Solution
0.3% TX-100 in 1x PBS
Protein Solubilization Buffer
30 mM Tris-HCl pH 8.0, 5 µM EDTA, 9M Urea, 1% DTT, 0.5% TX-100, in ddH_2O, storage at 4°C
Pulldown Lysis Buffer
50 mM HEPES-KOH pH7.5, 10 mM $MgCl_2$, 200 mM KCl, 0.1 mM EDTA, 10% Glycerol, 1% TX-100, in ddH_2O, storage at 4°C
Purification Buffer A
50 mM Tris-HCl pH8.0, 600 mM NaCl, 20% Glycerol, 10 mM β-mercaptoethanol, in ddH_2O
Purification Buffer C
0.5M NaPO4 pH6.8, 10% Glycerol, 10 mM β-mercaptoethanol, in ddH_2O
Purification High Salt Lysis Buffer
20 mM Tris-HCl pH8.0, 500 mM NaCl, 20% Glycerol, 0.5 mM β-mercaptoethanol, in ddH_2O
RIP-RIPA modified
790 mg Tris-HCl pH7.4, 900 mg NaCl, 1% NP-40, 0.25% Sodium-deoxycholoate, 1.25 mM EDTA, in DEPC treated ddH_2O, storage at 4°C
RIPA modified
790 mg Tris-HCl pH7.4, 900 mg NaCl, 1% NP-40, 0.25% Sodium-deoxycholoate, 1.25 mM EDTA, in ddH_2O, storage at 4°C
Solution A
25 mM Tris-HCl pH8.0, 10 mM EDTA, 50 mM Glucose, in ddH_2O, storage at 4°C
for Miniprep 10µg/ml RNase A
Solution B
0.2N NaOH, 1% SDS, in ddH_2O, freshly prepared
Solution C
60 ml 5M KAc, 11.2 ml Acetic Acid, for a volume of 100 ml, in ddH_2O, storage at 4°C
Sørensen Buffer[149,150]
0.5M Na_2HPO_4, in ddH_2O & 0.5M NaH_2PO_4 in ddH_2O
Sucrose Gradient KCl Buffer
50 mM Tris-HCl pH7.5, 100 mM KCl, 2 mM NaCl, 10 mM $MgCl_2$, 2 mM DTT, 1 % NP-40, 0.25% NaDOC, 1.25 mM EDTA, in ddH_2O; storage at 4°C
TCA Precipitation Solution
10% Trichloracetic Acid, 50% Aceton, in ddH_2O
Tissue Extraction Buffer
20 ml 1 M Tris-HCl pH 8.0, 20 g SDS, 0.744 g EDTA, in ddH_2O (for a volume of 200 ml)
Transport Buffer[146]
20 mM HEPES-KOH pH 7.9, 100 mM KAc, 2 mM MgAc, 1 mM EGTA, 2 mM DTT, in ddH_2O
TSB
5% DMSO, 10 mM $MgCl_2$, 10 mM $MgSO_4$, 10% PEG6000, in2x LB-0 medium
Wash Buffer
10 mM Tris-HCl pH 7.8, 250 mM EDTA, 2 M Sucrose, in ddH_2O; storage at 4°C

XI. Appendix

A. *List of Figures*

B. List of Tables

C. Abbreviations

%	percent
°C	Degree celcius
A488	Alexa dye 488
A594	Alexa dye 594
AA	Acrylamide
Ac	Acetate
Act D	Actinomycin D
Amp	Ampicillin
as	antisense
ATCC	American type culture collection
ATP	Adenosine triphosphate
BAA	Bisacrylamide
Bis-Tris	Bis(2-hydroxyethyl) aminotris (hydroxymethyl) methane
BPB	bromphenoblue

BSA	Bovine serum albumin
cDNA	Complementary deoxyribonucleic acid
Cl	Chloride
CO_2	Carbon dioxide
Cy2	Carbocyanine
Cy3	Indocarbocyanine
Dapi	4',6'-Diamidino-2-phenylindol
dd	Double distilled
DEPC	Diethylpyrocarbonate
Dept	Department
DMEM	Dulbecco's Modified Eagle Medium
DNA	Deoxyribonucleic acid
DOC	Deoxycholate
DTT	Dithiorethiol
e.g.	Lat. exempli gratia, for example
EDTA	Ethylenediaminetetraacetic acid
EGFP	Enhanced green fluorescent protein
f.c.	Final concentration
FCS	Fetal calf serum
Fw	Forward
g	Gravitational acceleration
GTP	Guanosine triphosphate
h	Hour
HCl	Hydrochloric acid
HEPES	2-(4-(2-Hydroxyethyl)-1-piperazinyl)-ethansulfonsäure
In vitro	Latin for „outside of the living organism"
IP	Immunoprecipitation
K	Potassium
Kan	Kanamycin
kb	Kilo bases
kDa	Kilo dalton
KOH	Potassium hydroxide
LMB	Leptomycin B
LSU	Large subunit (of the ribosome)
MCS	Multiple cloning site
MES	2-(N-morpholino)ethanesulfonic acid
MES	2-(N-Morpholino)-ethansulfonic acide
min	Minute
ml	Milli liter
MOPS	3-(N-morpholino)propanesulfonic acid
mRNA	messenger ribonucleic acid
mtDNA	Mitochondiral DNA
Na	Sodium
nm	Nano meter
nm	Nano meter (measure of wavelength)
NP-40	Nonidet P-40
Oligo	Oligo-nucleotide
PAGE	Polyacrylamide gel electrophoresis
PBS	Phophate buffered saline
PCR	Polymerase chain reaction
PFA	Para formaldehyde
PI	Protease inhibitors
PMSF	Phenylmethylsulfonylfluorid
PO_4	Phosphate
Rev	Reverse
RIP	RNA Immunoprecipitation
RNA	Ribonucleic acid
rRNA	Ribosomal ribonucleic acid
RT	Room temperature
RT-PCR	Reverse transcription polymerase chain reaction

S	Sense
SDS	Sodium dodecyl sulfate
sec	second
shRNA	Short-hairpin RNA
SSU	Small subunit (of the ribosome)
TAE	Tris-Acetic Acid-EDTA
TBE	Tris-Boric Acid-EDTA
TBS	Tris-Boric Acid-Sodium Chloride
TE	Tris-EDTA
Tris	Tris-(hydroxymethyl)-aminomethan
tRNA	Transfer ribonucleic acid
TX-100	Triton X-100
u	Unit
vs.	versus
µl	Micro liter
µm	Micro meter

D. List of oligonucleotides

The oligonucleotides were ordered from Sigma-Aldrich.

Name	Sequence 5'-3'	Application
18S rRNA fw	AAACGGCTACCACATCCAAG	PCR
18S rRNA rev	CCTCCAATGGATCCTCGTTA	PCR
Xcheck fw	CACGGAGGAACGCTTTCTGT	PCR
Xcheck rev	CGTCTGGAAACTCCGGGAC	PCR
ClpX fw	TGTTGTTGGCCAGTCGTTTG	PCR
ClpX rev	GCGATCTGAAGCAACTTTGT	PCR
ClpP fw	TGGGCCCGATTGACGACAGTG	PCR
ClpP rev	TAGATGGCCAGGCCCGCAGT	PCR
Lon fw	GCTCCATTGCCCGTGCCCTT	PCR
Lon rev	CCCCCACGTAGGTACGCCTGT	PCR
ClpX K300A a1935g_a1936c s	GGACCAACTGGGTCAGGTGCAACCCTTC TGGCACAAAC	Site directed Mutagenesis
ClpX K300A a1935g_a1936c as	GTTTGTGCCAGAAGGGTTGCACCTGACC CAGTTGGTCC	Site directed Mutagenesis
ClpX-mouse-BamHI fw	**GGATCC**ATGTCCAGTTGCGGCGCTTGT	Amplification
ClpX-mouse-XhoI rev	**CTCGAG**TTAGCTGTTTGCAGCATCCGCT TGAC	Amplification
NOA1XhoIN-3KK-AAStoprev	**CTCGAG**TCATCTGTGGGCGGCCAGGTT GTGCACCAGGGACGGAGGGGCGG CGGTTTTATAGGCCACACTGGCGGCCAT GCGCTG	Mutation
NOA1XhoIN-3KK-AAnoStop	**CTCGAG**TCTGTGGGCGGCCAGGTTGTG CACCAGGGACGGAGGGGCGGCG GTTTTATAGGCCACACTGGCGGCCATGC GCTG	Mutation
XhoI rev	**CTCGAG**TCATCTGTGCTTCTTCAGGTTG	Amplification
XhoIFlag rev	**CTCGAG**TCACTTATCATCATCATCCTTA TAATCTCTGTGCTTCTTCAGGT TG	Amplification
NOA1 sense	TTTAAA**GGATCC**ATGCTGCCCGCGCGC CTGGCTTGCGGGCTGCTCTGCGGG	Amplification (#1)
ΔNOA1 sense	TTTAAA**GGATCC**ATGCCCGCGCCGGCC GCTGCGTGCTACGGCCCAGCACGG	Amplification (#2)
ΔNOA1-C25 sense	TTTAA**AGGATCC**ATG*TCC*CTGGCCTTTG ACATGGGAAGTGAACCAGTTGTGT	Amplification (#3)
77-Flag-Stop revcompl	TAA**CTCGAG**TCACTTATCATCATCATCC TTATAATCTCTGTGCTTCTTCAGGTTG	Amplification (#4)

N52-Flag-Stop revcompl	TAA**CTCGAG**TCACTTATCATCATCATCCTTATAATCGTCGGCATCAAACTCAAAG	Amplification (#5)
MTS s (BamH1-XhoI compatible overhangs)	**GATC**CATGCTGCCCGCGCGCCTGGCTTGCGGGCTGCTCTGCGGGCTCCGGCGGGGCC	Signal sequence cloning upstream of GFP
MTS as (BamH1-XhoI compatible overhangs)	**TCGAG**GCCCCGCCGGAGCCCGCAGAGCAGCCCGCAAGCCAGGCGCGCGGGCAGCATG	Signal sequence cloning upstream of GFP
NLS s (BamH1-XhoI compatible overhangs)	**GATC**CATGTTGAAGCGGCTGCGGAAGCGGCTGC	Signal sequence cloning upstream of GFP
NLS as (BamH1-XhoI compatible overhangs)	**TCGAG**CAGCCGCTTCCGCAGCCGCTTCAACATG	Signal sequence cloning upstream of GFP
MTS-NLS s (BamH1-XhoI compatible overhangs)	**GATC**CATGCTGCCCGCGCGCCTGGCTTGCGGGCTGCTCTGCGGGCTCCGGCGGGGCTTGAAGCGGCTGCGGAAGCGGCTGC	Signal sequence cloning upstream of GFP
MTS-NLS as (BamH1-XhoI compatible overhangs)	**TCGAG**CAGCCGCTTCCGCAGCCGCTTCAAGCCCCGCCGGAGCCCGCAGAGCAGCCCGCAAGCCAGGCGCGCGGGCAGCATG	Signal sequence cloning upstream of GFP
NLS-NES s (BamH1-XhoI compatible overhangs)	**GATC**CATGTTGAAGCGGCTGCGGAAGCGGCTGCTAGACCTGCCGGACGCCCTGCTACCCGACCTGCCCAAGCTGC	Signal sequence cloning upstream of GFP
NLS-NES as (BamH1-XhoI compatible overhangs)	**TCGAG**CAGCTTGGGCAGGTCGGGTAGCAGGGCGTCCGGCAGGTCTAGCAGCCGCTTCCGCAGCCGCTTCAACATG	Signal sequence cloning upstream of GFP
fw1	ATGCTGCCCGCGCGCCTGGCTTGCGG	Splice variant PCR
fw2	ATGCAGAAGGCCCGGACACGGAGGAAC	Splice variant PCR
fw3	CCCAGCGGCATCTACTGCTCGGGCTGC	Splice variant PCR
fw4	CACCACTAATGCTGGCAAGTCCACTCT	Splice variant PCR
fw5	ACCGGGCCACCATCTCCCCCTGGCCAG	Splice variant PCR
fw6	GCACCACATTAAACCTCCTGAAGTTTC	Splice variant PCR
fw7	GAAGAGTTGGAAGAACATTCTCGTACT	Splice variant PCR
fw8	ATTTTAAATCTTCTAACAGAAAAAGAA	Splice variant PCR
fw9	GGAAATCAGTCAGCCTGGTTCACAGTT	Splice variant PCR
fw10	GTTCCAATGGGTGGAAAAGAACGAATG	Splice variant PCR
fw11	GTTGGGTTGCAGTAACACCTTATTCTGA	Splice variant PCR
rev1	AGAGTGGACTTGCCAGCATTAGTGGTG	Splice variant PCR
rev2	CTGGCCAGGGGGAGATGGTGGCCCGGT	Splice variant PCR
rev3	CTACTATGTAGCCGTGCTTTTTCAGTT	Splice variant PCR
rev4	ACAGCTTTCTTTTGTAATTCCAGGGGT	Splice variant PCR
rev5	CTGTAGGAAATCTATTCGGGCTATCCC	Splice variant PCR
rev6	CAGCAGTAGCTCGTGACCTGCATGTTT	Splice variant PCR
rev7	CTGCAGAGGAGAACTTGATATCAGCTA	Splice variant PCR
rev8	TCATCTGTGCTTCTTCAGGTTGTGCAC	Splice variant PCR
CMV fw	CGCAAATGGGCGGTAGGCGTG	Sequencing
BGH rev	TAGAAGGCACAGTCGAGG	Sequencing
FLAG tag s (BamH1-XhoI compatible overhangs)	**TCGAG**GATTATAAGGATGATGATGATAAGTGAT	Introduction of tag to pcDNA5/TO
FLAG tag as (BamH1-XhoI compatible overhangs)	**CTAGA**TCACTTATCATCATCATCCTTATAATC	Introduction of tag to pcDNA5/TO
HA tag s (BamH1-XhoI compatible overhangs)	**TCGAG**TACCCATACGATGTTCCAGATTACGCTTGAT	Introduction of tag to pcDNA5/TO
HA tag as	**CTAGA**TCAAGCGTAATCTGGAACATCG	Introduction of tag

(BamH1-XhoI compatible overhangs)	TATGGGTAC	to pcDNA5/TO
myc tag s (BamH1-XhoI compatible overhangs)	**TCGAG**GAACAAAAACTTATTTCTGAAGA AGATCTGTGAT	Introduction of tag to pcDNA5/TO
myc tag as (BamH1-XhoI compatible overhangs)	**CTAGA**TCACAGATCTTCTTCAGAAATAA GTTTTTGTTCC	Introduction of tag to pcDNA5/TO

E. Nucleotide and Amino acid sequence of NOA1

NM_019836

BamH1**G'GATCC**ATGCTGCCCGCGCGCCTGGCTTGCGGGCTGCTCTGCGGGCTCCGGCG
GGGCCCCGCGCCGGCCGCTGCGTGCTACGGCCCAGCACGGTGGCTTCTGGAGGGGAAGT
GTGAGGTCCCCATCCGCCAGCGTGCATCATCCTTGGGCCGTCGGGTTCCCCCGAGCTCCA
CGGCGACCGAGGACTATGCAGAAGGCCCGGACACGGAGGAACGCTTTCTGTTCCCGGAG
TACGTCCCGGAGCGGACCCCGGAGGAACAAGTGCGGGAGTTGCAGGAGCTGCGGGAGTT
GCAGCAGCTGCAGCAGGAGAAGGAACGAGAGAGATTGCAGCAGCGGGAGGAGCGGCTTC
AGCAGAAGCTGCGGGCGGGCTTCCGGACGCTGCCTGTCCCGGAGTTTCCAGACGCCTCG
GTGCCGCCCAGCGGCATCTACTGCTCGGGCTGCGGAGCCGAGCTGCACTGCCAGCATCC
CGGCCTGCCGGGCTACCTGCCGGAGGAGAAGTTCCGCGACGCTGCCCAGGCGGAAGGC
GGCCCGGCGCGGACCGTGTGCCAACGCTGCTGGCTGCTGGTGCACCACGGACGAGCCCT
GCGCCTGCAGGTAAGCCGCGATCAGTACCTGGAGCTTGTGAGCGCAGCGCTGCGGCGTC
CCGGGCCGGCTCTGGTGCTCTATATGGTGAATCTTCTAGACCTGCCGGACGCCCTGCTAC
CCGACCTGCCCAAGCTGGTGGGCCCCAAGCAACTCATCGTGCTGGGGAACAAAGTGGAC
CTGCTGCCCCAGGACGCTCCCGGCTACTTGAAGCGGCTGCGGAAGCGGCTGTGGGACGA
TTGCATCCGCGCCGGGCTCGTGGTGGCTCCTGGTCATCAAGGACCACAGTACCCTGCCG
GGGATGAGCCACTGGAGGAGATAAAGAATCAGAATCCGTCCTCCAGGTCCCGCACGGTAG
TCAAGGACGTGCGACTGATCAGCGCCAAGACGGGCTATGGAGTTGAAGAAATGATCTCTG
CTCTTCAGCGCTCCTGGCGCTACCGTGGTGATGTCTACCTGGTGGGCACCACTAATGCTG
GCAAGTCCACTCTCTTTAACACACTCCTGGAGTCTGATTACTGCACCGCCAAGGGCTCCG
AAGCCATCGACCGGGCCACCATCTCCCCCTGGCCAGGCACCACATTAAACCTCCTGAAGT
TTCCTATTTGCAACCCGACTCCTTACAGAATGTTCAAAAGACAAAGAAGGCTTCAAGAAGA
TGCGACCAAAGCTGAGGAAGATCTTAGTGAGGAAGAACAAAGTCAGCTCAATCAACTGAA
AAAGCACGGCTACATAGTAGGAAGAGTTGGAAGAACATTCTCGTACTCCAGAGAACAGGA
CGAAGTTCCCTTTGAGTTTGATGCCGACTCCCTGGCCTTTGACATGGGAAGTGAACCAGTT
GTGTCTGTGTGCAAAAGCACCAAGCAAATAGAGCTAACCCCAGAGGACGTGAAAGACGCC
CACTGGTTTTATGACACCCCTGGAATTACAAAAGAAAGCTGTATTTTAAATCTTCTAACAGA
AAAAGAAATAAATACTGTTTTGCCGACACATTCAATTATCCCAAGAACCTTTGTCCTCAAGC
CAGGAATGGTTTTATTTTTGGGTGGGATAGCCCGAATAGATTTCCTACAGGGAAATCAGTC
AGCCTGGTTCACAGTTGTGGCTTCCAACTTCCTTCCTGTTCATATTACTTCCTTGGACAAG
GCAGATGCTCTGTATGAGAAACATGCAGGTCACGAGCTACTGCTGGTTCCAATGGGTGGA
AAAGAACGAATGGCCCAGTTTCCCCCTCTTGTTGCTGAAGACATTACATTAAAGGGAGGTG
GAAAATTTGAAGCAGTAGCTGATATCAAGTTCTCCTCTGCAGGTTGGGTTGCAGTAACACC

TTATTCTGAGGGCACGCTGCATCTCCGAGGTCACACACCTGAAGGGACTGCTCTGACTGT
CCACCCCCCTGTCTTGCCATATATCGTTAATGTCAAAGGACAGCGCATGAAGAAAAGTGTG
GCCTATAAAACCAAGAAGCCTCCGTCCCTGGTGCACAACCTGAAGAAGCACAGATGA**C'T**
CGAG XhoI/SlaI

NLS, caspase-1 cleavage site, GTPase site, ClpX sites

NP_062810
MLPARLACGLLCGLRRGPAPAAACYGPARWLLEGKCEVPIRQRASSLGRRVPPSSTATEDYAEGPDTE
ERFLFPEYVPERTPEEQVRELQELRELQQLQQEKERERLQQREERLQQKLRAGFRTLPVPEFPDASVPPS
GIYCSGCGAELHCQHPGLPGYLPEEKFRDAAQAEGGPARTVCQRCWLLVHHGRALRLQVSRDQYL
ELVSAALRRPGPALVLYMVNLLDLPDALLPDLPKLVGPKQLIVLGNKVDLLPQDAPGYLKRLRKRLWD
DCIRAGLVVAPGHQGPQYPAGDEPLEEIKNQNPSSRSRTVVKDVRLISAKTGYGVEEMISALQRSWRY
RGDVYLVGTTNAGKSTLFNTLLESDYCTAKGSEAIDRATISPWPGTTLNLLKFPICNPTPYRMFKRQRR
LQEDATKAEEDLSEEEQSQLNQLKKHGYIVGRVGRTFSYSREQDEVPFEFDADSLAFDMGSEPVVSVC
KSTKQIELTPEDVKDAHWFYDTPGITKESCILNLLTEKEINTVLPTHSIIPRTFVLKPGMVLFLGGIARIDFL
QGNQSAWFTVVASNFLPVHITSLDKADALYEKHAGHELLLVPMGGKERMAQFPPLVAEDITLKGGGK
FEAVADIKFSSAGWVAVTPYSEGTLHLRGHTPEGTALTVHPPVLPYIVNVKGQRMKKSVAYKTKKPPSL
VHNLKKHR

Predicted MTS, NLS, caspase-1 cleavage site, GTPase site, ClpX sites

F. List of plasmids

Name	Description	Source
TO5	pcDNA5/TO vector for gene expression in mammalian cells; CMV promoter, Hygromycin resistance gene	Invitrogen
TO5 NOA1	pcDNA5/TO with coding sequence of NM_019836 NOA1 mRNA followed by a stop codon in the BamH1/Sla1 restriction sites	Provided by Dr. Szibor (Dept. Braun)
TO5 NOA1-Flag	1-4/A - amplification of fullength coding sequence of NOA1 with C-termanal Flag tag cloned into pcDNA5/TO in the BamHI/Sla1 restriction sites	cloned during this thesis
TO5 NOA1ΔMTS-Flag	2-4/B - amplification of NOA1 lacking N-terminal mitochondiral targeting sequence with C-termanal Flag tag cloned into pcDNA5/TO in the BamHI/Sla1 restriction sites	cloned during this thesis
TO5 NOA1ΔC-term-Flag	1-5- amplification of NOA1 lacking the C-terminus beginning from the caspase-1 cleavage site with C-termanal Flag tag cloned into pcDNA5/TO in the BamHI/Sla1 restriction sites	cloned during this thesis
TO5 NOA1ΔMTSΔC-term -Flag	2-5/L - amplification of NOA1 lacking N-terminal mitochondiral targeting sequence and lacking the C-terminus beginning from the caspase-1 cleavage site with C-termanal Flag tag cloned into pcDNA5/TO in the BamHI/Sla1 restriction sites	cloned during this thesis
TO5 C-term-Flag	amplification of the C-terminus of NOA1 beginning from the caspase-1 cleavage site with C-termanal Flag tag cloned into pcDNA5/TO in the BamHI/Sla1	cloned during this thesis

	restriction sites	
TO5 NOA1-ClpX-K690/91A	Introduction of the mutations by overlap PCR with Phusion Taq (Finnzymes) as described in the results section. A stop codon and the restriction sites were added by the amplification primers. The PCR product was cloned into pcDNA5/TO with BamH1/Sla1.	cloned during this thesis
TO5 NOA1-RNAmut-W629A	Introduction of the mutations by overlap PCR with Phusion Taq (Finnzymes) as described in the results section. A stop codon and the restriction sites were added by the amplification primers. The PCR product was cloned into pcDNA5/TO with BamH1/Sla1.	cloned during this thesis
TO5-cherry-Flag	mCherry (acc# AY678264) red fluorescent protein was amplified by PCR. The restriction sites AflII/NheI and a FLAG-tag were added by specific primer design and the fragment was cloned into the pcDNA5/TO vector.	Provided by Dr. Szibor (Dept. Braun)
TO5-NOA1ΔMTS-cherry	NOA1 without STOP codon (GeneID: 56412) and cherry were amplified by PCR. The restriction sites HindIII/XhoI (NOA1) and XhoI/XbaI (cherry) were introduced by specific primer design and the fragments were ligated into the pcDNA 3.1 (+) vector.	Provided by Dr. Szibor (Dept. Braun)
TO5-NOA1-EGFP	NOA1 without STOP codon (GeneID: 56412) and EGFP were amplified by PCR. The restriction sites BamHI/XhoI (NOA1) and XhoI/XbaI (EGFP) were introduced by specific primer design and the fragments were ligated into the pcDNA5/TO vector.	Provided by Dr. Szibor (Dept. Braun)
TO5 EGFP	EGFP-stop was amplified by PCR and cloned into the pcDNA5/TO backbone with the restriction sites XhoI/XbaI that were introduced by primer design; the MCS is N-terminal to the EGFP.	Provided by Dr. Szibor (Dept. Braun)
TO5 MTS-EGFP	Oligonucleotides containing the MTS sequence with BamH1/Sla1 compatible ends were annealed and ligated into the TO5-EGFP backbone	cloned during this thesis
TO5 NLS-EGFP	Oligonucleotides containing the NLS sequence with BamH1/Sla1 compatible ends were annealed and ligated into the TO5-EGFP backbone	cloned during this thesis
TO5 MTS/NLS-EGFP	Oligonucleotides containing the MTS/NLS sequence with BamH1/Sla1 compatible ends were annealed and ligated into the TO5-EGFP backbone	cloned during this thesis
TO5 NLS/NES-EGFP	Oligonucleotides containing the NLS/NES sequence with BamH1/Sla1 compatible ends were annealed and ligated into the TO5-EGFP backbone	cloned during this thesis
Omp25-GFP	Outer mitochondrial membrane protein marker protein OMP25 (NM_018373) was truncated containing the transmembrane domain and cloned into pEGFP-C1 in the restriction sites BglII/EcoRI	Provided by Dr. Szibor (Dept. Braun) (original source: Alexandra Kukat[67])
TO5 ClpX	Amplification of fullength coding sequence of ClpX with stop codon cloned into pcDNA5/TO in the BamHI/Sla1 restriction sites	cloned during this thesis
U6i	U6 RNA pol. III promoter fragment subcloned into a promoter-less pcDNA 3.1-derived vector.	Provided by Dr. Szibor (Dept. Braun)
U6i Luci (Mock)	Oligonucleotides coding for shRNA against luciferase are cloned into the BsmBI restriction sites. U6_RNAi knock-down control vector.	Provided by Dr. Szibor (Dept. Braun)
ClpXshRNA 1	Oligonucleotides coding for shRNA against ClpX are cloned into the BsmBI restriction sites. U6_RNAi knock-down control vector.	cloned during this thesis
ClpXshRNA 1	Oligonucleotides coding for shRNA against ClpX are	cloned during this

	cloned into the BsmBI restriction sites. U6_RNAi knock-down control vector.	thesis
pBacPAK9-NOA1ΔMTS-His_6	Wiltype NOA1 lacking the MTS was cloned in the pBacPAK9 (Clontech) vector backbone with the restriction sites HindIII/Sla1 and the His_6-tag was fused downstream with SalI/NotI.	Provided by Dr. Szibor (Dept. Braun)
pBacPAK9-NOA1-A460G-ΔMTS-His_6	Caspase-1 mutant (A460G) NOA1 lacking the MTS was cloned in the pBacPAK9 (Clontech) vector backbone with the restriction sites HindIII/Sla1 and the His_6-tag was fused downstream with SalI/NotI.	Provided by Dr. Szibor (Dept. Braun)
pBacPAK9-NOA1-K353R-ΔMTS-His_6	GTPase mutant (K353R) NOA1 lacking the MTS was cloned in the pBacPAK9 (Clontech) vector backbone with the restriction sites HindIII/Sla1 and the His_6-tag was fused downstream with SalI/NotI.	Provided by Dr. Szibor (Dept. Braun)

XII. Acknowledgements

Prof. Dr. Dr. Thomas Braun gave me the chance to develop my skills as a researcher and supported my work throughout the years with fruitful discussions. Thanks to him I attended excellent conferences and had a great research stay abroad.
Thank you for believing in me!

Prof. Dr. Robert Tampé supported me by being my supervisor at Frankfurt University where I already did my studies. I appreciate his directness when he assessed the status quo of my work.
Thank you for your honesty!

Dr. Jaakko Pohjoismäki provided a lot of intellectual support during the years of his stay in the Braun lab and was a great door opener. He introduced me to the "mito-society" at the Euromit8 conference and also arranged collaborations for me.
Thank you for everything!

Prof. Dr. Maria Falkenberg allowed me to purify the recombinant NOA1 protein in her lab in Gothenburg. Without the protein a major part of this work would not have been possible. I am very thankful for the fast supply of new NOA1-protein pellets (special thanks to Emily Hoberg).
Thank you for the kind accommodation!

Dr. Sjoerd Wanrooij supported my lab work in Gothenburg and also commented this thesis. He intensively supported the manuscript on G-quadruplexes.
Thank you for your constant support, the very good suggestions and discussions!

Dr. Steffi Goffart provided me with supervision and practical support concerning the work in the isotope lab. From her I learned the preparation of mitochondria and other helpful lab stuff.
Thank you for the great time in the lab!

Prof. Dr. Tania Baker accepted my request for collaboration about the ClpXP story and I am very honored that she supports my work with her expertize.
Thank you for the straightforward help!

Dr. Julia Kardon is my direct collaboration partner in the Baker lab and provided the first data on the ClpXP *in vitro* degradation of NOA1. She showed me around during my short stay in Boston.
Thanks for sending me your proteins and supporting my ideas!

Dr. Stefanie Köhler-Bachmann became a dear friend during the last years.
Thank you very much for reading and commenting my thesis in a very positive but particularly effective way. Thank you for your kind support and for your friendship!

Kerstin Richter was a major contact point in the lab. She supported my work with her technical expertise and the daily routine. And she was happy when I was happy because some result or experimental setup was rather nice to look at.
Thank you for you endurance, assistance and for the never-ending milk supply!

Dr. Thomas Böttger never hesitated to criticize my project in labmeetings leading to improvement of the experiments and their presentation. He was always willing to share protocols and gave advice when needed.

Dr. Marcus Krüger supported my project in the proteomics field and was always helpful in discussing experimental settings for proteomic studies. Thanks to Soraya Hölper for sample preparation and data evaluation.

A big thank you to the many people at the MPI supporting our research every single day: utility management, janitor, the scullery ladies and the receptionists. Especially, I want to thank the workshop team around Herr Burk for the many emergency case repairings, device exchanges and self-made labware.

Der allergrößte Dank gebührt jedoch meiner Familie, die mir erst die schulische Ausbildung, dann das Hochschulstudium und schließlich auch noch meinen lange währenden Wunschtraum einer Promotion durch ihre unermüdliche (auch finanzielle) Unterstützung erst ermöglicht haben. Nach Jahren der unangenehmen Fragerei "Wann isch se endlich fertich? Verdient se bald e'mol ebbes g'scheits?" auf die es lange keine verlässliche Antwort gab, kannst du nun endlich sagen: "Mein Kind ist jetzt Frau Doktor".

Mama - danke für Alles!

XIII. Curriculum Vitae

Name:	Natalie Al-Furoukh
Date of Birth:	21.12.1981
Place of Birth:	Freudenstadt im Schwarzwald
Nationality:	German
Family status:	unmarried

Doctorate:

12.2007-04.2013	Max-Planck-Institute for Heart and Lung Research (W.G. Kerckhoff Insitute), Department of Cardiac Development and Remodelling, Bad Nauheim, Germany Supervisor: Prof. Dr. Dr. Thomas Braun

Research Stays:

01.2011	Department of Medical Biology, University of Gothenburg, Gothenburg, Sweden Supervisor: Prof. Dr. Maria Falkenberg, Dr. Sjoerd Wanrooij Production and purification of recombinant NOA1-His_6.
08.2006-11.2007	Pathobiochemistry Department, University Hospital Frankfurt/Main, Germany Supervisor: Prof. Dr. Bernhard Brüne, Dr. Emeka Igwe Impact of hypoxia and nitric oxide on the transcriptional regulation of mouse macrophages.

Scientific Education:

03.06.2006	Degree: Diploma in Biochemistry
12.2005-07.2006	Diploma Thesis at the Institute of Biochemistry, Biocenter, Johann-Wolfgang Goethe University, Frankfurt/Main, Germany Supervisor: Prof. Dr. Robert Tampé, Dr. Jacob Piehler Reversible fluorescence-labelling of proteins on living cells.
11.2005	Diploma examination (Biochemistry, Biophysical Chemistry, Infection Biology with focus on Virology)

10.2001-11.2005	Studies in Biochemistry at the Johann-Wolfgang Goethe University, Frankfurt/Main, Germany

Internship:

02.2005-04.2005	Department 2/4, Pathological Virology, Paul-Ehrlich Institute, Langen, Germany Supervisor: PD Dr. Michael Nübling Specific detection of West-Nile-Virus proteins by western blot.

Conferences:

07.2012	Poster Presentation: NOA1 binds G-quadruplexes and is degraded by the mitochondrial ClpXP protease. Gordon Research Conference Mitochondria & Chloroplasts 2012, Bryant University, Smithfield, Rhode Island, USA
09.2011	Participant: Molecular Life Sciences 2011, International Meeting oft he German Society of Biochemistry and Molecular Biology (GBM), University Campus Westend, Frankfurt/Main, Germany
06.2011	Poster Presentation: A Caspase-1 processed NOA1 fragment is a putative mediator of proliferation. Euromit8 - European Meeting on Mitochondrial Pathology, Zaragossa, Spain
06.2011	Poster Presentation: ECCPS 2nd Symposium, Bad Nauheim, Germany
11.2010	Participant: New Frontiers in Bioenergetics Symposium, Nijmegen, Netherlands.
10.2007	Poster Presentation: Nitric oxide modulates hypoxic gene regulation. 12th NO Forum of the german speaking countries, Mainz, Germany

08.2006	Speaker: Type I Interferon Receptor Assembly in Live Cells Cytokines 2006, Molecular Biology and Human Disease, Wien, Austria
11.2005	Participant: Katzir Conference on Molecular Perspectives on Protein-Protein Interactions, Eilat, Israel

Basic Education:

20.06.2001	German Abitur (Focus English, Chemistry)
1992-2001	German Gymnasium (Albeck Gymnasium, Sulz am Neckar)
1988-1992	German Elementary School (Dornhan)

Memberships:

Since 2001	GBM (Gesellschaft für Biochemie und Molekularbiologie)
Since 2010	GRADE (Goethe Graduate Academy at the Goethe University Frankfurt/Main)

For references you may apply to:

Prof. Dr. Dr. Thomas Braun
Thomas.braun@mpi-bn.mpg.de

Prof. Dr. Robert Tampé
Tampe@em.uni-frankfurt.de

Dr. Jaakko Pohjoismäki
Jaakko.pohjoismaki@uef.fi

Dr. Steffi Goffart
Steffi.goffart@uef.fi

Dr. Sjoerd Wanrooij
Sjoerd.wanrooij@medkem.gu.se

XIV. Eidesstattliche Versicherung

Ich erkläre hiermit an Eides Statt, dass ich die vorgelegte Dissertation über

„Characterization of Mouse NOA1: Subcellular Localization, G-Quadruplex Binding & Proteolysis."

selbständig angefertigt und mich anderer Hilfsmittel als der in ihr angegebenen nicht bedient habe, insbesondere, dass alle Entlehnungen aus anderen Schriften mit Angabe der betreffenden Schrift gekennzeichnet sind.

Ich versichere, nicht die Hilfe einer kommerziellen Promotionsvermittlung in Anspruch genommen zu haben.

Bad Nauheim, den 13.03.2013 Natalie Al-Furoukh

(Unterschrift)

XV. Table of Contents

XVI. References

1. Ash MR, Maher JJ, Mitchell G, Jormakka M. The cation-dependent G-proteins: in a class of their own. FEBS Lett. 20142;586(16):2218-24.
2. Britton RA. Role of GTPases in bacterial ribosome assembly. Annu Rev Microbiol. 2009;63:155-76.
3. Moreau M, Lee GI, Wang Y, Crane BR, Klessig DF. AtNOS/AtNOA1 is a functional Arabidopsis thaliana cGTPase and not a nitric-oxide synthase. J Biol Chem. 2008;283(47):32957-67.
4. Heidler J, Al-Furoukh N, Kukat C, et al. Nitric oxide-associated protein 1 (NOA1) is necessary for oxygen-dependent regulation of mitochondrial respiratory complexes. The Journal of biological chemistry. 2011 Sep 16;286(37):32086-93.
5. Kolanczyk M, Pech M, Zemojtel T, et al. NOA1 is an essential GTPase required for mitochondrial protein synthesis. Molecular biology of the cell. 2011 Jan 1;22(1):1-11.
6. Anand B, Surana P, Bhogaraju S, Pahari S, Prakash B. Circularly permuted GTPase YqeH binds 30S ribosomal subunit: Implications for its role in ribosome assembly. Biochemical and biophysical research communications. 2009 Sep 4;386(4):602-6.
7. He J, Cooper HM, Reyes A, et al. Human C4orf14 interacts with the mitochondrial nucleoid and is involved in the biogenesis of the small mito-chondrial ribosomal subunit. Nucleic Acid Research. 2012;40(13):6097-108.
8. Anand B, Surana P, Prakash B. Deciphering the catalytic machinery in 30S ribosome assembly GTPase YqeH. PloS one. 2010;5(4):e9944.
9. Uicker WC, Schaefer L, Koenigsknecht M, Britton RA. The essential GTPase YqeH is required for proper ribosome assembly in Bacillus subtilis. Journal of bacteriology. 2007 Apr;189(7):2926-9.
10. Lewis MR, Lewis WH. Mitochondria in the tissue culture. Science. 1914 27 February 1914:330-3.
11. McBride HM, Neuspiel M, Wasiak S. Mitochondria: more than just a powerhouse. Curr Biol. 2006;16(14):R551-60.
12. Davies KM, Anselmi C, Wittig I, Faraldo-Gomez JD, Kühlbrandt W. Structure of the yeast F1F0-ATP synthase dimer and its role in shaping the mitochondrial cristae. PNAS. 2012;109(34):13602-7.
13. Sharma MR, Koc EC, Datta PP, Booth TM, Spremulli LL, Agrawal RK. Structure of the mammalian mitochondrial ribosome reveals an expanded functional role for its component proteins. Cell. 2003;115:1-20.
14. Bogenhagen DF, Clayton DA. The mitochondrial DNA replication bubble has no burst. Trends Biochem Sci. 2003;28(7):357-60.
15. Clayton DA. Mitochondrial DNA replication: what we know. IUBMB Life.2003;55(4-5):213-7.
16. Kasiviswanathan R, Collins TR, Copeland WC. The interface of transcription and DNA repliation in mitochondria. Biochim Biophys Acta. 2012;1819(9-10):970-8.
17. Pohjoismäki JL, Goffart S. Of circles, forks and humanity: Topological organization and replication of mammalian mitochondrial DNA. Bioessays. 2011;33(4):290-9.
18. Nunnari J, Suomalainen A. Mitochondria: In sickness and health. Cell. 2012;148(6):1145-59.
19. Wallace DC. Bioenergetic origin of complexity and disease. Cold Springs Harb Symp Quant Biol. 2011;76:1-16.
20. Schaefer AM, Taylor RW, Turnbull DM, Chinnery PF. The epidemiology of mitochondrial disorders - past, present and future. BBA-Bioenergetics. 2004;1659(2-3):115-20.
21. Agrawal RK, Sharma MR. Structural aspects of mitochondrial translational apparatus. Curr Opin Struct Biol. 2012.
22. Smirnov A, Entelis N, Martin RP, Tarassov I. Biological significance of 5S rRNA import into human mitochondria: role of ribosomal protein MRP-L18. Genes Dev. 2011;25(12):1289-305.
23. Smirnov A, Comte C, Mager-Heckel AM, et al. Mitochondrial enzyme rhodanese is essential for 5S ribosomal RNA import into human mitochondria. J Biol Chem. 2010;285(40):30792-803.
24. Christian BE, Spremulli LL. Mechanism of protein biosynthesis in mammalian mitochondria. Biochim Biophys Acta. 2012;1819(9-10):1035-54.
25. Chrzanowska-Lightowlers ZM, Pajak A, Lightowlers RN. Termination of protein synthesis in mammalian mitochondria. The Journal of biological chemistry. 2011 Oct 7;286(40):34479-85.

26. Lightowlers RN. Mitochondrial transformation: time for concerted action. EMBO reports. 2011 Jun;12(6):480-1.
27. Richter R, Pajak A, Dennerlein S, Rozanska A, Lightowlers RN, Chrzanowska-Lightowlers ZM. Translation termination in human mitochondrial ribosomes. Biochemical Society transactions. 2010 Dec;38(6):1523-6.
28. Becker T, Böttinger L, Pfanner N. Mitochondrial protein import: from transport pathways to an integrated network. Trends Biochem Sci. 2012;37(3):85-91.
29. Bachmair A, Finley D, Varshavsky A. In vivo half-life of a protein is a functino of its amino-terminal residue. Science. 1986;234(4773):179-86.
30. Gonda DK, Bachmair A, Wünning I, Tobias JW, W.S. L, Varshavsky A. Universality and structure of the N-end rule. J Biol Chem. 1989;264 (28):16700-12.
31. Stuart R. Insertion of proteins into the inner membrane of mitochondria: the role of the Oxa1 complex. Biochim Biophys Acta. 2002;1592(1):79-87.
32. Hildenbeutel M, Theis M, Geier M, et al. The membrane insertase oxa1 is required for efficient import of carrier proteins into mitochondria. J Mol Biol. 2012;423(4):590-9.
33. Moreno-Lastres D, Fontanesi F, Garcia-Consuegra I, et al. Mitochondrial complex I plays an essential role in human respirasome assembly. Cell Metab. 2012;15(3):324-35.
34. Richter CV. Analyse verschiedener chloroplastidärer SRP-Transportsysteme in pflanzlichen Organismen. Bochum: Ruhr-Universität Bochum, 2009.
35. Bonnefoy N, Fiumera HL, Dujardin G, Fox TD. Roles of Oxa1-related inner-membrane translocases in assembly of respiratory chain complexes. Biochim Biophys Acta. 2009;1793:60-70.
36. Ott M, Herrmann JM. Co-translational membrane insertion of mitochondrially enceded proteins. Biochim Biophys Acta. 2010;1803(6):767-75.
37. Hartl FU, Neupert W. Protein sorting to mitochondria: evolutionary conservations of folding and assembly. Science. 1990;247(4945):930-8.
38. Wang P, Dalbey RE. Inserting membrane proteins: The YidC/Oxa1/Alb3 machinery in bacteria, mitochondria, and chloroplasts. Biochim Biophys Acta. 2044;1808:866-75.
39. von Heijne G. Membrane protein structure prediction. Hydrophobicity analysis and the positive-inside rule. J Mol Biol. 1992;225:487-94.
40. Blobel G. Intracellular protein topogenesis. Proc Natl Acad Sci U S A. 1980;77(3):1496-500.
41. van Loon AP, Schatz G. Transport of proteins to the mitochondrial inner membrane space: the "sorting" domain of the cytochrome c1 presequence is a stop-transfer sequence for the inner mitochondrial membrane. EMBO J. 1987;6(8):2441-8.
42. Kaput J, Goltu S, Blobel G. Nucleotide sequence of the yeast nuclear gene for cytochrome c peroxidase precursor. Functional implications of the pre sequence for protein transport into mitochondria. J Biol Chem. 1982;257(24):15054-8.
43. Stuart RA, Ono H, Langer T, Neupert W. Mechanisms of protein import into mitochondria. Cell Struct Funct. 1996;21(5):403-6.
44. von Heijne G. Membrane-protein topology. Nat Rev Vol Cell Biol. 2006;7(12):909-18.
45. Samuelson JC, Chen M, Jiang F, et al. YidC mediates membrane protein insertion in bacteria. Nature. 2000;406(6796):637-41.
46. Samuelson JC, Jiang F, Yi L, et al. Function of YidC for the insertion of M13 procoat protein in Escherichia coli: translocation of mutants that show differences in their membrane potential dependence and Sec requirement. J Biol Chem. 2001;276(37):34847-52.
47. van Bloois E, Nagamori S, Koningstein G, et al. The Sec-independet function of Escherichia coli YidC is evolutionary conserved and essential. J Biol Chem. 2005;280(13):12996-3003.
48. Kohler R, Boehringer D, Greber B, et al. YidC and Oxa1 form dimeric insertion pores on the translating ribosome. Mol Cell. 2009;34(3):344-53.
49. Matsushima Y, Kaguni LS. Matrix proteases in mitochondrial DNA function. BBA-Gene Regulatory Mechanisms. 2012;1819(9-10).
50. Bonn F, Tatsuta T, Petrungaro C, Riemer J, Langer T. Presequence-dependent folding ensures MrpL32 processing by the m-AAA protease in mitochondria. EMBO J. 2011;30(13):2545-56.
51. Matsushima Y, Goto Y, Kaguni LS. Mitochondiral Lon protease regulates mitochondrial DNA copy number and transcription by selective degradation of mitochondrial transcription factor A (Tfam). PNAS. 2010;107(43):18410-5.
52. Baker TA, Sauer RT. ClpXP, an ATP-powered unfolding and protein-degradation machine. Biochimica et biophysica acta. 2012 Jan;1823(1):15-28.

53. Flynn JM, Neher SB, Kim YI, Sauer RT, Baker TA. Proteomic discovery of cellular substrates of the ClpXP protease reveals five classes of ClpX-recognition signals. Molecular cell. 2003 Mar;11(3):671-83.
54. Gottesman S. Proteases and their targets in Escherichia coli. Annu Rev Genet. 1996;30:465-506.
55. Gottesman S, Clark WP, de Crecy-Lagard V, Maurizi MR. ClpX, an alternative subunit for the ATP-dependent Clp protease of Escherichia coli. Sequence and in vivo activities. J Biol Chem. 1993;268:22618-626.
56. Guo FQ, Okamoto M, Crawford NM. Identification of a plant nitric oxide synthase gene involved in hormonal signaling. Science. 2003 Oct 3;302(5642):100-3.
57. Sudhamsu J, Lee GI, Klessig DF, Crane BR. The structure of YqeH. An AtNOS1/AtNOA1 ortholog that couples GTP hydrolysis to molecular recognition. The Journal of biological chemistry. 2008 Nov 21;283(47):32968-76.
58. Tang T, Zheng B, Chen SH, et al. hNOA1 interacts with complex I and DAP3 and regulates mitochondrial respiration and apoptosis. The Journal of biological chemistry. 2009 Feb 20;284(8):5414-24.
59. Paul MF, Alushin GM, Barros MH, Rak M, Tzagoloff A. The putative GTPase encoded by MTG3 functiona in a novel pathway for regulating assembly of the small subunit of yeast mitochondrial ribosomes. J Biol Chem. 2012;287(29):24346-55.
60. Claros MG, Vincecs P. Computational method to predict mitochondrially imported proteins and their targting sequences. Eur J Biochem. 1996;241:770-86.
61. Bairoch A, Bucher P, Hofmann K. Nucleic Acid Research. 1997;25(217-221).
62. Rost B, Yachdav G, Liu J. The PredictProtein Server. Nucleic Acid Research 2004;32(Web Server Issue):W321-W326.
63. Dingwall C, Laskey RA. Nuclear targeting sequences -- a consensus? Trends Biochem Sci. 1991;16(12):478-81.
64. Turowec JP, Duncan JS, Gloor GB, Litchfield DW. Regulation of caspase pathways by protein kinase CK2: Identification of proteins with overlapping CK2 and caspase consensus motifs. Mol Cell Biochem. 2011;356(1-2):159-67.
65. Krissinel E. On the relationship between sequence and structure similarities in proteomics. Bioinformatics. 2007;23(6):717-23.
66. Szymczak AL, Workman CJ, Wang Y, et al. Correction of multi-gene deficiency in vivo using a single 'self-cleaving' 2A peptide based retroviral vector. Nat Biotechnol. 2004;22(5):589-94.
67. Kukat A. Mitochondriale Fusions- und Fissionsvorgänge am Modellsystem von Mega-Mitochondrien einer rho0-Zelllinie. Würzburg: Bayerische Julius-Maximilians-Universität, 2007.
68. Nemoto Y, De CP. Recruitment of an alternatively spliced form of synaptojanin 2 to mitochondria by the interaction with the PDZ domain of a mitochondrial outer membrane protein. EMBO J. 1999;18(2991-3006).
69. Chuderlund D, Marmor G, Shainskaya A, Seger R. Calcium-mediated interactions regulate the subcellular localization of extracellular signal-regulated kinases. J Biol Chem. 2008;283(17):11176-88.
70. Asscher Y, Pleban S, Ben-Shushan M, Levin-Khalifa M, Yao Z, Seger R. Leptomycin B: An important tool for the study of nuclear export. Homepage Sigma-Aldrich
71. Li W, Jain MR, Chen C, et al. Nrf2 possesses a redox-insensitive Nuclear Export Signal overlapping with the Leucine Zipper Motif. Jounal of Biological Chemistry. 2005;280(31):28430-38.
72. Schneider TD, Stephens RM. Sequence Logos: A New Way to Display Consensus Sequences. Nucleic Acid Research. 1990;18:6097-100.
73. Grooks GE, Hon G, Chandonia JM, Brenner SE. WebLogo: A sequence logo generator. Genome Research. 2004;14:1188-90.
74. Kikin O, D'Antonio L, Bagga PS. QGRS Mapper: a web-based server for predicting G-qudaruplexes in nucleotide sequnces. Nucleic Acid Research. 2006;34 (Web Server Issue):W676-W82.
75. Joachimi A, Benz A, Hartig J. A comparison of DNA and RNA quadruplex structures and stabilities. Bioorganic and Medicinal Chem. 2009;17(19):6811-15.
76. Menendez C, Frees S, Bagga P. QGRS-H Predictor: A Web Server for Predicting Homologous Quadruplex forming G-Rich Sequence Motifs in Nucleotide Sequences. Nucleic Acids Res. 2012;40(W96-W103).

77. von Knethen A, Tzieply N, Jennewein C, Brüne B. Casein-kinase-II-dependent phosphorylation of PPARγ provokes CRM1-mediated shuttling of PPARγ from the nucleus to the cytosol. J Cell Sci. 2010;123:192-201.
78. Gnad F, Ren S, Cox J, et al. PHOSIDA (phophorylation site database): management, structural and evolutionary investigation, and prediction of phophosites. Genome Biology. 2007.
79. Gnad F, Gunawardena J, Mann M. PHOSIDA 2011: the posttranslational modifiation database. Nucleic Acid Research. 2011.
80. Varshavsky A. The N-end rule: Functions, mysteries, uses. Proc Natl Acad Sci. 1996;93:12142-49.
81. Käser M, Langer T. Protein degradation in mitochondria. Cell and Developmental Biology. 2000;11:181-90.
82. Koppen M, Langer T. Protein Degradation within Mitochondria: Versatile Activities of AAA Proteases and Other Peptidases. Critical Reviews in Biochemistry and Molecular Biology. 2007;42:221-42.
83. Santagata S, Bhattacharyya D, Wang FH, Singha N, Hodtsev A, Spanopoulou E. Molecular cloning and characterization of a mouse homolog of bacterial ClpX, a novel mammalian class II member of the Hsp100/Clp chaperone family. The Journal of biological chemistry. 1999 Jun 4;274(23):16311-9.
84. Wojtyra UA, Thibault G, Tuite A, Houry WA. The N-terminal Zinc Binding Domain of ClpX Is a Dimerization Domain That Modulates the Chaperone Function. J Biol Chem. 2000;278(49):48981-90.
85. Loh PC, Morimoto T, Matsuo Y, Oshima T, Ogasawara N. The GTP-binding protein YqeH participates in biogenesis of the 30S ribosome subunit in Bacillus subtilis. Genes & genetic systems. 2007 Aug;82(4):281-9.
86. Morimoto T, Loh PC, Hirai T, et al. Six GTP-binding proteins of the Era/Obg family are essential for cell growth in Bacillus subtilis. Microbiology. 2002 Nov;148(Pt 11):3539-52.
87. Karniely S, Pines O. Single translation-dual destination: mechanisms of dual protein targeting in eukaryotes. EMBO reports. 2005;6(5):420-25.
88. Yogev O, Pines O. Dual targeting of mitochondrial proteins: Mechanism, regulation and function. Biochim et Biophys Acta. 2011;1808:1012-20.
89. Spector DL, Lamond AI. Nuclear Speckles. Cold Springs Harb Perspect Biol. 2011;3(a000646).
90. Kim SJ, Kwon MC, Ryu MJ, et al. CRIF1 is essential for the synthesis and insertion of oxidative phophorylation polypeptides in the mammalian mitochondrial membrane. Cell Metab. 2012;16(2):274-83.
91. He J, Cooper HM, Reyes A, et al. Mitochondrial nucleoid interacting proteins support mitochondrial protein synthesis. Nucleic Acids Res. 2012;40(13):6109-21.
92. Chung HK, Yi YW, Jung NC, et al. CR6-interacting Factor 1 Interacts with Gadd45 Family Proteins and Modulate Cell Cycle. J Biol Chem. 2003;278:28079-88.
93. Sen D, Gilbert W. A sodium-potassium switch in the formation of four-stranded G4-DNA. Nature. 1990;344:410-344.
94. Bugaut A, Balasubramanian S. 5'-UTR RNA G-quadruplexes: translation regulation and targeting. Nucleic Acid Res. 2012;40(11):4727-41.
95. Millevoi S, Moine H, Vagner S. G-quadruplexes in RNA biology. Wiley Interdiscip Rev RNA. 2012;3(4):495-507.
96. Booy EP, Meier M, Okun N, et al. The RNA helicase RHAU (DHX36) unwinds a G4-quadruplex in human telomerase RNA and promotes the formation of the P1 helix temlate boundary. Nucleic Acid Res. 2012;10(6):1000-24.
97. Lattman S, Stadler MB, Vaughn JP, Akman SA, Nagamine Y. The DEAH-box RNA helicase RHAU binds and intramolecular RNA G-quadruplex in TERC and associates with telomerase holoenzyme. Nucleic Acid Res. 2011;39(21):9390-404.
98. Palumbo SL, Memmott RM, Uribe DJ, Krotova-Khan Y, Hurley LH, Ebbinghaus SW. A novel G-quadruplex-forming GGA repeat region in the c-myb promoter is a critical regulator of promoter activity. Nucleic Acid Res. 2008;36(6):1755-69.
99. Morris MJ, Negishi Y, Pazsint C, Schonhoft JD, Basu S. An RNA G-quadruplex is essential for cap-independent translation initiation in human VEGF IRES. J Am Chem Soc. 2010;132(50):17831-9.

100. Capra JA, Paeschke K, Singh M, Zakian VA. G-quadruplex DNA sequenes are evolutionarily conserved and associated with distinct genomic features in Saccharomyces cerevisiae. Plos Computational Biology. 2010;6(7).
101. Kaushik M, Kaushik S, Bansal A, Saxena S, Kukreti S. Structural diversity and specific recognition of four stranded G-quadruplex DNA. Curr Mol Med. 2011;11(9):744-69.
102. Düchler M. G-quadruplexes: targets and tools in anticancer drug design. J Drug Target. 2012;20(5):389-400.
103. Collie GW, Parkinson GN. The application of DNA and RNA G-quadruplexes to therapeutic medicine. Chem Soc Rev. 2011;40(12):5867-92.
104. Sissi C, Gatto B, Palumbo M. The evolving world of protein-G-quadruplex recognition: a medicinal chemist's perspective. Biochimie. 2011;93(8):1219-30.
105. Entelis N, Brandina I, Kamenski P, Krasheninnikov IA, Martin RP, Tarassov I. A glycolytic enzyme, enolase, is recruited as a cofactor of tRNA targeting toward mitochondria in Sacharomyces cerevisiae. Genes Dev. 2006;20:1606-20.
106. Summers WA, Wilkins JA, Dwivedi RC, Ezzati P, Court DA. Mitochondrial dysfunction resulting from the absence or mitochondrial porin in Neurospora crassa. Mitochondrion. 2012;12(2):220-9.
107. Nijtmans LG, de Jong L, Artal Sanz M, et al. Prohibitins act as a membrane-bound chaperone for the stabilization of mitochondrial proteins. EMBO J. 2000;19(11):2444-51.
108. Osman C, Merkwirth C, Langer T. Prohibitins and the functional compartmentalization of mitochondrial membranes. J Cell Sci. 2009;122:3823-30.
109. Osman C, Haa M, Potting C, et al. The genetic interactome of prohibitins: coordinated control of cardiolipin and phosphatidylethanolamine by conserved regulators in mitochondria. Journal of Cell Biology. 2009;184(4):593-96.
110. Merkwirth C, Langer T. Prohibitin function within mitochondria: essential roles for cell proliferation and cristae morphogenesis. Biochim Biophys Acta. 2009;1793(1):27-32.
111. Artal-Sanz M, Tavernarakis N. Prohibitin and mitochondrial biology. Trends Endocrinol Metab. 2009;20(8):394-401.
112. Tschopp F, Charrière F, Schneider A. In vivo study in Trypanosoma brucei links mitochondrial transfer RNA import to mitochondrial protein import. EMBO Rep. 2011;12(8):825-32.
113. Seidman D, Johnson D, Gerbasi V, Golden D, Orlando R, Hajduk S. Mitochondrial membrane complex that contains proteins necessary for tRNA import in Trypanosoma brucei. J Biol Chem. 2012;287(12):8892-903.
114. Mick DU, Dennerlein S, Wiese H, et al. MITRAC links mitochondrial protein translocation to respiratory-chain assembly and translational regulation. Cell. 2012 Dec 21;151(7):1528-41.
115. Hao L, Yu C, Li B, Wang D. Molecular cloning and preliminary analysis of TaNOA in common wheat. Article in chinese - abstract cited. 2010.
116. Almajan ER, Richter R, Paeger L, et al. AFG3L2 supports mitohochondrial protein synthesis and Purkinje cell survival. JCI. 2012:1-11.
117. Labzebnik YA, Kaufmann SH, Desnoyers S, Poirier GG, Earnshaw WC. Cleavage of poly (ADP-ribose) polymerase by a proteinase with properties like ICE. Nature. 1994;371:346-7.
118. Schmidt O, Harbauer AB, Rao S, et al. Regulation of mitochondrial protein import by cytosolic kinases. Cell. 2011;144(2):227-39.
119. Heidler J. Adaptation der mitochondrialen Energiebereitstellung an subzelluläre Unterschiede der Sauerstoffversorgung im Herzen. Hallo-Wittenberg: Martin-Luther-Universität, 2011.
120. Pohjoismaki JL, Boettger T, Liu Z, Goffart S, Szibor M, Braun T. Oxidative stress during mitochondrial biogenesis compromises mtDNA integrity in growing hearts and induces a global DNA repair response. Nucleic Acid Research. 2012;40(14):6595-607.
121. Burton BM, Baker TA. Mu transpososome architecture ensures that unfolding by ClpX or proteolysis by ClpXP remodels but does not destroy the complex. Chem Biol. 2003;10(5):463-72.
122. Grosshans H, Deinert K, Hurt E, Simos G. Biogenesis of the Signal Recognition Particle (SRP) Involves Import of SRP proteins into the Nucleolus, Assembly with the SRP-RNA and Xpo1p-mediated Export. J Cell Biol. 2001;153(4):745-61.
123. Jacobson MR, Pederson T. Localization of signal recognitino particle RNA in the nucleolus of mammalian cells. Proc Natl Acad Sci. 1998;95:7981-6.
124. Walter P, Blobel g. Disassembly and reconstitution of signal recognition particle. Cell. 1983;34:525-33.

125. Luirink J, Dobberstein B. Mammalian and Escherichia coli signal recognition particles. Molecular Microbiology. 1994;111(1):9-13.
126. Gundelfinger ED, Krause E, Melli M, Dobberstein B. The organization of the 7SL RNA in the signal recognition particl. Nucleic Acids Res. 1983;11(21).
127. Ullu E, Murphy S, Melli M. Human 7SL RNA consists of a 140 nucleotide middle-repetitive sequence inserted in an Alu sequence. Cell. 1982;29:195-202.
128. Zwieb C. The secondary structure of the 7SL RNA in the signal recognition particle: functional implications Nucleic Acids Rec. 1982;13:6105-24.
129. Walter P, Blobel G. Purification of a membrane-associated protein complex required for protein translocation acros the endoplasmic reticulum. Proc Natl Acad Sci. 1980;77:7112-6.
130. Sakaguchi M, Mihara K, Sato R. Signal recognition particle is required for co-translational insertion of cytochrome P-450 into microsomal membranes. Proc Natl Acad Sci. 1984;81:3361-64.
131. Halic M, Becker T, Pool MR, et al. Structure of the signal recognition particle interacting with the elongation-arrested ribosome. Nature. 2004;427:808-14.
132. Shan S, Walter P. Co-translational protein targeting by the signal recognition particle. FEBS Letters. 2005;579:921-6.
133. Shan SO, Chandrasekar S, Walter P. Conformational changes in the GTPase modules of the signal recognition particle and its receptor drive initiation of protein translocation. J Cell Biol. 2007;178(4):611-20.
134. Miller JD, Walter P. A GTPase cycle in initiation of protein translocation across the endoplasmic reticulum membrane. Ciba Found Symp. 1993;176:147-63.
135. Arnold CE, Wittrup KD. The Stress Response to Loss of Signal Recognition Particle Function in Saccharomyces cerevisiae. J Biol Chem. 1994;269(48):30412-418.
136. Utz P, Hottelet M, Le TM, et al. The 72kDa Component of the Signal Recognition Particle is Cleaved during Apoptosis. J Biol Chem. 1998;273(52):35362-70.
137. Birnboim HC, Doly J. A rapid alkaline extraction prodedure for screening recombinant plasmid DNA. Nucleic Acids Research. 1979;7(6):1613-23.
138. Chomczynski P, Sacchi N. Single-step method of RNA isolation by acid guanidinium thiocyanate-phenol-chloroform extraction. Anal Biochem. 1987;162:156-9.
139. Chomczynski P, Sacchi N. The single-step method of RNA isolation by acid guanidinium thiocyanate-phenol-chloroform extraction: twenty-something years on. Nature Protocols. 2006;1(2):581-5.
140. Hyvarinen AK, Pohjoismaki JL, Reyes A, et al. The mitochondrial transcription termination factor mTERF modulates replication pausing in human mitochondrial DNA. Nucleic acids research. 2007;35(19):6458-74.
141. Englehorn TV, Updyke TV; System for pH neutral longlife precast electrophoresis gel. U.S. 1996.
142. Hachmann JP, Amshey JW. Models of protein modification in Tris-glycine and neutral pH Bis-Tris gels during electrophoresis: Effect of gel pH. Analytical Biochemistry. 2005;342(2):237-45.
143. Moore S. bis-Tris SDS-PAGE, the very best Accessed. OpenWetWare, 2009.
144. Zatsepina OV, Dudnic OA, Chentsov YS, Thiry M, Srping H, Trendelenburg MF. Reassembly of Functional Nucleoli Following In Situ Unraveling by Low-Ionic-Strength Treatment of Cultured Mammalian Cells. Experimental Cell Research. 1997;233(1):155-68.
145. Igwe EE, Essler S, Al-Furoukh N, Dehne N, Brüne B. Hypoxic transcription gene profiles under the modulation of nitric oxide in nuclear run on-microarray and proteomics. BMC Genomics. 2009;10(408).
146. Melchior F. Nuclear Protein Import in a Permeabilized Cell Assay. Mehtods in Molecular Biology. 1998;88:265-73.
147. Gaines G, Attardi G. Highly efficient RNA-synthesizing system that uses isolated human mitochondria: nes initiation events and in vivo-lke processing patterns. Mol Cell Biol. 1984;4:1605-17.
148. Laemmli UK. Cleavage of Structural Proteins during the Assembly of the Head of Bacteriophage T4. Natrue. 1970;227:680-5.
149. Sørensen SPL. Enzymstudien II. Biochem Z. 1909;22(352).
150. Gomori G. Preparation of buffers for use in enzyme studies. Methods Enzymol. 1955:138-46.